MONOTONIC AND CYCLIC SHEAR RESPONSE OF RECONSTITUTED NATURAL SILT

by

Daniel Mark Barnes

B.Eng., Civil Engineering, University of Newcastle, 2009

A THESIS SUBMITTED IN PARTIAL FULFILLMENT OF

THE REQUIREMENTS FOR THE DEGREE OF

MASTER OF APPLIED SCIENCE

in

THE FACULTY OF GRADUATE AND POSTDOCTORAL STUDIES

(Civil Engineering)

THE UNIVERSITY OF BRITISH COLUMBIA

(Vancouver)

December 2015

Abstract

A triaxial apparatus was upgraded and a specimen preparation device was developed to enable monotonic and cyclic triaxial testing of low plastic reconstituted silts. The silt reconstitution technique involves consolidating silt slurry inside a cylindrical split mold, directly on the triaxial base pedestal. The slurry is carefully poured into the split mold using a flexible hose. A vertical load is then applied to slurry using a top cap and loading ram. Loading is applied in an incremental manner and the slurry is allowed to consolidate, creating a specimen firm enough to carry on with triaxial testing. The newly developed silt reconstitution device was verified with respect to specimen uniformity, saturation and test repeatability.

Using the new triaxial apparatus and silt reconstitution device, the monotonic and cyclic shear response of Kamloops silt was investigated, contributing to the understanding of the material behaviour of relatively low plastic silt. Silt specimens, initially hydrostatically consolidated to various stress levels, displayed cyclic mobility type strain development during both monotonic and cyclic loading. The specimen preparation technique was capable of producing laboratory test specimens having Skempton's B values of greater than 0.98, indicating a high level of saturation of prepared specimens.

The undrained shear strength measured in undrained monotonic triaxial extension was found to be 20% lower than the undrained shear strength measured in monotonic triaxial compression. This difference is in accord with the stress-path dependency typically found in gravity deposited sediments, and is considered to be due to the anisotropic soil fabric.

Liquefaction in the form of strain softening accompanied by loss of shear strength did not manifest in the reconstituted Kamloops silt regardless of the applied cyclic stress ratio (CSR). The cyclic shear resistance of the material was found to be relatively insensitive to the applied confining stress level. The cyclic mobility type stress-strain behaviour was observed in spite of the initial static shear stress bias. The potential for excess pore water pressure generation was observed to decrease significantly with increasing level of initial static shear.

Preface

I was involved in soil sample retrieval process, laboratory equipment development and conducted all the tests in the laboratory experimental program in this research project. Dr. Wijewickreme was the supervisory author and was involved in the formation of concept during the conductance of experiments, organizing the content and final editing of the manuscript. One publication arising from this research is detailed below.

Version of parts in chapter 2, 3 and 4 has been published at the 2015 Canadian Geotechnical Society annual conference:

Barnes, D., Verma, P., & Wijewickreme (2015) Some initial experimental findings on the influence of mode of shear on the monotonic shear response of reconstituted silts, Sep 20- Sept 23, 2015, Quebec City, Quebec.

It is noteworthy to acknowledge the presentation of previously published data and results extracted from other sources in the following figures:

For the illustration purpose of soil response, figures from Atkinson (1993), Kuerbis (1989) have been reproduced and presented in Figure 2.1 and Figure 2.2 respectively. Similarly figures from Vaid & Chern (1985) have been used to reproduce and present Figure 2.3, Figure 2.4 and Figure 2.5. Figures from Idriss & Boulanger (2008) and Andersen (2009) are reproduced and presented in Figure

2.7 and Figure 2.8. Data points from Sanin (2010) have been reproduced and presented in Figure 2.24 for comparative purposes.

All the figures were prepared by the current author with the results obtained from publication from aforementioned researches reproduced accordingly.

Table of Contents

Abstract ..... **ii**

Preface ..... **iv**

Table of Contents ..... **vi**

List of Tables ..... **x**

List of Figures ..... **xi**

List of Symbols ..... **xix**

List of Abbreviations ..... **xxi**

Acknowledgements ..... **xxii**

Dedication ..... **xxiv**

Chapter 1: Introduction **1**

1.1 Background 1

1.2 Objectives 3

1.3 Organisation 4

Chapter 2: Literature Review **5**

2.1 General 5

2.2 Mechanical response of sand 7

2.3 Mechanical response of clay 19

2.4 Mechanical response of silt and fine grained tailings 23

2.5 Specimen reconstitution methods 26

2.5.1 Moist tamping 26
2.5.2 Air pluviation 27
2.5.3 Water pluviation 28
2.5.4 Slurry deposition method 29
2.5.5 Slurry consolidation method 30
2.5.6 Slurry displacement method 33
2.6 Influence of reconstitution method on shear response of soil 34
2.7 Uniformity of reconstituted specimens 39
2.8 Closure 41
Chapter 3: Materials Tested and Experimental Aspects 44
3.1 Materials tested 45
3.2 Triaxial apparatus 48
3.2.1 Loading system 49
3.2.2 Pore-water pressure and specimen volume measuring system 52
3.2.3 Data acquisition and control system 53
3.2.4 Specimen reconstitution method 55
3.2.4.1 UBC slurry consolidometer for triaxial testing 56
3.2.4.2 Silt pulverisation 59
3.2.4.3 Slurry preparation 59
3.2.4.4 Selection of a suitable slurry deposition technique 59
3.2.4.5 Slurry deposition 62

3.2.4.6 Slurry consolidation 65
3.2.4.7 Specimen homogeneity 67
3.2.4.8 Specimen geometry and strain uniformity 70
3.2.5 Assembly of triaxial test apparatus 71
3.2.6 Specimen saturation 75
3.2.7 Consolidation phase 76
3.2.8 Static shear bias phase 77
3.2.9 Undrained shear loading phase 77
3.2.9.1 Arrest of secondary consolidation 77
3.2.9.2 Monotonic shearing 78
3.2.9.3 Cyclic shearing 79
3.2.10 Post-cyclic reconsolidation 80
3.2.11 Error and uncertainty 80
3.3 Replication 82
3.4 Test program 85
Chapter 4: Experimental Results and Discussion 87
4.1 Monotonic undrained shear loading response 92
4.2 Monotonic drained shear loading response 96
4.3 Cyclic shear loading response 100
4.3.1 Effect of initial effective confining stress 100
4.3.1.1 General stress-strain and pore water pressure response 100

4.3.1.2 Cyclic shear resistance 105
4.3.2 Effect of initial static shear bias 109
4.3.2.1 General stress-strain and pore-water pressure response 109
4.3.2.2 Cyclic shear resistance 113
4.3.3 Comparison with typical cyclic response of sands 114
4.3.4 Post-cyclic reconsolidation 115
4.3.5 Error in pore water pressure measurement 117
Chapter 5: Summary and Conclusions 119
5.1 Upgrade of the UBC triaxial device 120
5.2 Development of specimen preparation methods 120
5.3 Undrained monotonic response of reconstituted Kamloops silt 121
5.4 Drained monotonic response of reconstituted Kamloops silt 122
5.5 Cyclic shear response of reconstituted Kamloops silt 122
5.6 Limitations and recommendations for future research 123
References 126
Appendices 136
Appendix A Rate of loading 136
A.1 Drained shear tests 136
A.2 Undrained triaxial tests 138
Appendix B Additional cyclic shear test results 140

List of Tables

Table 3.1 Summary of index parameters 46

Table 3.2 Composition of Kamloops silt 47

Table 3.3 X-ray diffraction of clay fraction of Kamloops silt only 47

Table 3.4 Capacity and resolution of sensors on the UBC-CTX device 53

Table 3.5 Test program 86

Table 4.1 Test parameters and summary results (Test Series I) 88

Table 4.2 Test parameters and summary results (Test Series II) 89

Table 4.3 Test parameters and summary results (Test Series III) 90

Table 4.4 Test parameters and summary results (Test series IV) 91

Table 4.5 Mobilised undrained shear strength at relatively large axial strain 93

List of Figures

Figure 2.1 Typical direct shear response of sands [Reproduced after Atkinson(1993)] 11

Figure 2.2 Characteristic triaxial undrained monotonic response of sands [reproduced after Kuerbis (1989)]..... 12

Figure 2.3 Typical "liquefaction" response during undrained cyclic loading. a) stress-strain response. b) stress path. c) shear strain development [reproduced after Vaid & Chern (1985)]..... 13

Figure 2.4 Typical "limited liquefaction due to cyclic loading" type of response during undrained cyclic loading. a) stress-strain response. b) stress path. c) shear strain development [reproduced after Vaid & Chern (1985)]. 14

Figure 2.5 Typical 'cyclic mobility' type of response during undrained cyclic loading. a) stress-strain response. b) stress path. c) shear strain development [reproduced after Vaid & Chern (1985)] 15

Figure 2.6 Typical loading conditions and laboratory simulation models..... 18

Figure 2.7 Cyclic stress ratios required to cause some failure criteria versus number of uniform cycles at a frequency of 1Hz in different clays [reproduced after Idriss & Boulanger (2008)]..... 21

Figure 2.8 Effective stress paths for undrained tests with monotonic and cyclic loading [reproduced after Andersen(2009)] 22

Figure 3.1 Particle size distribution of tested Kamloops silt 46

Figure 3.2 General arrangement of UBC cyclic triaxial apparatus..... 49

Figure 3.3 Schematic diagram rolling diaphragm double acting piston 51

Figure 3.4 General arrangement of data acquisition and control system (DACS) 54

Figure 3.5 General arrangement of UBC slurry consolidometer..... 58

Figure 3.6 Trial slurry pouring techniques 61

Figure 3.7 The main steps of the slurry deposition process..... 64

Figure 3.8 Typical slurry consolidation curves over a 24-hr period..... 66

Figure 3.9 Specimen uniformity – particle size analysis 67

Figure 3.10 Water content variation at end of undrained monotonic shear tests.. 69

Figure 3.11 Specimen diameter following removal of vacuum split mold..... 70

Figure 3.12 Schematic diagram of specimen preparation process..... 73

Figure 3.13 Repeatability of the slurry deposited Kamloops silt –monotonic shear 83

Figure 3.14 Repeatability of the slurry deposited Kamloops silt –cyclic shear.... 84

Figure 4.1 Undrained monotonic TC and TE testing on reconstituted specimens of Kamloops silt at varying confining stress levels: Stress-strain curves; $\sigma'3c \sim$ 100, 200 and 300kPa. 94

Figure 4.2 Undrained monotonic TC and TE testing on reconstituted specimens of Kamloops silt at varying confining stress levels: Stress path curves; $\sigma'3c \sim$ 100, 200 and 300kPa. 95

Figure 4.3 Undrained monotonic TC and TE testing on reconstituted specimens of Kamloops silt at varying confining stress levels: Normalized stress path curves; $\sigma'3c \sim$ 100, 200 and 300kPa. 95

Figure 4.4 Drained monotonic TC testing on reconstituted specimens of Kamloops silt at varying confining stress levels: Stress-strain curves; $\sigma'3c \sim$ 100, 200 and 300kPa 98

Figure 4.5 Drained monotonic TC testing on reconstituted specimens of Kamloops silt at varying confining stress levels: Volumetric strain curves; $\sigma'3c \sim$ 100, 200 and 300kPa 98

Figure 4.6 Drained monotonic TC testing on reconstituted specimens of Kamloops silt at varying confining stress levels: Stress path curves; $\sigma'3c \sim$ 100, 200 and 300kPa. (Undrained response superimposed). ... 99

Figure 4.7 Drained monotonic TC testing on reconstituted specimens of Kamloops silt at varying confining stress levels: Normalized stress path curves; $\sigma'3c \sim$ 100, 200 and 300kPa. 99

Figure 4.8 Undrained triaxial cyclic shear test on reconstituted specimen of Kamloops silt: Applied single amplitude deviator stress ($qcyc$) vs. number of loading cycles for different CSR values; $\sigma'3c \sim$ 100; Kc=1.0. 103

Figure 4.9 Undrained triaxial cyclic shear test on reconstituted specimen of Kamloops silt: Excess pore water pressure ratio (ru) vs. number of loading cycles for different CSR values; $\sigma'3c \sim 100$; Kc=1.0. 103

Figure 4.10 Undrained triaxial cyclic shear test on reconstituted specimen of Kamloops silt: axial strain (εa) vs. number of loading cycles for different CSR values; $\sigma'3c \sim 100$; Kc=1.0. 104

Figure 4.11 Undrained triaxial cyclic shear test on reconstituted specimen of Kamloops silt: Stress-strain and stress path curves; $\sigma'3c \sim$ 100kPa; CSR = 0.150; Kc=1.0. 104

Figure 4.12 Undrained triaxial cyclic shear test on reconstituted specimen of Kamloops silt: Stress-strain and stress path curves; $\sigma'3c \sim$ 100kPa; CSR = 0.180; Kc=1.0. 105

Figure 4.13 Undrained triaxial cyclic shear test on reconstituted specimen of Kamloops silt: Stress-strain and stress path curves; $\sigma'3c \sim$ 100kPa; CSR = 0.210; Kc=1.0. 105

Figure 4.14 Cyclic resistance ratio from undrained cyclic triaxial tests on reconstituted specimens of Kamloops silt at varying initial effective confining stress levels; Kc = 1.0. 107

Figure 4.15 Cyclic strength ratio ($qcyc/su$) from undrained cyclic triaxial tests on reconstituted specimens of Kamloops silt at varying initial confining stress levels. 108

Figure 4.16 Undrained triaxial cyclic shear test on reconstituted specimen of Kamloops silt: Applied single amplitude deviator stress ($qcyc$) vs. number of loading cycles for different Kc values; $\sigma'3c \sim 100$; CSR = 0.21. 110

Figure 4.17 Undrained triaxial cyclic shear test on reconstituted specimen of Kamloops silt: Excess pore water pressure ratio (ru) vs. number of loading cycles for different Kc values; $\sigma'3c \sim 100$; CSR = 0.21. 111

Figure 4.18 Undrained triaxial cyclic shear test on reconstituted specimen of Kamloops silt: axial strain (εa) vs. number of loading cycles for different Kc values; $\sigma'3c \sim 100$; CSR = 0.21. 111

Figure 4.19 Undrained triaxial cyclic shear test on reconstituted specimen of Kamloops silt: Stress-strain and stress path curves; $\sigma'3c \sim$ 100kPa; CSR = 0.210; Kc=1.0. 112

Figure 4.20 Undrained triaxial cyclic shear test on reconstituted specimen of Kamloops silt: Stress-strain and stress path curves; $\sigma'3c \sim$ 100kPa; CSR = 0.210; Kc=1.2. 112

Figure 4.21 Undrained triaxial cyclic shear test on reconstituted specimen of Kamloops silt: Stress-strain and stress path curves; $\sigma'3c \sim$ 100kPa; CSR = 0.210; Kc=1.4. 113

Figure 4.22 Cyclic resistance ratio from constant volume cyclic DSS tests on reconstituted specimens of Kamloops silt at varying initial static shear bias (Kc) levels; $\sigma'3c \sim 100$. 114

Figure 4.23 Typical post cyclic volumetric strain ($\varepsilon v - pc$) versus time characteristics of reconstituted Kamloops silt during post cyclic consolidation (Test Series III) 116

Figure 4.24 Post cyclic volumetric strain ($\varepsilon v - pc$) versus excess pore water pressure ratio (ru) of reconstituted Kamloops (Test Series III) and normally consolidated Fraser River Silt (Sanin, 2010). 117

Figure A.1 Estimation of t_{100} from typical consolidation curve.....134

Figure B.1 Undrained triaxial cyclic shear test on reconstituted specimen of Kamloops silt: Applied single amplitude deviator stress (q_{cyc}) vs. number of loading cycles for different CSR values; $\sigma'_{3c} \sim 200$; K_c=1.0.....140

Figure B.2 Undrained triaxial cyclic shear test on reconstituted specimen of Kamloops silt: Excess pore water pressure ratio (r_u) vs. number of loading cycles for different CSR values; $\sigma'_{3c} \sim 200$; K_c=1.0.....140

Figure B.3 Undrained triaxial cyclic shear test on reconstituted specimen of Kamloops silt: Axial strain (ε_a) vs. number of loading cycles for different CSR values; $\sigma'_{3c} \sim 200$; K_c=1.0.....141

Figure B.4 Undrained triaxial cyclic shear test on reconstituted specimen of Kamloops silt: Stress-strain and stress path curves; $\boldsymbol{\sigma'_{3c}}$ ~ 200kPa; CSR = 0.130; $\mathbf{K_c}$=1.0.....141

Figure B.5 Undrained triaxial cyclic shear test on reconstituted specimen of Kamloops silt: Stress-strain and stress path curves; σ'_{3c} ~ 200kPa; CSR = 0.190; K_c=1.0.....142

Figure B.6 Undrained triaxial cyclic shear test on reconstituted specimen of Kamloops silt: Stress-strain and stress path curves; σ'_{3c} ~ 200kPa; CSR = 0.230; K_c=1.0.....142

Figure B.7 Undrained triaxial cyclic shear test on reconstituted specimen of Kamloops silt: Applied single amplitude deviator stress (q_{cyc}) vs. number of loading cycles for different CSR values; σ'_{3c} ~ 300; K_c=1.0.....143

Figure B.8 Undrained triaxial cyclic shear test on reconstituted specimen of Kamloops silt: Excess pore water pressure ratio (r_u) vs. number of loading cycles for different CSR values; σ'_{3c} ~ 300; K_c=1.0.....143

Figure B.9 Undrained triaxial cyclic shear test on reconstituted specimen of Kamloops silt: Axial strain (ε_a) vs. number of loading cycles for different CSR values; σ'_{3c} ~ 300; K_c=1.0.....144

Figure B.10 Undrained triaxial cyclic shear test on reconstituted specimen of Kamloops silt: Stress-strain and stress path curves; σ'_{3c} ~ 300kPa; CSR = 0.120; K_c=1.0.....144

Figure B.11 Undrained triaxial cyclic shear test on reconstituted specimen of Kamloops silt: Stress-strain and stress path curves; $\boldsymbol{\sigma'_{3c}}$ ~ 300kPa; CSR = 0.155; $\mathbf{K_c}$=1.0.....145

Figure B.12 Undrained triaxial cyclic shear test on reconstituted specimen of Kamloops silt: Stress-strain and stress path curves; σ'_{3c} ~ 300kPa; CSR = 0.185; K_c=1.0.....145

List of Symbols

K_c	effective consolidation stress ratio
k	hydraulic conductivity (m/s)
N_{cyc}	number of shear stress cycles to reach a certain failure condition
q_{cyc}	single amplitude cyclic deviator stress (kPa)
r_u	excess pore water pressure ratio
r_{u-av}	average excess pore water pressure ratio
s_u	undrained shear strength (kPa)
s_{u-mob}	mobilised undrained shear strength measured from triaxial tests (kPa)
u	pore water pressure (kPa)
α	initial static shear bias on DSS apparatus
ε_a	axial strain (%)
ε_v	volumetric strain (%)
ε_{v-pc}	post cyclic reconsolidation volumetric strain (%)
σ_3	cell pressure (kPa)
σ'_1	major effective principle stress (kPa)
σ'_3	minor effective principle stress (kPa)
σ_d	deviator stress (kPa)
σ_v	vertical stress (kPa)

σ_{3c}	cell pressure (kPa)
σ'_{3c}	initial effective confining stress level (kPa)
ϕ_{MO}	friction angle at maximum obliquity (^{o})
ϕ_{PT}	friction angle at phase transformation state (^{o})
ϕ_{SS}	friction angle at steady state (^{o})
Δu	excess pore water pressure (kPa)
τ_{stat}	initial static shear stress on DSS apparatus (kPa)
σ'_{v}	initial effective vertical consolidation stress (kPa)
σ'_{vc}	initial effective vertical stress on DSS apparatus (kPa)

List of Abbreviations

CDSS	cyclic direct simple shear
CPT	cell pressure transducer
CSR	cyclic stress ratio
CTX	cyclic triaxial
DACS	data acquisition and control system
DPWPT	differential pore water pressure transducer
DSS	direct simple shear
EPR	electro-pneumatic regulator
FG	function generator
LC	load cell
LVDT	linear variable differential transformer
PI	plasticity index
PWPT	pore water pressure transducer
SCT	slurry consolidation device for triaxial testing
SHANSEP	stress history and normalised soil engineering properties
TC	triaxial compression
TE	triaxial extension
TSC	triaxial slurry consolidation
QSS	quasi-steady state

Acknowledgements

Many people contributed in some way to the culmination of this thesis. I would like to express my sincere appreciation to those who supported me throughout this process. Without their assistance this research would not have been possible.

First, I wish to express my most sincere gratitude to my research supervisor, Dr. Dharma Wijewickreme, for his constant guidance and encouragement throughout this journey. His experience, knowledge and positive attitude made possible the culmination of this work. His friendship and unconditional support made the path easier and enjoyable.

I also wish to thank the members of the faculty, Dr. John Howie and Dr. Yogi Vaid for their constructive comments and encouragement. Their lessons, input and support during the preparation of my thesis and during my years at UBC are deeply appreciated.

Financial support provided by the National Research Council of Canada (NSERC), the University of British Columbia is deeply appreciated. Without this funding, this research would not have been possible.

I would also like to extend my gratitude to Bruce Bosdet of Golder Associates in Kamloops for his generous input and help with the collection of samples from Kamloops.

I am grateful to my colleagues at the geotechnical group for interesting, critical and enjoyable conversations regarding this research, laboratory techniques and extracurricular activities. Technical assistance of Harald Schremp, Bill Leung, Scott Jackson of the Department of Civil Engineering Workshop during development of the test equipment is also acknowledged with deep regard.

This thesis is dedicated to

All of the lives affected by strong motion earthquakes

Chapter 1: Introduction

1.1 Background

Fine-grained silty soils with high levels of saturation are commonly found both as natural soil deposits and man-made waste product in mine tailings derived from the processing of ore in the mining industry. Evidence of ground failure in fine-grained soils during strong motion earthquakes has suggested that certain saturated low plastic fine-grained soils can be susceptible to earthquake-induced softening and potential strength reduction. Although wide-ranging studies have been undertaken to understand the performance of sands over the past 40 years, the available published information on the undrained shear response of fine-grained soils with respect to cyclic loading is limited. In particular, there is a need for understanding the response of silts in a more fundamental manner and laboratory testing plays an important role in this regard.

In addition to the shear deformations associated with loss of stiffness and/or strength in some situations, another key mechanism of earthquake induced deformations is the overall volume changes in the soil mass that take place due to the dissipation of shear-induced excess pore water pressures. These volume changes manifest in the field as post-liquefaction settlements, and they may occur both during and after earthquake shaking. Recent evidence of ground failure

during strong earthquakes has indicated that certain saturated fine-grained soils can be susceptible to earthquake-induced softening and strength reduction, in turn, leading to post-cyclic settlements, foundation sliding, tilting and collapsing of structures.

The response of a given soil to monotonic and cyclic loading is controlled by many parameters such as packing density, microstructure, fabric, level/duration of cyclic loading, confining stress, initial static bias, etc. These parameters have been noted to primarily govern the development of excess pore water pressures, stiffness, and strength in a soil mass, in turn, controlling the overall shear response. While cyclic shear tests are valuable in assessing the performance of soils under seismic loading conditions, data from monotonic shear tests have often provided insight into the fundamental soil behavior and assisted interpretation of the behavioral patterns observed in cyclic shear tests.

Due to the difficulties associated with field sampling as well as the need to obtain systematic data sets for the development of meaningful soil behaviour frameworks, most of the laboratory research on low plastic fine grained soils has been conducted using reconstituted soil specimens. While the possibility of obtaining reasonably undisturbed samples of certain low-plastic silts have been already demonstrated, in general, it is fair to state that the development of mechanical behavior of a given soil type is best examined in the laboratory by

element testing of repeatable and homogenous test specimens. One of the ways in which this could be achieved is through specimen reconstitution. Having said this, the influence of specimen reconstitution technique can have a profound influence on the observed soil behavior, and the differences have been found to be due to fabric and microstructure.

1.2 Objectives

With the above background, the main goal of this study was to develop a triaxial device and suitable silt reconstitution technique to enable cyclic shear testing of reconstituted silts at the University of British Columbia (UBC). Once developed, the UBC cyclic triaxial (CTX) device was used to investigate the mechanical response of reconstituted silts and included the following components:

- Drained monotonic shear response in triaxial compression;
- Undrained monotonic shear response in triaxial compression and extension;
- Undrained cyclic shear response;
- Effect of initial effective confining stress on the monotonic and cyclic shear loading response;
- Effect of static shear bias on the cyclic shear loading response; and

- Post-cyclic re-consolidation response due to dissipation of pore water pressures.

1.3 Organisation

The thesis is organised into five Chapters. Chapter 1 introduces the thesis topic of shear loading response of fine-grained materials, and a high-level basis of the thesis objectives, followed by identification of those objectives. A detailed survey of literature on the shear response of soils and assessment of both fine and coarse grained material and different silt reconstitution techniques is summarised in Chapter 2, thus presenting the rationale for this thesis. A detailed description of the test apparatus, test material, testing procedures and an outline of the test program is presented in Chapter 3.

Results obtained from the test program conducted under this study are explained in Chapter 4. This includes the findings of monotonic shear, cyclic shear and post cyclic response of tested silts.

Chapter 5 presents the summary of findings and main conclusions arising from this study. This is followed by the list of references, and appendices containing: relevant calculations, additional test results, and discussions not include in the main body of the thesis.

Chapter 2: Literature Review

2.1 General

A proper understanding of the monotonic and cyclic shear response of soils is an important consideration in the solution of geotechnical engineering problems. In this regard, laboratory element testing that can mimic field loading conditions plays an important role in understanding and characterising basic soil behaviour.

Fine-grained silty soils with high levels of saturation are common in most earth-quake prone areas. Recent evidence of ground failure during strong motion earthquakes has indicated certain saturated fine-grained soils can be susceptible to earthquake-induced softening and strength reduction, in turn, leading to post-cyclic settlements, foundation sliding, tiling and collapsing of structures. Although there are major advances in the understanding of shear response of sands and clays, our understanding of the mechanical response of silts is still very limited and there is still no standard procedure to assess the potential for cyclic softening/liquefaction. As such, there is a strong need to characterize the shear behaviour of fine grained silty soils using laboratory element testing methods.

Testing of homogeneous (uniform) specimens under uniform states of stress and strain is required for fundamental laboratory element studies of soil property characterization. The use of uniform specimens yielding repeatable test results has

resulted in the use of reconstituted soils in preference to natural materials for fundamental investigations of soil behaviour. Kuerbis & Vaid (1988) identified the following criteria to define specimen uniformity: 1) specimens should achieve target densities expected within an in situ soil deposit; 2) there should be uniform void ratio throughout the specimen; 3) specimens should be fully saturated; and 4) specimens should not display particle size segregation, regardless of particle size distribution or fines content. These criteria will be used in subsequent sections of this thesis as a qualitative measurement of specimen uniformity.

In addition to specimen uniformity and test repeatability, it is also important that under a given initial state (void ratio and effective stress), the selected specimen preparation method should simulate the in situ deposition process of the type of soil type. This is because soil behaviour is known to be profoundly influenced by the specimen reconstitution method (Ladd, 1974; Mulilis et al., 1977; Miura & Toki, 1982; Vaid & Negussey, 1984; Kuerbis & Vaid, 1988; Vaid et al., 1999).

With the above in mind, this thesis presents a silt reconstitution method that was developed at UBC. This technique was then used to obtain some initial experimental observations on low plastic silt. In order to provide the required background and rationale for the work proposed in this thesis, this chapter presents a review of literature on laboratory observations with particular reference made to the fundamental shear response of soils and the different specimen

reconstitution methods available for laboratory element testing. Section 2.2 provides a brief outline of the mechanical response of sand emphasising the monotonic and cyclic loading response. In Sections 2.3 and 2.4, past work on the shear loading response of clay and silts are summarised respectively. A detailed treatment of aspects related to different specimen reconstitution methods is provided in Sections 2.5, 2.6 and 2.7.

2.2 Mechanical response of sand

It has been well established that initial state variables, relative density and confining stress are two important factors that govern the shear response of sands. As such, a combination of void ratio and confining stress has been adopted in critical state soil mechanics to characterise sand behavior (Schofield & Wroth, 1968; Atkinson, 1993). Based on the combination of the prevalent confining stress and void ratio, a dilative response (tendency for volume increase) or a contractive response (tendency for volume decrease) may occur during shear loading of a given sand specimen.

The monotonic and cyclic shear response of sands have been widely studied by researchers such as; Castro (1969); Lee & Seed (1967); Seed & Lee (1967); Finn et al. (1970); Ishihara et al. (1975); Seed et al. (1975); Vaid & Finn (1979); Ishihara & Yamazaki (1980); Vaid & Chern (1985); Ishihara (1993); Boulanger & Seed (1995); Vaid & Thomas (1995); Yamamuro & Lade (1997); Vaid et al.

(2001); Sriskandakumar (2004). The typical behaviour of sand under direct shear is shown below in Figure 2.1. Two typical stress-strain curves exist; "looser" side of critical (loose sands) and "denser" side of critical (dense sands). During shear, soils on the looser side of critical typically exhibit a tendency to contract (reduce volume) while soils the denser side typically dilate (expand) after a small amount of contraction. Both ultimately reach states at which the shear stress is constant and there are no more volumetric strains. Soils on the denser side reach peak shear stresses before reaching the ultimate state.

The typical response of sand to monotonic undrained triaxial compression loading is shown in Figure 2.2 and show three characteristic behavior types:

- Type 1 response; there is an initial increase in stress ratio, defined as the ratio of major effective principal stress (σ'_1) to minor effective principal stress (σ'_3), or simply (σ'_1/σ'_3) with increase in axial strain (strain hardening). After reaching a peak value of σ'_1/σ'_3 at relatively small strains (generally <1%) this is then followed by a significant reduction of σ'_1/σ'_3, (strain softening) , until a steady state condition of constant σ'_1/σ'_3 with increase in axial strain is reached. The initial mobilised peak strength at relatively small strain followed by strain softening is identified as a brittle type response. The deformation at constant σ'_1/σ'_3 has been termed 'steady state liquefaction' by Vaid & Chern (1985). In the effective

stress path space, the soil experiences contractive type behaviour at all strain levels.

- Type 2 response; similar to Type 1 response, except at some point following the initial peak σ'_1/σ'_3, a phenomenon known as phase transformation occurs. This is where the sand response transitions from dilative to contractive type behaviour and starts to exhibit a strain hardening. This type of response has been referred by as 'limited liquefaction' by Castro (1969). The point at which phase transformation and subsequent strain hardening occurs has been identified as quasi-steady state (QSS) by Ishihara et al. (1975).
- Type 3 response; the sand exhibits a strain hardening type behaviour with no initial brittle type response. The effective stress path response is similar to Type 2, except the contractive behaviour occurs to a lesser degree and a significantly higher shear stress is observed.

The friction angle at phase transformation (ϕ_{PT}) which is observed in Type II and Type III sand behaviour has been shown to be unique for a given sand and is equal to the friction angle mobilised at steady state (Vaid & Chern, 1985). Results of large displacement ring shear test indicate that the value of ϕ_{PT} is equal to the constant-volume friction angle (ϕ_{CV}) (Wijewickreme, 1986; Negussey et al., 1986).

The resistance of sand to cyclic loading, simulating liquefaction type behaviour, has been studied using undrained cyclic shear loading tests such as the cyclic triaxial (CTX) and constant-volume cyclic direct simple shear (CDSS) tests. Under cyclic loading, similar to undrained monotonic shear responses, three typical cyclic shear behaviours are observed, they are; liquefaction, limited liquefaction and cyclic mobility (Castro, 1969; Vaid & Chern, 1985). A schematic representation of the stress-strain response and stress-path response of each of these behavioral types is presented in Figure 2.3, Figure 2.4 and Figure 2.5. The limited liquefaction type response is similar to the Type 1 monotonic response where the sand exhibits a contractive behaviour with increase in number of cycles until a point is reached at relatively low strain level where there is complete loss of strength and steady state is reached. In the limited liquefaction type response, the sand is also seen to experience an initially contractive behaviour, except a dilative response is seen to occur after σ'_1/σ'_3 reaches QSS during the loading phase of shear. Following this, large cyclic strains develop and the sand experiences excursions through states of transient zero effective stress followed by momentary gain in strength during the loading phase. This is accompanied by a significant amount of excess pore water pressure generation. In the cyclic mobility type response, strain development, excess pore water pressure buildup and strength loss is gradual with increasing number of cycles.

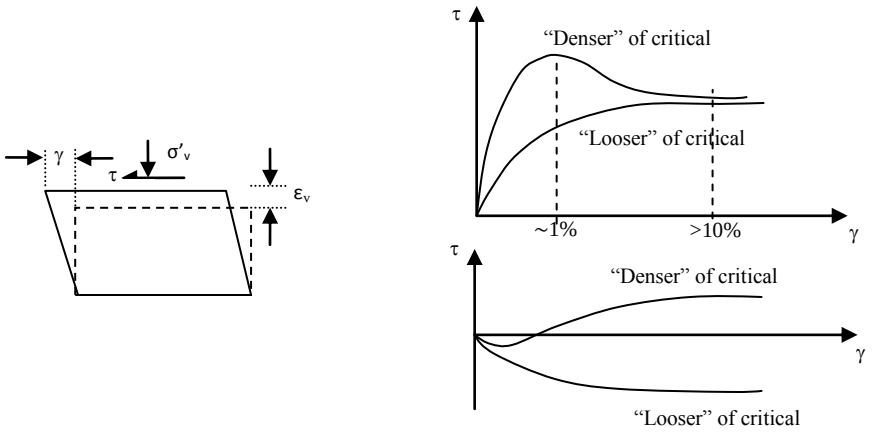

Figure 2.1 Typical direct shear response of sands [reproduced after Atkinson (1993)]

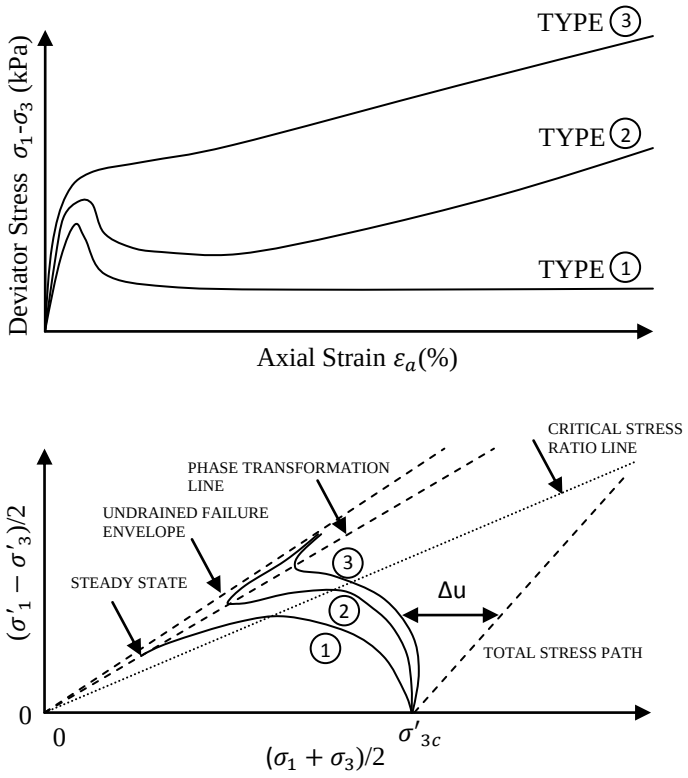

Figure 2.2 Characteristic triaxial undrained monotonic response of sands [reproduced after Kuerbis (1989)]

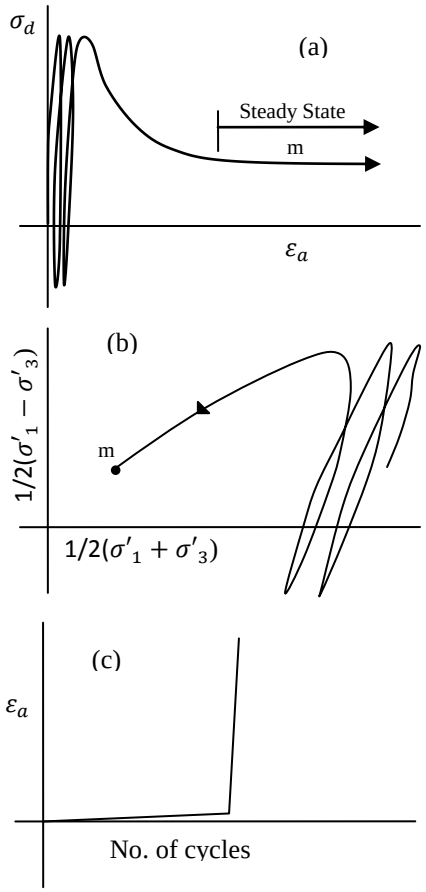

Figure 2.3 Typical "liquefaction" response during undrained cyclic loading. a) stress-strain response. b) stress path. c) shear strain development [reproduced after Vaid & Chern (1985)]

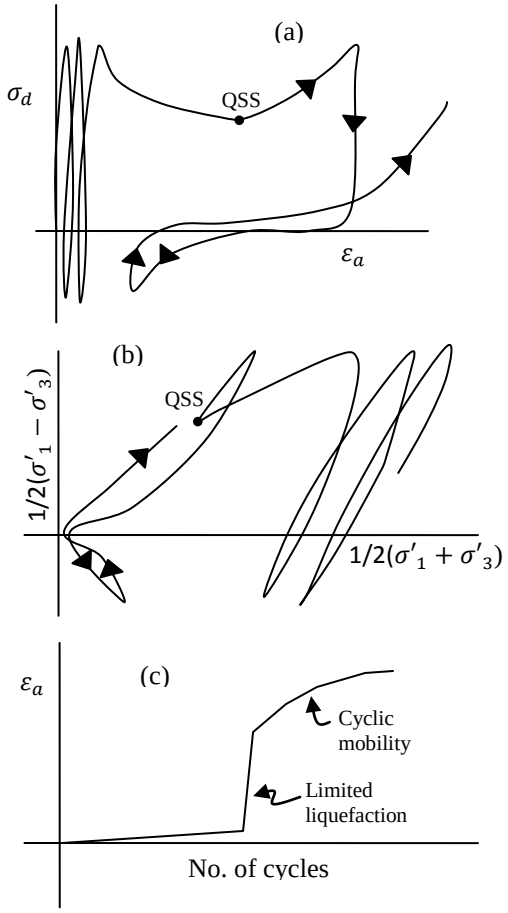

Figure 2.4 Typical "limited liquefaction due to cyclic loading" type of response during undrained cyclic loading. a) stress-strain response. b) stress path. c) shear strain development [reproduced after Vaid & Chern (1985)]

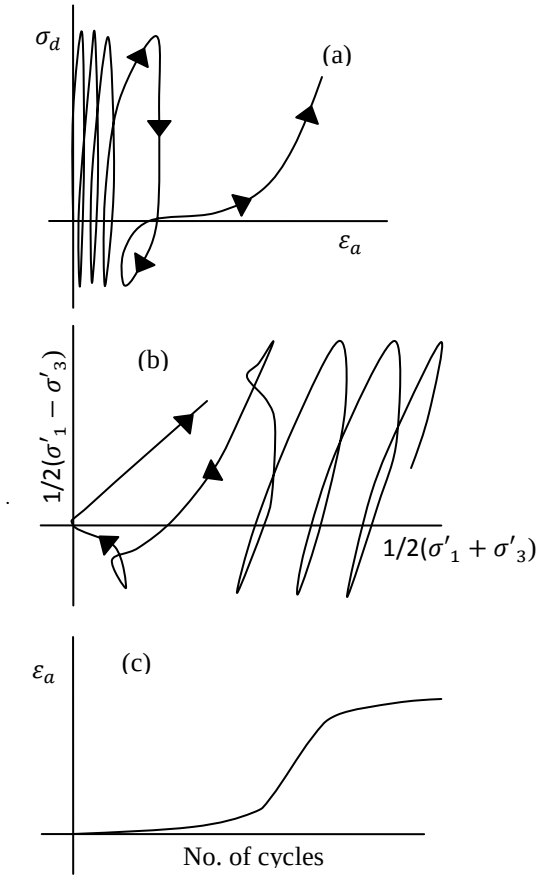

Figure 2.5 Typical "cyclic mobility" type of response during undrained cyclic loading. a) stress-strain response. b) stress path. c) shear strain development [reproduced after Vaid & Chern (1985)]

In liquefaction assessment, the effects of sloping ground can be simulated in laboratory testing by applying an initial static shear stress after consolidation and just before cyclic loading. These types of tests are typically referred to as cyclic shear tests with initial static shear (stress) bias. The influence of initial static shear bias can be assessed using both the constant volume CDSS and CTX devices. In the CDSS device, the level of initial static shear is characterized by the static shear stress ratio (α), defined as the ratio of initial shear stress on the horizontal plane (τ_{stat}) to the initial vertical effective consolidation stress (σ'_{vc}) or simply (τ_{stat}/σ'_{vc}). In the CTX device, the level of initial static shear is characterized by an initial anisotropic consolidation stress ratio (K_c), defined as the ratio of major effective principal stress (σ'_1) to minor effective principal stress (σ'_3) or simply (σ'_1/σ'_3). Figure 2.6 schematically shows typical field conditions and laboratory element test models to simulate these types of conditions.

It has been found that the presence of an initial static shear bias has a major influence on the cyclic resistance of sands, although the findings have not always been in agreement. While some researchers have found that the presence of initial static shear increases the cyclic resistance to liquefaction (Lee & Seed, 1967; Seed et al., 1975), others have observed that the increase in static shear stress would decrease the cyclic resistance to liquefaction (Castro, 1969; Vaid & Finn, 1979; Vaid & Chern, 1985). Furthermore, Vaid et al. (2001) and Sriskandakumar

(2004) have found that the effect of static shear stress on the cyclic resistance of sands is influenced by the initial density. The presence of an initial static shear has been found to result in a reduction in cyclic resistance for loose sands and an increase in cyclic resistance for dense sands.

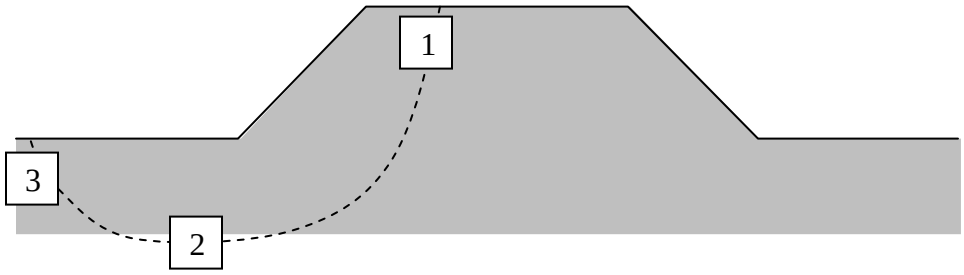

Embankment or sloping ground

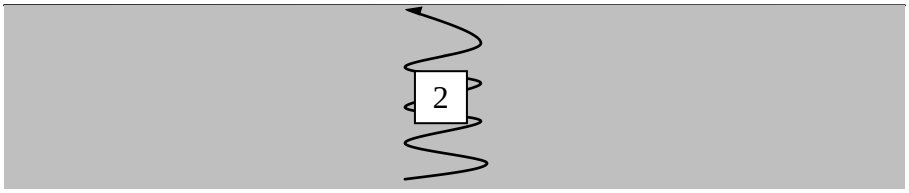

Vertically propagating shear wave – level ground

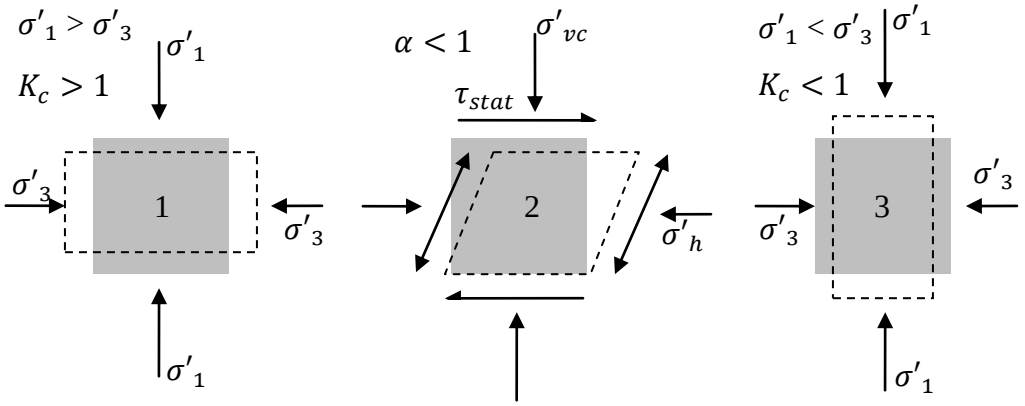

Triaxial Compression Direct Simple Shear Triaxial Extension

Figure 2.6 Typical loading conditions and laboratory simulation models

2.3 Mechanical response of clay

The mechanical response of fine-grained materials such as silty and clayey soils has been found to be different to that of sands. Ladd (1964) noted that the undrained shear strength (s_u) of fine grained soils can be characterized by normalizing with respect to σ'_{vc}. This is known as the Stress History and Normalized Soil Engineering Properties or SHANSEP approach which has been widely used for characterizing fine-grained soils in engineering practice. For example, identical stress-path characteristics can be observed for normally consolidated clay when stresses are divided by the initial effective confining stress.

Ground failures in deposits of clays have been observed during earthquakes but are less common than in saturated sands. Zergoun & Vaid (1994) investigated the cyclic response of natural Cloverdale clay with slow (low frequency) undrained triaxial cyclic load testing. Cyclic loading has been found to cause a progressive increase in excess pore water pressure accompanied by increasing strains potentially leading to significant ground deformation during an earthquake. This type of behaviour is called “cyclic softening” which is different to the term liquefaction used for cyclic loading response in saturated sands. The cyclic strength of clays has been generally expressed as a relatively unique function of monotonic shear strength (Idriss & Boulanger, 2008) as shown in Figure 2.7 .

Consequences of cyclic softening in clays depend on the soils sensitivity (defined as ratio of intact s_u to remoulded s_u. Soft, normally consolidated clays with generally large water contents will have higher sensitivity and will be most prone to loss of strength during earthquake loading compared to those of stiff overconsolidated clays. Anderson (2009) compared the effective stress paths of undrained monotonic and cyclic shear testing carried out on Drammen clay (Figure 2.8). He suggested soil structure would break down during cyclic shear loading causing a contractive tendency in the clay material and result in significant increase in excess pore water pressure as the clay reaches the monotonic undrained failure envelope.

The effects of strain rate development during cyclic shear testing have been investigated by Zergoun & Vaid (1994) and Lefebvre & Pfendler (1996) through constant volume CDSS tests on Cloverdale clay and St. Lawrence clay respectively. The influence of the loading rate was illustrated by the observation that the cyclic shear stresses required for failure in one cycle exceeded the undrained shear strength observed under relatively slow conventional monotonic loading rates.

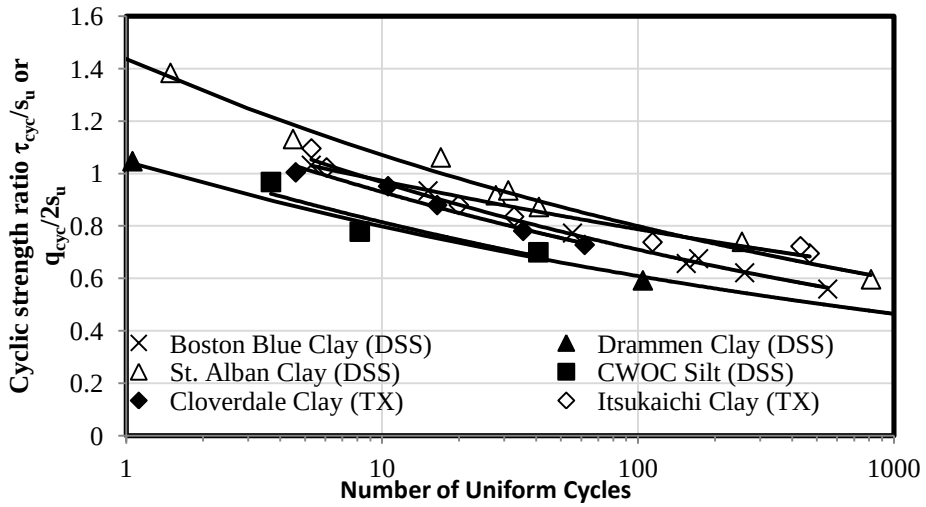

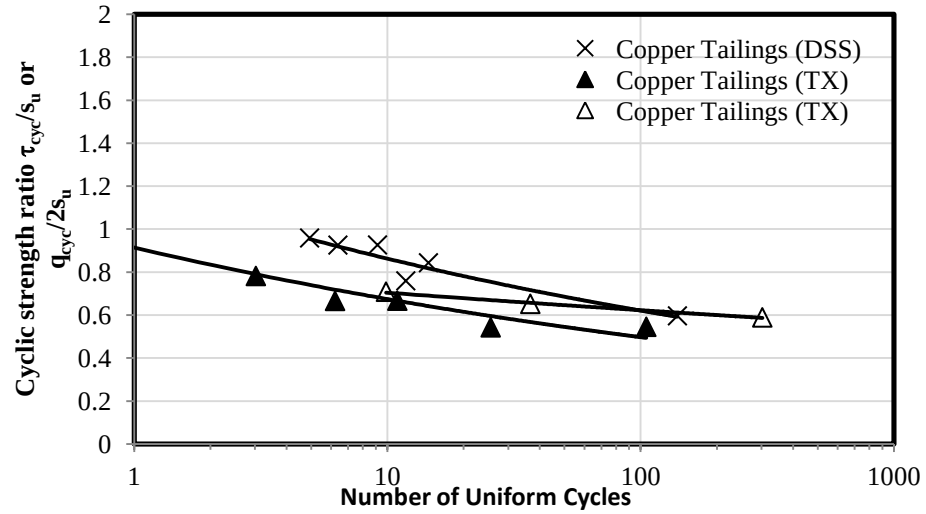

Figure 2.7 Cyclic stress ratios required to cause some failure criteria versus number of uniform cycles at a frequency of 1Hz in different clays [reproduced after Idriss & Boulanger (2008)]

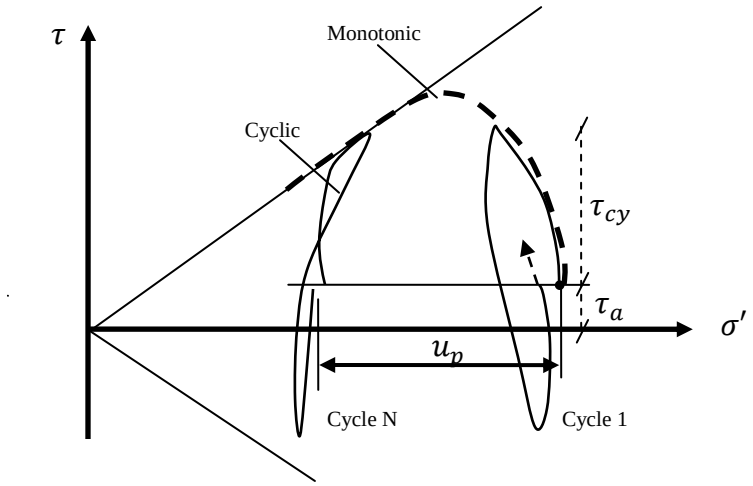

Figure 2.8 Effective stress paths for undrained tests with monotonic and cyclic loading [reproduced after Andersen (2009)]

u_p = permanent pore-pressure component; σ' = effective normal stress; τ = shear stress; τ_a = average shear stress; τ_{cy} = single-amplitude cyclic shear stress

2.4 Mechanical response of silt and fine grained tailings

A number of researchers have carried out laboratory experimental research looking at the shear response of silts (El Hosri et al., 1984; Puri, 1990; Prakash & Sandoval, 1992; Guo & Prakash, 1999; Høeg et al., 2000; Bray & Sancio, 2006; Hyde et al., 2006; Sanin & Wijewickreme, 2006; Donahue et al., 2007; Sanin, 2010; Soysa, 2015). It is also of relevance to note that significant laboratory research has been undertaken to study the mechanical response of fine-grained tailings (Ishihara et al., 1980; Troncoso, 1986; Wijewickreme et al., 2005; Kim et al. 2011; Geremew & Yanful, 2011; Seidalinova, 2014).

Experimental observations of silt during cyclic shear loading (Guo & Prakash, 1999; Prakash & Sandoval, 1992; Sanin & Wijewickreme, 2006; Bray & Sancio; 2006) suggest silts develop a gradual 'cyclic mobility type' strain development, accompanied by gradual increase in excess pore water pressure (Δu) becoming equal or close to the initial effective confining pressure. Sanin (2010) and Soysa (2015) reported that the cyclic resistance of undisturbed and reconstituted, relatively young, channel-fill Fraser River silt is relatively insensitive to confining stress. Sanin (2010) also noted that an increase of initial static shear (α) generally increased the cyclic resistance of this soil.

When the applied CSR in a laboratory test is plotted against the number of cycles to reach a certain condition of failure (N_{cyc}) on a linear-logarithmic type graph, a relationship between the two can be developed. Such relationships have been derived by Donahue et al. (2007); Guo & Prakash (1999); Hyde et al. (2006); Sanin & Wijewickreme (2006); Sanin (2010) and Soysa (2015) with differing results. These differences are likely to be attributed to factors such as plasticity, fabric, microstructure and mineralogy. With regards to plasticity, there is currently no clear consensus on the effect it has on the monotonic and cyclic response of silts. The results of cyclic shear testing by Puri (1990) and Soysa (2010), on samples of reconstituted silt/clay mixtures and undisturbed Fraser River silts respectively, both indicate that an increase in plasticity index (PI) increases resistance against liquefaction. Conflicting observations have been made by El hosri et al. (1984) and Prakash & Sandoval (1992) on samples of low plastic silts, where a reduction in resistance to liquefaction has been observed with increase in PI up to a certain PI threshold level. Beyond this threshold level, the shear resistance is seen to increase with increase PI. In addition, Soysa (2015) observed a reduction in cyclic shear resistance with increase in coarse (sand) fraction as well as destructuration effects.

Høeg et al. (2000); Sanin & Wijewickreme (2006); Sanin (2010); and Soysa (2015) investigated the difference of shear response between undisturbed and

reconstituted specimens originating from natural soils. It was noted that the shear response of reconstituted specimens deviated from the response of undisturbed specimen and concluded that fabric/microstructure in natural specimens influence the cyclic shear resistance.

With regards to mine tailings, experimental observations by Ishihara et al. (1980); Troncoso et al. (1988) and Wijewickreme et al. (2005) suggests that such material experiences a gradual ‘cyclic mobility’ type response similar to that of natural silts. From the results of CTX testing performed on fine-grained tailings, Ishihara et al. (1980) observed that the cyclic shear resistance of fine-grained tailings are significantly influenced by plasticity.

Wijewickreme et al. (2005) conducted constant volume CDSS on various tailings material with varying results. For one particular type of tailings material, a greater cyclic resistance was observed with increase in confining stress, suggesting that that the contractive tendency due to increase in confining stress could be overridden by the dilative tendency arising due to stress densification. The cyclic shear resistance of other tailings materials, on the other hand, were observed to be insensitive to initial density condition and confining pressure.

With respect to static shear bias, Seidalinova (2014) conducted CDSS tests on fine-grained gold tailings and noted a reduction in cyclic shear resistance with increasing level of initial static shear bias.

2.5 Specimen reconstitution methods

2.5.1 Moist tamping

The oldest laboratory reconstitution technique is moist or dry tamping of soil in layers (Lambe, 1951). The moist tamping method best models the soil fabric of rolled construction fills, for which the method was originally designed.

The moist tamping method has been used by researchers to assess the shear response of both naturally occurring and engineered silts and sands (Ladd, 1974; Miura & Toki, 1982; Vaid et al, 1999; Høeg et al. 2000; Bradshaw & Baxter, 2007; Guo & Wang 2009). The main advantage of the moist tamping method is the ability to achieve a desired densities ranging from extremely loose to dense (Ladd, 1974; Mulilis et al. 1977; Miura & Toki, 1982; Kuerbis & Vaid, 1988; Bradshaw & Baxter, 2007). In liquefaction assessment, moist tamping has been shown to be able to produce a very loose soil specimen that is possible due to capillary effects between grains. This may unjustifiably condemn sand as potentially liquefiable (Vaid, et al, 1999).

It is also recognised that specimens prepared using this method requires subsequent saturation, removing the capillary tension between soil particles and possibly altering the soil fabric, reducing density and inducing particle size segregation (Kuerbis & Vaid, 1988; Høeg at al., 2000). In addition, specimens

prepared using such a method have been found to be less uniform than those prepared using the water pluviation method (Mululis et al., 1977; Vaid et al., 1999).

Bradshaw & Baxter (2007) acknowledged the difficulties associated with specimen non-uniformity and developed the modified moist tamping method, for preparation of low plastic silt specimens. This method allows for target densities to be achieved while ensuring uniformity in density by applying a specified amount of tamping energy to each layer. A relationship between dry density and hammer drop height was established and a uniform density along the length of the specimen was achieved by increasing the tamping effort as each layer was placed.

2.5.2 Air pluviation

The air pluviation technique is typically used for sands. The sand is deposited by pouring dry soil, either through a concentrated opening or raining from a surface which may cover the full cross sectional area of the specimen. The technique best simulates the natural deposition process of aeolian deposits, typically comprising of well sorted sands or well sorted silts (Kuerbis & Vaid, 1988). In liquefaction assessment, this technique has been used to conduct constant volume CDSS testing of sands whereby saturation of the specimen is not required (Sivathayalan & Ha, 2004; Wijewickreme et al, 2005).

The density of sand prepared by air pluviation may be controlled by drop height and rate of deposition. Miura & Toki, (1982) demonstrated that high densities could be achieved by air pluviation, with the density greatly affected by the rate of deposition. Vaid & Negussey (1984) observed the drop height to also be a major contributing factor to specimen density. Wijewickreme et al. (2005) noted that the as-placed densities increase with increasing fall height and decreasing flow rate.

Vaid & Negussey, (1984) indicated that preparation of uniform specimens using air pluviation is not as successful for well graded sands with such material being prone to particle size segregation. In triaxial testing, subsequent saturation is required which may possibly disrupt the initial sand fabric and produce segregation due to washing out of fines from the sample (Kuerbis & Vaid, 1988).

2.5.3 Water pluviation

The water pluviation technique has been used my many researchers in liquefaction assessment of sands (Vaid & Negussey, 1984). The technique typically involves raining a sample of saturated sand through de-aired water into a specimen split mold. In this method, specimens easily reach specimen saturation requirements during specimen preparation with the sand being deposited in a saturated state. This minimises the amount of disruption to soil fabric, otherwise

observed during the saturation process in air pluviation and moist tamping methods.

Oda et al. (1978) suggested that natural water pluviated soils have a similar fabric and behaviour to that of natural alluvial soils. Vaid, et al, (1999) reported similar undrained triaxial shear responses between a frozen undisturbed specimen and water pluviated sand specimens, providing further evidence to suggest that a similar fabric exists.

During water pluviation, specimens are initially prepared in a loose state. Soils are found to reach a terminal velocity in water within a short distance and as such the drop height and rate of deposition are not effective in influencing the density of the specimen (Vaid & Negussey, 1984). The density may be increased from the initial loose state by applying external vibrations to the specimen.

Specimen uniformity is easily achieved using the water pluviation method; however particle size segregation has been found to be a problem for well graded sands and silty sands.

2.5.4 Slurry deposition method

To overcome the inherent problems of particle segregation of well-graded or silty sand samples, Kuerbis & Vaid, (1988) developed a slurry deposition technique specifically for well graded sands and sands with fines. In this method, fine

grained material is added to water in a sedimentation cylinder. After the fine grained material is allowed to settle, sand is pluviated through water in the sedimentation cylinder. The silt/sand mixture is then thoroughly mixed in the sedimentation cylinder, ensuring no entrapped air, and the mixture is allowed to settle once again. The sedimentation cylinder is then carefully lowered into a vacuum split mold sitting directly on a triaxial base pedestal with an expanded membrane in place. The sedimentation cylinder is carefully removed leaving the deposited soil sitting inside the split mold ready for triaxial testing. Through a series of verification tests, this method has demonstrated very good specimen uniformity regardless of particle size distribution and fines content.

2.5.5 Slurry consolidation method

The slurry consolidation method is typically used to prepare saturated specimens of fine grained soil (Khalili & Wijewickreme, 2008). The slurry consolidation method is distinctly different to the slurry deposition method, described in the previous section, with the main difference being in the way that the slurry is consolidated. In the slurry deposition method, the slurry is predominantly a coarse grained material which, through water pluviation, can form a soil skeleton under its own weight in a relatively short period of time. This material can be readily densified by application of external vibration. In the slurry consolidation method, the slurry is predominantly a fine grained material which is difficult to density. As

such, this type of material requires an external vertical load to achieve K_o-consolidation to form a solid state. Like the slurry displacement method, a major benefit of the slurry consolidation method is that saturation is easily achieved during specimen preparation. Unlike the slurry deposition method, a major limitation of the preparation method is that densities of in-situ natural silts are not necessarily achieved.

The slurry consolidation method has been used by recent researchers such as Hyde et al. (2006); Bradshaw & Baxter (2007)' and Wang et al., (2011) to investigate the undrained monotonic and cyclic shear response of low plastic reconstituted silts. With clays, slurry consolidation is typically achieved through a large consolidometer, where multiple specimens may be prepared from one batch. With low plastic silts, specimen preparation using such a method is difficult due to disturbance (Hyde et al., 2006). An alternative method has been to consolidate the specimen inside a split mold directly on the triaxial base pedestal, minimising specimen disturbance. However with this method, individually prepared specimens require verification testing to demonstrate uniformity and test repeatability.

Hyde et al. (2006) investigated the undrained monotonic shear response of low plastic silts, manufactured from powdered limestone". Specimens were prepared using a "one-dimensional (ID) preconsolidation" method and "sedimentation"

method. In the "1D pre-consolidation" method, the slurry was initially consolidated to a maximum vertical stress of 80kPa in a steel cylinder with dimensions slightly larger than the final trimmed triaxial specimen. During preparation for triaxial testing, the specimens were observed to be 'highly variable' which was reported to be due to friction inside the consolidation tube and sample disturbance. An alternative "sedimentation technique" was developed with the aim of producing an initially loose specimen that would be more prone to liquefaction. This technique involved pouring silt slurry prepared from rock powder into a split mold with an expanded membrane in place. The slurry was then allowed to settle under its own weight and the top cap applied. Following this, a 10kPa or 40kPa vacuum was applied through the bottom specimen drainage, providing a reasonably firm specimen to carry on with triaxial testing. In all tests, reported Skempton's B values were in excess of 0.96.

The method adopted by Wang et al., (2011) involved depositing a natural low plastic silt material using a similar method to Hyde et al., (2006), except following settlement under self-weight and application of a vacuum, an external vertical load was applied in an incremental manner to a maximum vertical stress of 40kPa, achieving a firm enough specimen for triaxial testing. It was noted that the vacuum assisted in providing uniform stresses along the full height of the specimen during application of vertical load, reducing shear stresses at the

specimen boundary. In all tests, Skempton's B values were reported to be in excess of 0.98. Through verification testing, very good specimen uniformity and excellent test repeatability were noted.

2.5.6 Slurry displacement method

As mentioned in Section 2.1, specimen reconstitution plays an important role in developing our fundamental understanding of the mechanical response of soils. Another important use of specimen reconstitution is to characterize man-made materials for engineering purposes, with one particular application being mine waste material.

In an attempt to simulate the deposition of highly gap-graded mine waste material, Khaili & Wijewickreme (2008) developed a slurry displacement technique for triaxial tests. As mentioned in previous sections, commonly used techniques such as pluviation, slurry displacement and slurry consolidation are not considered suitable for highly gap graded material. The slurry displacement method involves preparing the waste material in both paste and slurry form. The paste is carefully spooned into a split mold filled with the slurry medium, displacing the slurry. A rod is used to carefully level the paste rock during the deposition process. Once the paste has fully displaced the slurry, the top cap is placed carefully onto the paste and the membrane is rolled from the split mold onto the top cap and sealed with an o-ring. A 25kPa vacuum is then applied to the

specimen, providing an initial effective stress to hold the specimen in place while the split mold is carefully removed.

A number of tests were conducted to confirm saturation and uniformity of specimens prepared using such a method. In most of the tests, Skempton's B values were reported to be in excess of 0.95. Density and particle size analysis indicated reasonably uniform specimens and no evidence of segregation. The results of undrained monotonic and cyclic shear testing indicated very good test repeatability.

2.6 Influence of reconstitution method on shear response of soil

Since the pioneering work of Seed & Lee (1967), the liquefaction behaviour of different soil types, as determined by laboratory testing, has been studied in detail with earlier studies focussed on the liquefaction testing of sands. It was generally considered during these earlier studies that the manner in which a particular density was achieved had little effect on the shear response of soils (Mulilis et al., 1977). The specimen preparation procedure most commonly used in these earlier studies were described as sand initially saturated in a container, poured through water into a water-filled forming mold, and then densified to a required density by some means, usually vibration (Ladd, 1974). This method is referred to in more recent studies as the water pluviation technique (Mulilis et al., 1977; Vaid & Negussey, 1984; Vaid et al, 1999; Khalili & Vaid, 2008) and later modified to

become the slurry displacement technique for sands with fines (Kuerbis & Vaid, 1988; Carraro & Prezzi, 2005).

The influence of specimen reconstitution technique on laboratory observed soil behaviour, and the differences in the soil fabric and mechanical response between different reconstitution techniques has been widely studied. In earlier years, the dominant interest revolved primarily around the cyclic resistance of sands for liquefaction assessment (Ladd, 1974; Mulilis, 1977; Miura & Toki, 1982; Vaid & Negussey; 1984; Vaid et al., 1999).

Ladd (1974) initially observed that the specimen preparation method can have a major influence on strength-deformation behavior of sand when comparing the shear response of specimens prepared using a moist vibration method and dry vibration method. In response to this initial observation, Mulilis et al. (1977) compared the undrained cyclic shear response of a sand compacted to same density using multiple reconstitution methods such as; pluviation through air, pluviation through water, high and low frequency vibrations applied to dry and moist samples, tamping and rodding of moist and dry samples. From these results, the weakest samples were found to be those formed by pluviating soil through air and a stronger response was observed specimens prepared using the vibration and moist tamping methods. Microscope and electrical conductivity measurements of thin vertical specimen slices suggest that the differences in measured strength

were probably due to the differences soil fabric (orientations of soil particles and packing density).

Miura & Toki (1982) compared the drained and undrained triaxial shear response of clean sands, comparing the moist tamping and air pluviation specimen preparation methods. The results indicate that for both preparation methods, the difference in shear response and dilatancy performance is more significant in triaxial extension and triaxial compression modes of shear. In addition, the dilatancy performance was found to be greater in specimens prepared by air pluviation than moist tamping. These differences can be attributed to the difference of fabrics developed during sample preparation. The results of undrained cyclic shear testing indicated the air pluviation method had a much higher strength when compared to the moist tamping method.

Vaid et al. (1999) compared the monotonic triaxial and direct simple shear (DSS) response of Fraser River sand using the air pluviation, water pluviation and moist tamping methods. The results of triaxial testing indicated that preparation method has a profound influence on shear response with the water pluviation method resulting in a significant strain hardening, dilative type response and the moist tamping method resulting in a significant strain softening, contractive type response. The results of DSS testing indicate that specimens prepared using the

air pluviation method have a strength that is roughly midway between that of specimens prepared using the water pluviation and moist tamping methods.

In recent years, research has turned to the shear response of silts for liquefaction assessment (Hyde et al., 2006; Bradshaw & Baxter, 2007; Wang et al., 2011). Hyde et. al. (2006) compared the undrained monotonic triaxial shear response of low plastic silts formed using a "1D slurry consolidation method" and a "sedimentation method" (see Section 2.5.5). The results of the testing indicate the slurry consolidation produces a dilative strain hardening response typical to that of dense sands. The "sedimentation method", on the other hand, resulted in a loose specimen which displayed a more contractive type response. Wang et al., (2011) also demonstrated a dilative type response of low plastic silt prepared using a slurry consolidation method (see section 2.5.5).

Høeg et al. (2000) compared the undrained shear response of undisturbed and reconstituted low plastic silt. Reconstitution methods included moist tamping and slurry consolidation. It was noted that the higher void ratios measured in the undisturbed state could not be achieved using the moist tamping and slurry consolidation methods. The results of monotonic triaxial shear testing indicated undisturbed specimens displayed a strain hardening dilative type response and the moist tamping and slurry consolidation methods displayed a strain softening type

response. Both the moist tamped and slurry consolidation methods displayed similarities in shear strength and pore water pressure development.

Bradshaw & Baxter (2007) developed a modified moist tamping method for silts addressing earlier specimen non-uniformity issues. The shear response of low plastic silt prepared using the modified moist tamping method, and slurry consolidation methods were compared against an undisturbed block sample. The results of cyclic shear testing indicated all methods displayed a strain hardening, dilative type response. However, the modified moist tamping method displayed either a similar or higher shear strength compared to the slurry displacement method and undisturbed block sample. This difference was found to be attributed to the molding water content during specimen preparation and the amount of energy required to compact specimens at the different molding water contents. The water content at specimen preparation is a possible explanation to the contradictory observations made by Mululis et al. (1977); Miura & Toki (1982); and Vaid et al. (1999).

Guo & Wang (2009) investigated the influence of initial water content during moist tamping on the drained and undrained shear response of natural silt. The results of drained monotonic triaxial testing indicated the specimens were more dilative at lower initial water content; however a similar strength was measured.

The results of undrained testing indicate a slight increase in shear strength and increase in dilative tendency with increase of initial water content.

2.7 Uniformity of reconstituted specimens

Uniformity of reconstituted specimens is a key consideration in laboratory element testing; in spite of this, the specimen uniformity is often assumed in testing, and only a few researchers have attempted to directly seek its confirmation (Mulilis et al, 1977; Miura et al., 1984; Vaid & Negussey, 1984, Kuerbis & Vaid, 1988; Vaid et al. 1999, Wijewickreme et al., 2005; Bradshaw & Baxter, 2007; Khalili & Wijewickreme, 2008; Wang et al., 2011). Various laboratory test investigations have been conducted to compare specimen uniformity of various specimen reconstitution techniques. Ladd (1974) initially identified a number of problems associated with the water pluviation techniques adopted in earlier studies, they included; the tendency for segregation of particles to occur when working with silty and relatively well-graded sands; and readily obtaining test specimens having an assured uniform density throughout.

In earlier research, verification of specimen uniformity focussed predominantly on sands and silty sand material (Mulilis et al., 1977; Miura et al., 1984; Vaid & Negussey, 1984; Kuerbis & Vaid, 1988). A study by Mulilis et al. (1977) included X-ray analyses on polyester-hardened specimens prepared using pluviation, vibration and tamping techniques. The results indicated the vibrated samples had

relatively uniform layers and the tamped samples were found have the most non-uniform layers. Miura et al. (1984) compared triaxial sample miniature cone penetration tests results for various methods of sample preparation. A high degree of sample uniformity was observed in air pluviated sand samples while considerable non-uniformity was observed in tamped sand specimens. The homogeneity of silty sand specimens prepared using the slurry deposition method was assessed by Kuerbis & Vaid (1988). Specimens of well graded sand and silty sand were set with gelatin under a confining pressure of 20kPa and four equal horizontal slices were obtained for particle size distribution and void ratio calculation. The results indicate that the samples were fairly homogenous with respect to particle size gradation and void ratio regardless of the fines content.

Wang et al., (2011) verified uniformity of low plastic silt specimens prepared using the consolidation method (see Section 2.5.5). Specimen uniformity was evaluated by taking five equally sized slices along the length of the specimen. Water content measurements and particle size analysis were carried out on each slice. The results of the analysis indicated very good uniformity in terms of water content (and void ratio) and excellent uniformity of particle size distribution. Khalili & Wijewickreme (2008) verified uniformity of highly gap-graded waste rock specimens prepared using the slurry displacement method (see Section 2.5.6). Specimens were “dissected” into four slices for density and particle size

distribution measurements. The results indicated the specimens had a relatively uniform density, with densities of each slice not deviating more than 3.7% of the corresponding average density. The results of particle size distribution analysis indicated essentially identical gradations suggesting no particle size segregation had occurred during the slurry displacement deposition process.

Despite earlier researchers concerns that the moist tamping method results in non-uniform specimens, Bradshaw & Baxter (2007) created a moist tamping method for silts which had better control of density by measuring the amount of energy applied to the specimen during compaction. The uniformity of silt specimens were verified using a non-destructive technique to obtain density measurements at 1mm increments along the full length of specimens. The density profiles indicated specimens to be 'very uniform' with subtle variation attributed due to layering. The variation in measured density was found to be significantly less than that initially reported by Vaid et al. (1999) on moist tamped silty sand specimens.

2.8 Closure

Liquefaction of saturated soils and associated geotechnical hazards are among the primary concerns related to the performance of structures located in areas of moderate to high seismicity. Over the past few decades, much of the laboratory research effort has focussed on the mechanical behaviour of sands and "relatively clean" sandy soils, whereas the behaviour of silts has been investigated on a very

limited scale. Natural silts and fine grained mine tailing materials are prevalent in most earthquake-prone areas, and there is evidence that sites underlain by such soils have experienced ground deformations and failure, including damage to structures (Boulanger et al., 1998). Controlled laboratory studies that have been conducted to assess the cyclic shear behaviour of silts are very few and there is no clear consensus position on the assessment of liquefaction potential of natural silts. Initial experimental research suggest silts develop a gradual 'cyclic mobility type' strain development, accompanied by gradual increase in excess pore water pressure (Δu) becoming equal or close to the initial effective confining pressure. The mechanical response of soils are controlled by many factors such as clay content, mineralogy, particle shape, particle fabric and there is a strong need for further investigate these factors to build on the fundamental knowledge of the seismic response of silts.

In the context of developing a mechanical framework for soils, reconstituted specimens are favoured over undisturbed specimens because tests can be conducted in a controlled and systematic manner. Reconstitution techniques reported in literature for preparing silt specimens include moist tamping, slurry consolidation and slurry displacement. The slurry consolidation method is considered to better simulate the deposition of silts found in an alluvial environment. Uniformity of reconstituted specimens is a key consideration in

laboratory element testing; in spite of this, much literature assumes or implies uniformity and only few researchers have attempted to directly seek its confirmation. Wang et al. (2011) has developed specimen reconstitution technique for low plastic silts based on the slurry consolidation method. Uniformity of specimens prepared using this technique was verified with respect to void ratio and particle size distribution. Specimen saturation and test repeatability was also confirmed.

In recognition of the above, a specimen reconstitution technique based on the slurry consolidation method was developed to enable triaxial testing of reconstituted silts at the University of British Columbia (UBC). In particular, the following activities were undertaken:

- Upgrade the UBC triaxial apparatus to enable monotonic and cyclic testing of reconstituted silt specimens;
- Develop a silt reconstitution technique based on the slurry consolidation design described by Wang et al. (2011);
- Verify uniformity and subsequent test repeatability of specimens prepared using the newly developed technique; and
- Apply the newly developed silt reconstitution technique to enable characterization of Kamloops silt, contributing to the understanding of the material behaviour of relatively low plastic silt.

Chapter 3: Materials Tested and Experimental Aspects

As indicated in the introductory chapters, monotonic and cyclic shear testing was carried out on reconstituted low plastic natural silt with the main objective to verify the newly developed UBC cyclic triaxial (UBC-CTX) device and slurry deposition technique.

This chapter presents the experimental aspects related to the present study. Initially, the information on material tested followed by details related to the new triaxial testing system with respect to mechanical components, data acquisition, and stress path control system are presented. A new method that was developed for preparing reconstituted silt specimens for element testing is then described and the ability of this new method to produce uniform specimens is demonstrated. Details pertaining to triaxial cell preparation and the different phases of triaxial testing are then described. Test repeatability of specimens prepared using the newly developed reconstitution method is then demonstrated through duplicate testing under both monotonic and cyclic modes of shear. An experimental program applying the newly developed silt reconstitution technique to characterise the shear response of Kamloops silt is then presented.

3.1 Materials tested

The silt material used in this research (named hereinafter as Kamloops silt) originates from the Kamloops bench lands bluffs, located on the south side of the South Thomson River just east of Kamloops, in the Province of British Columbia (BC), Canada. The Kamloops silt was deposited in a glacial lake referred to as Lake Thomson (Matthews, 1944) during the last deglaciation. Much of the silt was derived from the erosion of the till on the uplands and entered the Thomson Valley in the vicinity of Kamloops. The coarse portion of the till was left on the uplands while the silt was carried into the valley.

The Kamloops silt was selected due to its geographic uniformity in deposition, natural abundance, and ease of access for sampling, all of which are important factors when the intent is to conduct a large number of element tests on homogeneous and uniform specimens along with repeatability.

The results of particle size analysis obtained from five randomly selected samples of Kamloops silt used in this study are presented below in Figure 3.1 and Table 3.1.

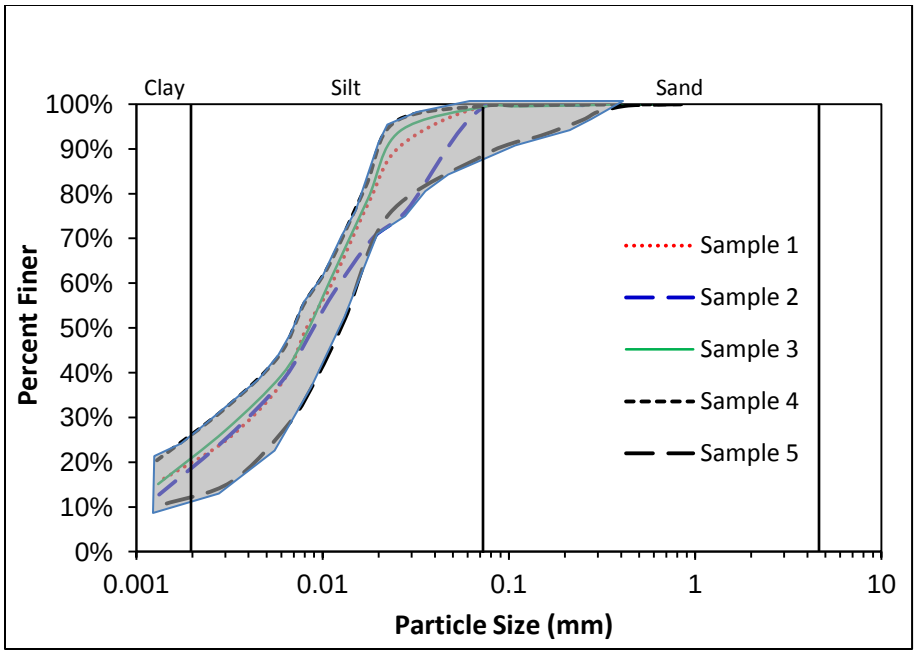

Figure 3.1 Particle size distribution of tested Kamloops silt

Table 3.1 Summary of index parameters

Soil Index Properties	Range of values	Average value
Liquid Limit, LL (%)	33-34	34
Plastic Limit, PL (%)	23-26	25
Plasticity Index, PI (%)	7-11	9
Unified soil classification	-	ML
Specific gravity, G_s	2.76-2.77	2.76

It can be seen from the results above that the Kamloops silt is reasonably uniform low plastic silt with clay content in the range of 10 to 20% and an average Plasticity Index of 9.

Mineralogy tests were not conducted as part of this study. However, Table 3.2 and Table 3.3 below are results of mineralogy analysis conducted by Fulton (1965) and Quigley (1976) on silt deposits located in the South Thomson River. It should be realized that Fulton analysed the silt and sand fractions optically while Quigley used X-ray powder analysis on the whole sample (i.e. with the clay fraction included).

Table 3.2 Composition of Kamloops silt

Mineral	Fulton (1965)	Quigly (1976)
quartz	main constituent	abundant
feldspar	major constituent	moderate
mica	major constituent	minor
Ferromagnesian minerals	minor constituent	minor

Table 3.3 X-ray diffraction of clay fraction of Kamloops silt only

Mineral	Fulton (1965)	Quigly (1976)
montmorillonite	35-40%	abundant
illite/mica	28-35%	moderate
chlorite	27-36%	minor
kaolinite	-	minor

3.2 Triaxial apparatus

All tests were conducted using the UBC-CTX apparatus. A schematic diagram of the UBC-CTX apparatus is given in Figure 3.2. The testing system consists of an instrumented triaxial cell and a loading system. The triaxial cell was designed to test cylindrical specimens approximately 73mm in diameter and approximately 150mm high, with one way drainage provided through the base pedestal. The loading system is capable of consolidating a given specimen under hydrostatic loading to a target initial effective confining stress level (σ'_{3c}), followed by monotonic shearing under strain controlled conditions or cyclic shearing under stress controlled conditions. At the end of hydrostatic consolidation, the specimen may be subjected to an initial static shear bias at a target effective consolidation stress ratio (K_c), defined as the ratio of major effective principal stress (σ'_1) to minor effective principal stress (σ'_3).

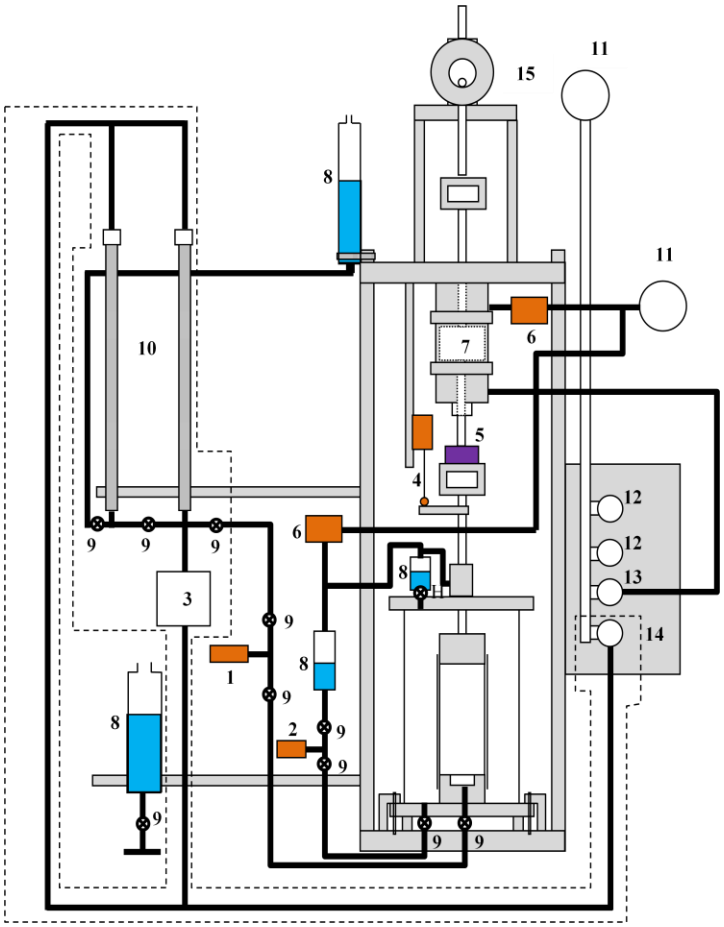

1. Pore water pressure transducer (PWPT)
2. Cell pressure transducer (CPT)
3. Differential pore water pressure transducer (DPWPT)
4. Linear variable differential transducer (LVDT)
5. Load cell (LC)
6. Electro-pneumatic regulator (EPR)
7. Double acting piston
8. Reservoir (air/water interface)
9. Valves
10. Pipettes
11. Compressed air supply 700kPa
12. Spare manual regulators
13. Manual regulator providing baseline pressure to double acting piston
14. Manual regulator providing back pressure to specimen
15. Variable speed motor

Figure 3.2 General arrangement of UBC cyclic triaxial apparatus

3.2.1 Loading system

The UBC-CTX apparatus consists of a strain controlled loading system for monotonic shear tests, and a stress controlled loading system for application of cell pressure and cyclic shearing. Two electro-pneumatic regulators (EPR) are driven by function generator (FG) code, written using National Instruments$_{TM}$ (Austin, Texas, United States of America), graphical user interface based code

LabVIEW$_{TM}$ and is used to control cell pressure (σ_{3c}) and deviator stress (σ_d). In cell pressure control, the EPR receives an input voltage from the FG and proportionally converts this signal into a pressure output. The voltage of the EPR is increased linearly to allow cell pressure to slowly increase to target values during Skempton's B value calculation, consolidation and is held at a constant voltage during the shearing phase.

During stress controlled cyclic shearing, a vertical load is applied to the specimen by means of a rolling diaphragm double acting piston controlled by an EPR connected to the top chamber and a constant pressure fed by a manually controlled regulator connected to the bottom chamber (refer to Figure 3.3). When the piston is not transmitting any load, a base pressure is supplied to both chambers from the manual regulator and EPR. The purpose of the base pressure is to maintain piston equilibrium and to allow the piston to apply both a positive and negative σ_d required for cyclic shearing and also to minimise wrinkling damage to the diaphragms when the system is not in use.

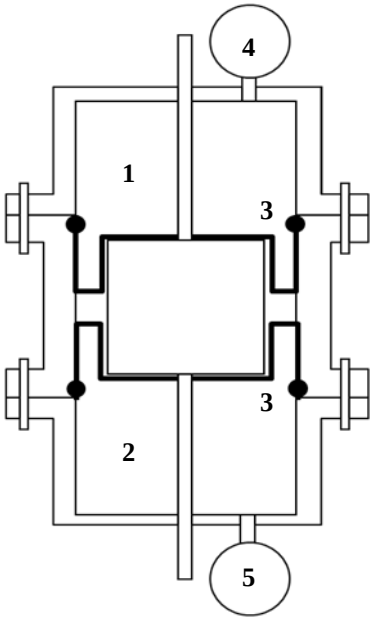

1. Top chamber
2. Bottom chamber
3. Rolling diaphragm with o-ring seal
4. Electro-pneumatic regulator (EPR)
5. Manual regulator at fixed baseline pressure

Figure 3.3 Schematic diagram rolling diaphragm double acting piston

The EPR for stress controlled shear tests is driven by a FG which defines the pulse shape, amplitude and frequency for cyclic loading. The baseline pressure in the double acting piston is set to a value which maximises the positive and negative deviator stress over the available EPR voltage range.

In strain controlled monotonic shear tests, the loading ram is connected to a variable speed motor, providing a constant rate of axial shear strain to the specimen. The direction and speed of shear can be changed manually using the

dial setting on the variable speed motor, as required, to achieve a desired strain rate.

For cyclic shear tests with initial static shear bias, the target anisotropic consolidation ratio (K_c) is achieved using the double acting piston and slowly increasing σ_d in 10kPa increments, keeping specimen drainage open. Between increments, the specimen is allowed to drain for 30 minutes. Once the final increment has been reached, the specimen is allowed to further drain for a set time of 60 minutes.

3.2.2 Pore-water pressure and specimen volume measuring system

The UBC-CTX device comprises of five transducers; a load cell (LC) measuring σ_d; a linear variable differential transformer (LVDT) measuring axial strain (ε_a); cell pressure transducer (CPT) for measuring cell pressure (σ_3); pore-water pressure transducer (PWPT) for measuring pore water pressure (u); and differential pore-water pressure transducer (DPWPT) measuring volumetric strain (ε_v). The capacity, measurements and resolutions of each transducer are summarised below in Table 3.4.

Table 3.4 Capacity and resolution of sensors on the UBC-CTX device

Measurement	Transducer Capacity	UBC-CTX Capacity	Resolution
Load Cell	225 kg	90 kg*	0.05kg
Axial displacement	17 mm	17 mm	0.005 mm
Cell pressure	700 kPa	700 kPa	0.15kPa
Pore-water pressure	1700 kPa	1700 kPa	0.15kPa
Specimen Volume	NA**	NA**	0.010cm^3

*For stress controlled tests only, limited by maximum applied stress from double acting piston. For strain controlled tests, UBC-CTX Capacity is equal to load cell capacity. ** Not applicable

3.2.3 Data acquisition and control system

The data acquisition and control system (DACS) of the UBC-CTX has four major components including; signal conditioning unit, data acquisition device, computation unit, and display panel. A schematic diagram of the set up is shown below in Figure 3.4.

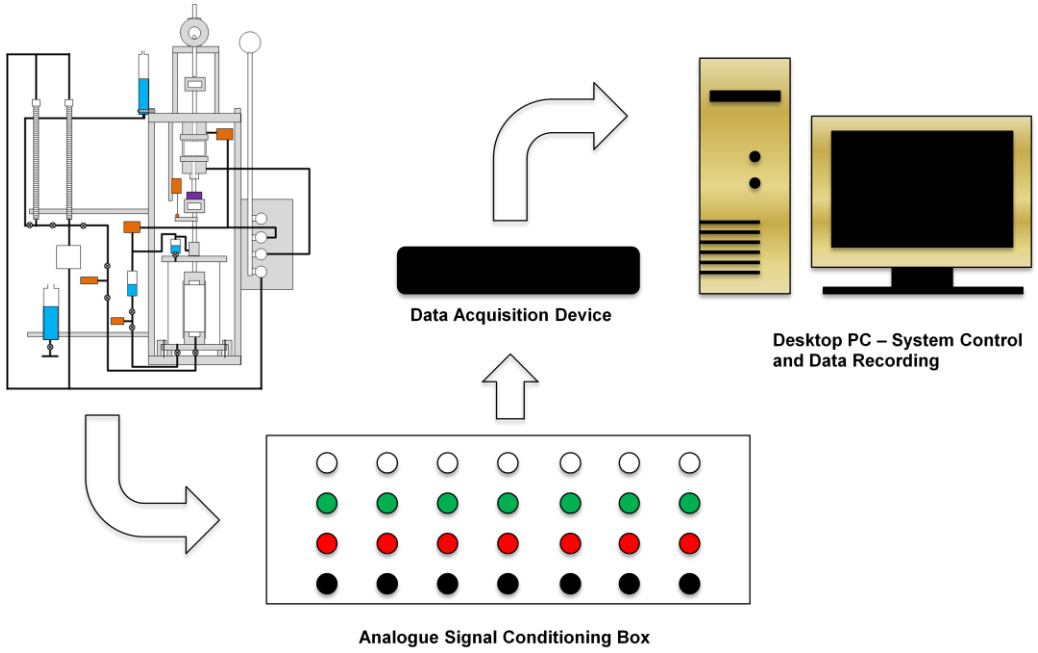

Figure 3.4 General arrangement of data acquisition and control system (DACS)

The signal conditioning unit was designed and constructed in the workshop of the department of Civil Engineering at UBC. The unit is capable of providing voltage excitation and conditioning to a maximum of eight sensors at any one given time. Signal conditioning involves a low pass filter to reduce electrical noise and amplification can be applied to improve resolution of sensors that operate over a relatively narrow voltage range. On the UBC-CTX, amplification was applied to DPWPT and PWPT sensors.

The data acquisition unit is a National Instruments$_{TM}$ (Austin, Texas, USA) DAQPad-6251$_{TM}$. The role of this device is to digitise voltage outputs from the signal conditioning unit and transfers this information to the computation unit.

The National Instruments$_{TM}$ (Austin, Texas USA) DAQPad-6251 $_{TM}$ unit comprises 16 analog input channels with a maximum sample rate of 1.25 milliseconds per second (MS/s), 16- bit resolution, voltage range of $\pm$10V and two analogue output channels with a sample rate of 2.86 MS/s, 16-bit resolution and a voltage range $\pm$10V.

The desktop computation unit runs National Instruments$_{TM}$ (Austin, Texas, USA) LabVIEW$_{TM}$ Version 8.2.1, a system-design platform and development environment which, through graphical code, allows the user to electronically record raw voltages from sensors, reduce sensor voltages, control the pressure output from EPRs and provide a continuous display of data during the testing period. As part of the development of the UBC-CTX and this research, customised code was developed to perform the triaxial test procedures described in the following sections. Data was acquired from each sensor simultaneously from the signal conditioning unit at a sampling rate of 1000 samples per second. Further noise reduction was applied to each sensor digitally by taking an average of 100 data points at a time before processing.

3.2.4 Specimen reconstitution method

A slurry consolidation approach with a vertical load application technique was developed to prepare reconstituted specimens of silt. The major advantage of the slurry consolidation technique is that it produces homogeneous well mixed

samples and repeatable tests (Wang et al., 2011). For this purpose, a new slurry consolidation device for triaxial testing of reconstituted silts was developed at UBC (called UBC-SCT). The reconstitution method developed herein is based on a previous design (Wang et al., 2011), allowing the silt slurry to be consolidated directly on the triaxial base pedestal inside a vacuum split mold with the expanded membrane in place. In contrast to the method by Wang et al. (2011) no vacuum is applied to the specimen during slurry consolidation in the new method, thus, forming the main difference between the two methods. The details related to the device and slurry consolidation approach are given in the following sections.

3.2.4.1 UBC slurry consolidometer for triaxial testing

A schematic of the UBC slurry consolidometer for triaxial testing (UBC-SCT) is given in Figure 3.5. Essentially, the device comprises four main components: (i) the triaxial base pedestal; (ii) vacuum split mold; (iii) extension collar; and (iv) slurry top cap and loading ram. The triaxial base pedestal and vacuum split mold accommodates triaxial testing of reconstituted silt specimens having diameter of 72 mm and final trimmed height of 145 mm. Slurry consolidation is performed directly on the triaxial base pedestal inside a cylindrical vacuum split mold and extension collar. The vacuum split mold serves two purposes: (i) to stretch the specimen membrane, forming a cylindrical shape having the same diameter as the base pedestal; and (ii) to provide radial support during slurry consolidation.

Vertical loading is applied through the slurry consolidation top cap and loading ram. The loading is applied in an incremental manner using the double acting piston in the triaxial loading frame. The extension collar provides additional height during slurry consolidation that is required due to the larger volume of slurry at the loosest state of deposition. At the end of slurry consolidation, the extension collar and loading ram is carefully removed exposing excess consolidated silt above the vacuum split mold which is carefully removed using a wire saw.

In the UBC-SCT device, the slurry consolidation top cap and loading ram is separate to the one that is used for subsequent triaxial testing. The sides of the slurry consolidation top cap have been recessed and chamfered to improve manoeuvrability through the extension collar during consolidation while, at the same time, minimising the chance for silt to squeeze between the extension collar and top cap. During slurry consolidation, two-way drainage is permitted through the top cap and the triaxial base pedestal.

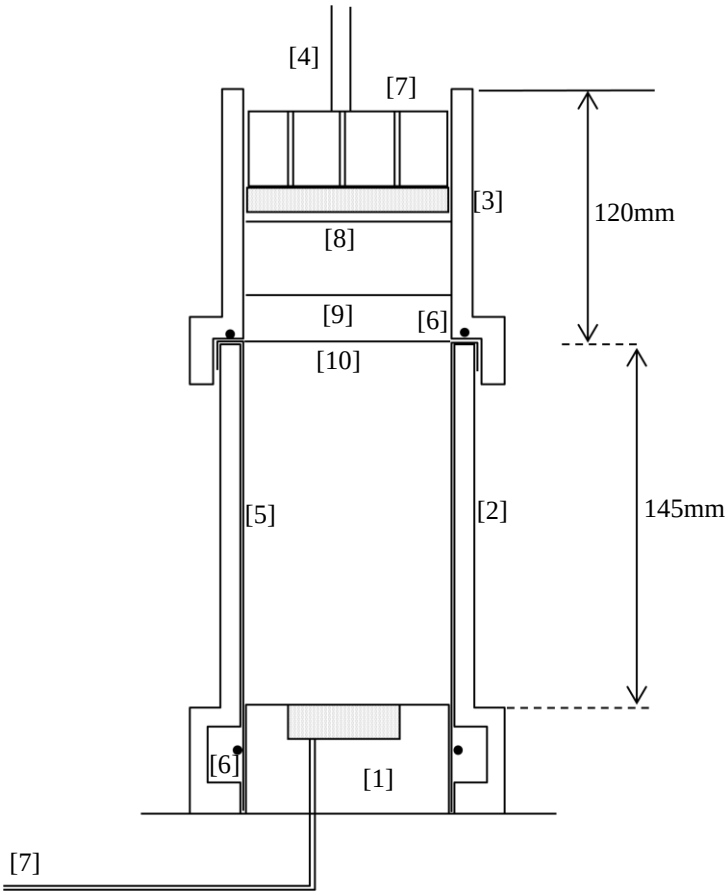

[1] Triaxial base pedestal
[2] Vacuum split mold
[3] Extension collar
[4] Slurry top cap and loading ram
[5] Triaxial membrane
[6] O-ring
[7] Drainage through porous stone
[8] Initial slurry height
[9] Excess consolidated silt
[10] Final trimmed specimen height

Figure 3.5 General arrangement of UBC slurry consolidometer

A detailed description of the adopted silt reconstitution process using the new device is described in the following sub-sections.

3.2.4.2 Silt pulverisation

Approximately 1.2kg of dry disturbed silt sample was selected from the bulk samples. This material was placed in a large metal tray and allowed to oven dry overnight. Following this, the silt was pulverised using a pestle and mortar. A No. 10 sieve (2.00mm opening size) was used to assist in the pulverisation process. Following pulverisation, the silt was thoroughly mixed using a spatula and placed in a plastic container for preservation.

3.2.4.3 Slurry preparation

The prepared dry pulverised silt was split into one thirds and placed into three 500-mL beakers. The material was mixed with a calculated volume of de-aired water resulting in a water content of 60%. The material was left under vacuum for 3 hours. The slurry was stirred every hour while under a vacuum environment to remove entrapped air bubbles and with the objective of achieving saturated homogeneous slurry.

3.2.4.4 Selection of a suitable slurry deposition technique

With slurry consolidation, it is important for silt slurry to be placed in a uniform manner. The slurry at deposition should have a high enough water content to allow mixing and pouring from a 500-mL glass beaker and the slurry should have a low enough water content such that particle settlement distance is kept to a

minimum and sedimentation currents do not segregate the soil during sedimentation (Kuerbis, 1989).

With this in mind, different slurry water contents and deposition techniques were tested to find the best method resulting in minimal air bubbles. Four pouring techniques were tested and included a funnel, pouring down a metal rod, rubber hose, and spooning in the slurry. A schematic diagram of each technique is given in Figure 3.6. For each technique, Kamloops silt slurry was prepared at water contents ranging from 50% to 80%. In each case, the rubber hose technique was the least time consuming and resulted in the least amount of air bubbles generating at the surface of the slurry. Considering the height of the extension collar, it was prudent to keep the water content to a minimum, by doing so reducing the required volume change during slurry consolidation.

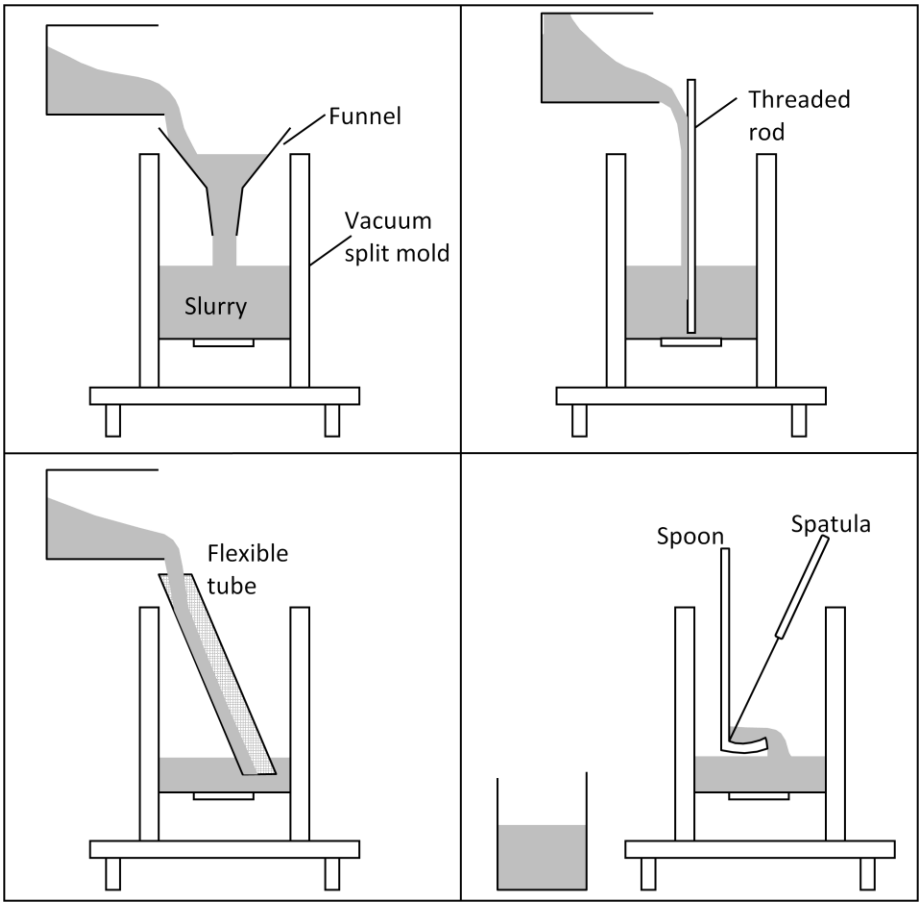

Figure 3.6 Trial slurry pouring techniques

It was found from the different specimen pouring techniques, and varying water contents, the flexible tube resulted in the least amount of bubbles visible at the surface of the slurry while maintaining ease of pouring from a 500-mL glass beaker at a minimum water content of 60%. On this basis, it was decided to proceed with a trial slurry preparation using the flexible tube and water content of 60%.

3.2.4.5 Slurry deposition

After conducting slurry deposition trials using Kamloops silt (Section 3.2.4.4), a procedure was developed with the aim of preparing a uniform reconstituted silt specimen using the UBC-SCT.

A schematic diagram of the main steps in the slurry deposition procedure are illustrated in steps (a) to (e) in Figure 3.7, and can be further described as follows: (a) Saturate the base pedestal drainage with de-aired water using a reservoir connected to a manual pressure regulator. Close the drainage valve when a meniscus of water has formed in the recess of the base pedestal. Insert a saturated porous stone into the recess. Place the membrane around the base pedestal, ensuring it remains fully saturated, and fit the bottom o-ring. Carefully place the vacuum split mold around the base pedestal, taking care to ensure that the membrane does not to catch in the vacuum split mold. Apply a vacuum to expand the membrane. (b) Place the flexible hose for pouring slurry inside the vacuum split mold and position the hose so that it sits slightly above the base pedestal; adjust the hose so that it is on a slight angle and carefully pour silt slurry through the hose; (c) while pouring, gradually raise the hose at the same rate as the increase in slurry height; (d) when slurry reaches almost the top of the vacuum split mold, carefully remove the flexible hose and add the extension collar. Continue to pour slurry as described in steps (b) and (c) until the slurry has

reached a target height; (e) allow the specimen to consolidate under self weight for 3 hours. After this period, decant any water that has risen to the slurry surface, carefully place the slurry top cap onto the specimen (equivalent to a surcharge of approximately 1.8kPa). Allow the specimen to settle under the weight of the slurry top cap overnight.

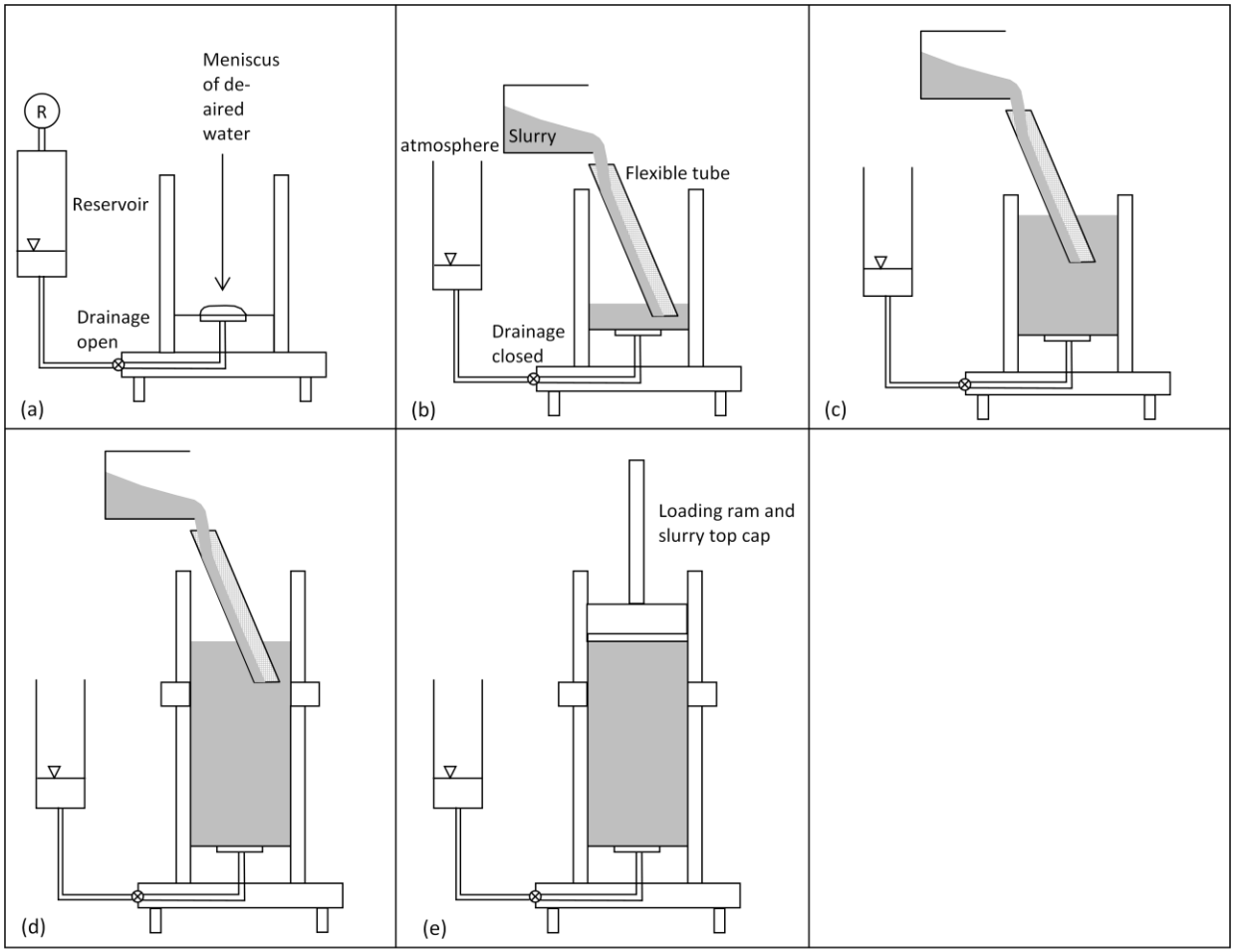

Figure 3.7 The main steps of the slurry deposition process

3.2.4.6 Slurry consolidation

After waiting for the slurry to consolidate under the weight of the slurry top cap, in preparation for applying load increments as per below, the slurry top cap was removed from the extension collar, cleaned with de-aired water and repositioned to minimise friction between the loading ram/top cap and extension collar.

The next step was to apply a vertical stress (σ_v) in an incremental manner on the slurry and allow the slurry to reach primary consolidation under each load increment. To minimize squeezing between the slurry top cap and extension collar, slurry consolidation was started at σ_v of 10kPa, and was subsequently increased to 20kPa and 40kPa. A final σ_v of 40kPa was found to provide a reasonably firm specimen to move forward with completing specimen preparation for triaxial testing, and keeping the initial specimen consolidation stress level at a value less than the minimum nominal σ'_{3c} of 100kPa, contemplated for triaxial testing.

A continuous record of test data was obtained by a computer interfaced data acquisition system (see Section 3.2.3). The monitored test variables consisted of full-time histories of σ_d, σ_3, u, ε_a and ε_v. Typical axial deformation versus time plots obtained during the slurry consolidation of Kamloops silt is shown below in Figure 3.8.

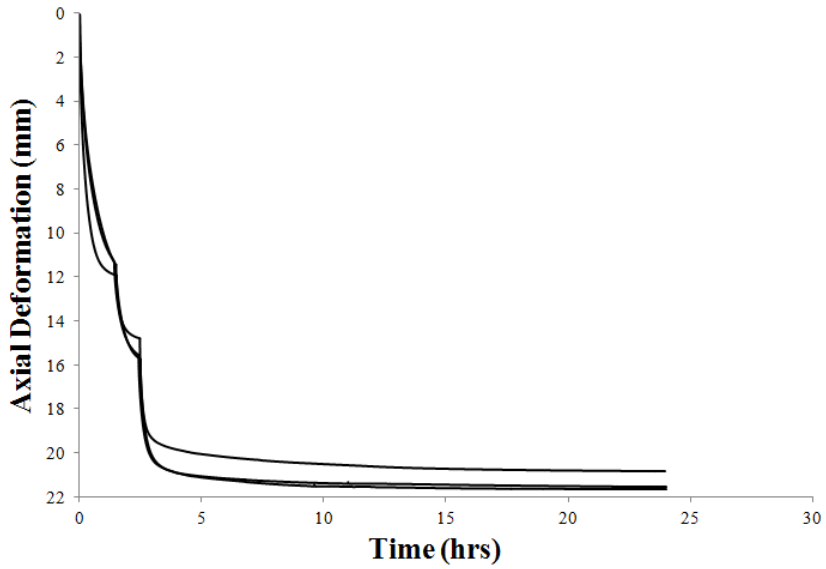

Figure 3.8 Typical slurry consolidation curves over a 24-hr period

It is important to note that in the Wang et al. (2011) method, the slurry consolidation is achieved by applying a vacuum to the specimen drainage with the intention of minimizing the shear stress development at the vertical boundary of the specimen. In the present application, the triaxial tests are conducted at a minimum nominal σ'_{3c} value of 100 kPa; as such, the effects arising from the shear stress development at the vertical boundaries of the specimen under low effective stresses (less than 50 kPa) during slurry consolidation, by vertical load application, can be considered negligible.

3.2.4.7 Specimen homogeneity

The two main factors that contribute to a homogeneous specimen include uniformity in void ratio and particle size distribution (Kuerbis, 1989).

To test the uniformity of the silt specimen with respect to particle size distribution, a Kamloops silt specimen was prepared using the methods described in the sections above. At the end of a triaxial shear tests, one of the specimens, initially consolidated to a target σ'_{3c} of 100kPa, was carefully removed and was cut into four equal horizontal slices. Grain size distributions results for the four slices are shown below in Figure 3.9.

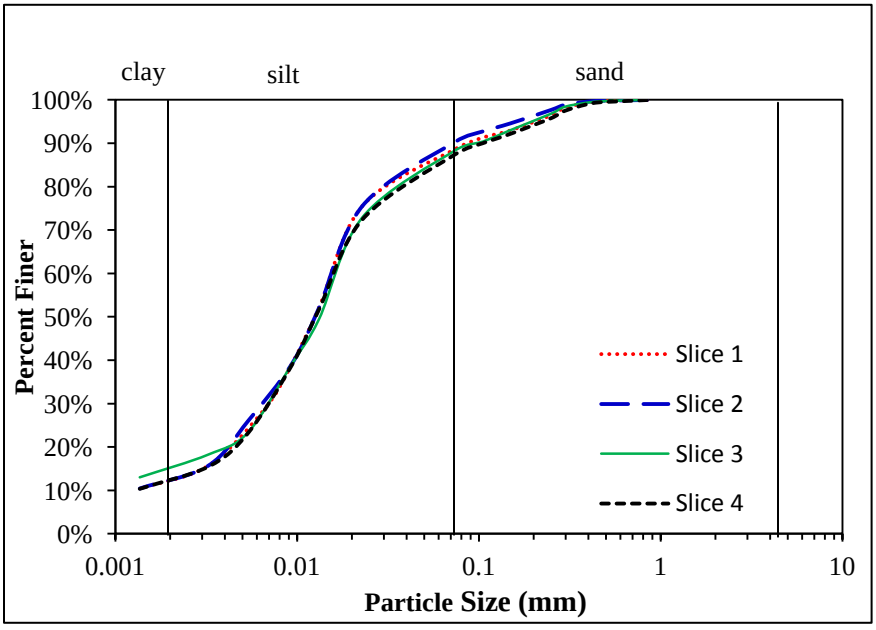

Figure 3.9 Specimen uniformity – particle size analysis

It can be seen from above in Figure 3.9 very good homogeneity exists within the reconstituted specimen with respect to particle size distribution.

To test for void ratio uniformity, the six specimens, prepared for undrained monotonic shear testing (See Section 3.4), were cut into three equal slices and moisture content (and void ratio) measurements were made. The variation of water content can be used as an indicator to any variation in void ratio. A plot of water content measurement with respect to the mid-height of each slice from the base of the specimen for the undrained monotonic shear tests is shown below in Figure 3.10. Information pertaining to test identification on the legend of this plot is provided in Table 3.5 in Section 3.4.

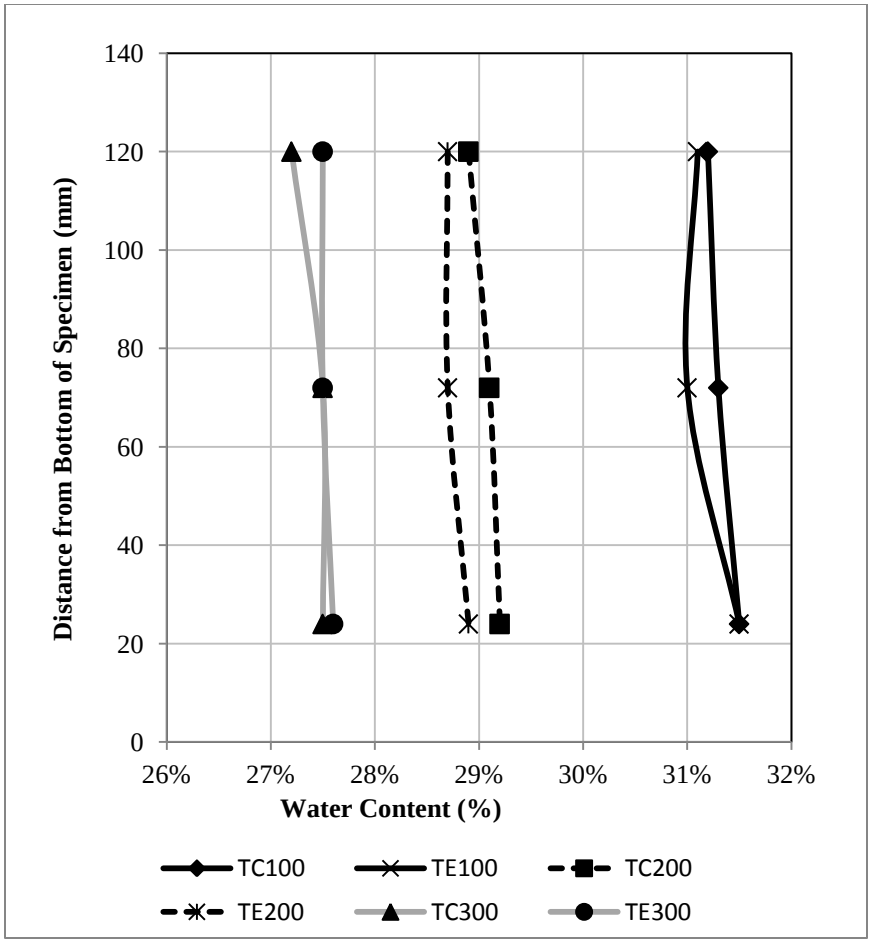

Figure 3.10 Water content variation at end of undrained monotonic shear tests

It can be seen from Figure 3.10, that distribution of water content and void ratio within the sample height is fairly uniform. These results are of similar findings to tests conducted on slurry deposited silty sands (Kuerbis, 1989).

3.2.4.8 Specimen geometry and strain uniformity

When the split mold was removed from the specimen, specimen uniformity in terms of geometry was observed by measuring the circumference of the specimen at the top middle and bottom of the specimen. A summary of specimen diameters measured for the monotonic undrained triaxial tests is provided below in Figure 3.11.

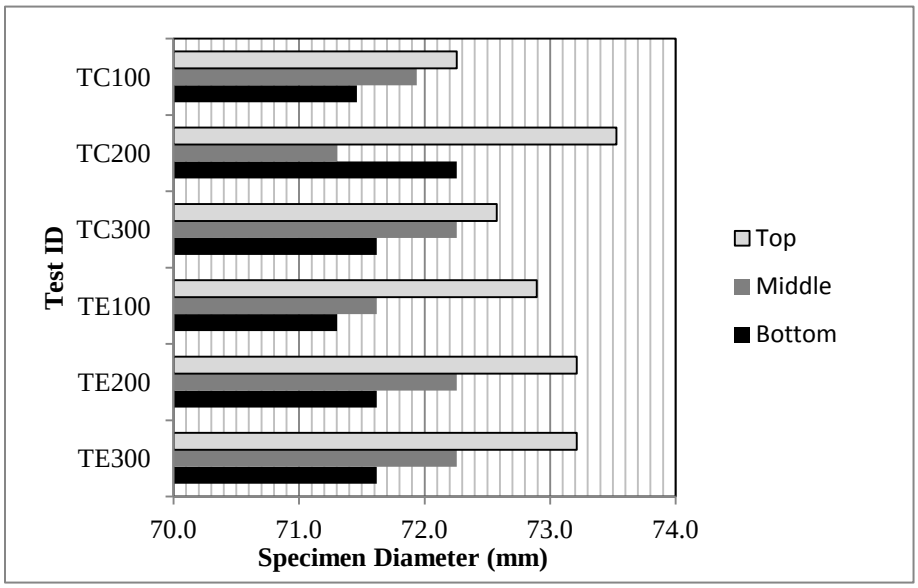

Figure 3.11 Specimen diameter following removal of vacuum split mold

The above results indicate good repeatability of specimen diameter following removal of the vacuum split mold. For all tests, the average of the measured diameter of the top, middle and bottom diameters was found to be 72mm. There is a slight tapering effect whereby the diameter reduced by an average of 1mm from

the top to the bottom of the specimen. This may be due to the effect of small shear stresses being developed at the side boundary of the specimen during slurry consolidation along the expanded membrane (see Section 3.2.4.6).

3.2.5 Assembly of triaxial test apparatus

Following slurry consolidation, the specimen was removed from the triaxial loading frame, ready for specimen preparation. A schematic diagram outlining the preparation process is provided below in Figure 3.12, and it can be further described as follows: (a) The extension collar was carefully removed from the vacuum split mold, exposing a disc of excess consolidated silt above the split mold. (b) The slurry top cap was carefully removed and a sponge was used to clean any film of excess water/silt around the vacuum split mold. (c) The excess silt was then trimmed using a thin wire saw, resulting in a specimen that was flush with the top of the split mold. When trimming the specimen, particular care was taken to ensure that the wire saw does not tear/puncture the expanded membrane. (d) The triaxial top cap was then carefully placed onto the trimmed specimen. The rubber membrane was flipped up from the vacuum split mold to encapsulate the top cap. An o-ring was used to seal the rubber membrane to the top cap, as usually undertaken in securing specimens for triaxial testing. A 30kPa vacuum was then applied to the specimen through the bottom drainage. The specimen was left to stabilize under vacuum for 30 minutes. (e) After the water level in the reservoir

stabilized, the vacuum split mold was carefully removed; the specimen height and membrane axial strain was recorded. (f) The triaxial cell was carefully assembled, filled with water and a final specimen height was recorded.

Upon completion of the above, the triaxial cell was moved back into the triaxial loading frame, and an initial σ_3, approximately equal to the applied vacuum, was applied to the cell. At this point the specimen ready was ready for saturation checks using Skempton's B value testing, as described in Section 3.2.6.

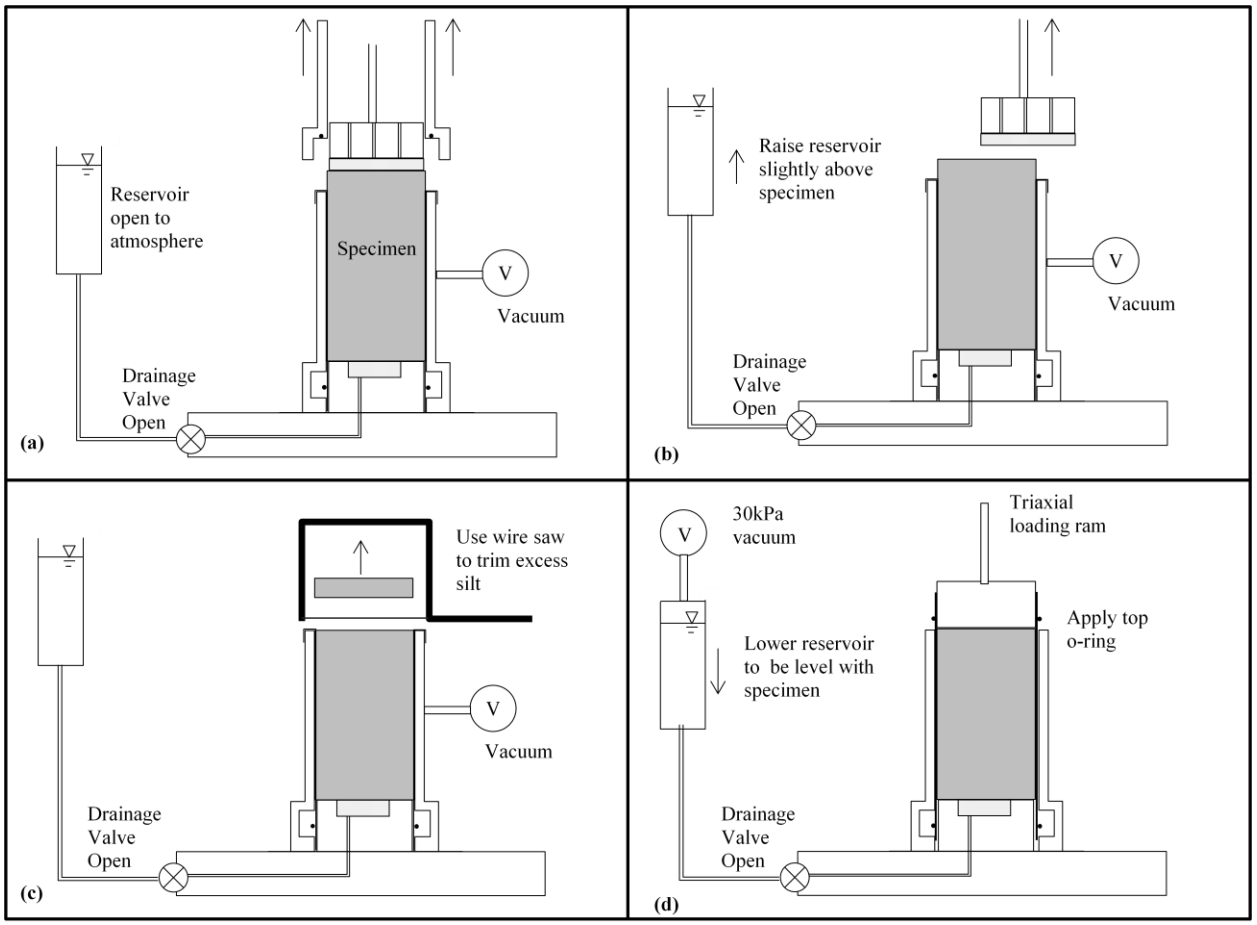

Figure 3.12 Schematic diagram of triaxial cell assembly process

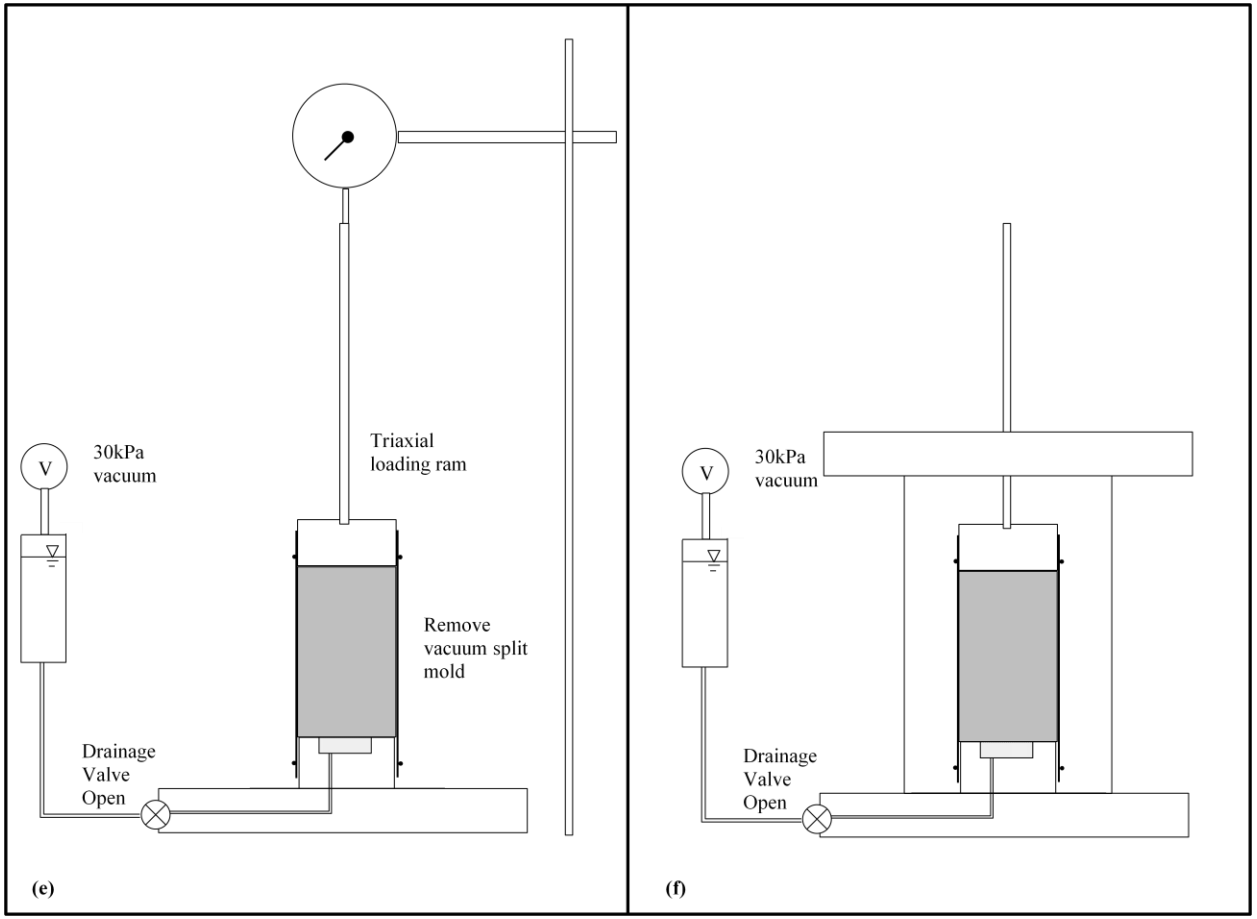

Figure 3.12 (continued) Schematic diagram of triaxial cell assembly process

3.2.6 Specimen saturation

Once the triaxial cell is assembled and positioned within the loading frame, the degree of saturation of the specimen must be checked by incrementally increasing the cell pressure and monitoring the pore-water pressure response of the specimen with drainage closed. Skempton's B values can be calculated at the end of each cell pressure increment. Increasing hydrostatic pressure requires computer control of the axial load to maintain K_c of 1.0.

In this study, Skempton's B values were calculated by increasing σ_3 by 30 kPa, waiting two minutes, and measuring the resulting increase in u. The increase of σ_3 causes any air in the specimen and pore water pressure measuring system to dissolve, which would increase the degree of saturation. Calculation was performed until u reached around 120 kPa. For all tests, the calculated Skempton's B values were greater than 0.98. At this point, back pressure was set to match the final u value reading of the specimen at the end of Skempton's B value calculation, and then the specimen drainage was opened to the back pressure. Since the pore water pressure and back pressure is matched the specimen does not undergo any volumetric strain (ε_v) at the time of opening the drainage valve.

3.2.7 Consolidation phase

Following specimen saturation, the sample was ready for consolidation to the target σ'_{3c} values. The consolidation phase comprises two sequential steps: (i) Step 1: The drainage to the specimen is closed and the cell pressure is raised while adjusting the axial load simultaneously to maintain $\sigma_1 = \sigma_3$. σ_3 and at a constant rate of 0.5 kPa per second using the EPR and double acting piston until desired σ_3 was achieved. (ii) Step 2: The drainage is opened and consolidation is allowed to occur to reach the final σ'_{3c}.

The specimen was consolidated incrementally, firstly to a σ'_{3c} of 50kPa. Then, σ'_{3c} was increased by a factor of two until the final desired value was achieved. At each load increment, the specimen was left to consolidate for 60 minutes, which was the estimated time required for primary consolidation to occur based on the observed time-volume change characteristics. To aid in test repeatability, the drainage line was kept open for an additional 1.5 hours at the final target σ'_{3c}. The intent was to allow for a set amount of secondary consolidation (or creep) to occur and aid in test repeatability.

During the consolidation process, ε_v, axial strain (ε_a) and $\sigma_d$were continually monitored by the DACS.

3.2.8 Static shear bias phase

For tests with an initial static shear bias, the desired K_c was achieved following consolidation under drained condition by applying a static shear stress at a rate of 0.5kPa/s. This stress rate was selected based on drained monotonic shear stress results, whereby the selected stress rate was less than the time required to reach the same target σ'_1. The specimen was sheared by increasing σ_d in 10 kPa increments, followed by a waiting period of 30 minutes to ensure there is no remaining buildup of excess pore water pressure (Δu) due to shear. To aid in test repeatability, each test specimen was allowed to sit for a period of 60 minutes after the final target K_c had been reached.

During the application of static shear bias, ε_v, ε_a and σ_d were continually monitored by the DACS.

3.2.9 Undrained shear loading phase

3.2.9.1 Arrest of secondary consolidation

After completion of the consolidation and static shear bias (if needed) phases, the specimen drainage was closed. Due to continued secondary consolidation, specimens were observed to experience a gradual increase in u. This phenomenon is commonly referred to as 'pore water pressure rise due to arrest of secondary consolidation'. To aid in test repeatability, a time period of 30 minutes was

allowed for the arrest of secondary consolidation (it was estimated that this time period would allow for at least 90% of the pore water pressure rise due to arrest of secondary consolidation).

3.2.9.2 Monotonic shearing

A series of strain controlled monotonic loading tests were performed on the Kamloops silt and included conventional drained and undrained triaxial compression (TC) and conventional undrained triaxial extension (TE) tests.

The rate of axial loading during drained shear must provide sufficient time for pore water pressure to dissipate from the drainage provided at the end of the specimen so that there would not be any significant excess u within the specimen. An appropriate rate of strain was selected using a method based on consolidation theory suggested by Bishop and Henkel (1957) and later by Germaine and Ladd, (1988). Using this method, a rate of axial strain of 2% per hour was found to be sufficiently slow to ensure dissipation of excess u within the tested Kamloops silt specimens. Calculation of this rate of axial strain can be found in Appendix A.1.

In undrained shear tests, the rate of loading should be sufficiently slow to allow equalization of u throughout the specimen during shear, and in doing so allowing for reliable measurement of u at the base of the specimen. Using the method suggested by Germaine and Ladd (1988), a rate of axial strain of 6% per hour was

found to be sufficiently slow to ensure equilibration of u within the specimen. Calculation of this rate of axial strain can be found in Appendix A.2.

3.2.9.3 Cyclic shearing

A sinusoidal wave form was used for stress controlled cyclic loading. Research to date investigating the cyclic shear response of silt material has used sinusoidal wave pulses with frequencies typically ranging between 0.1Hz and 1Hz (Prakash and Sandovol, 1992; Hyde et al., 2006; Bray and Sancio, 2006). A wave pulse frequency of 0.1Hz has been selected for DSS research at UBC (Sanin & Wijewickreme, 2006; Wijewickreme et al., 2005, Sanin (2010), Seidalinova, 1014; Soysa 2015). These frequencies are lower than those typically encountered during an earthquake, however a slower frequency allows for better measurement of pore water pressure. Zergoun and Vaid (1994) noted that the behaviour of clay in undrained cyclic triaxial shear cannot be confidently interpreted in 'fast' loading tests due to inadequate time for equalization of u throughout specimen.

Due to the time constraints and the requirement to conduct a meaningful number of tests in this study a sinusoidal frequency of 0.1Hz was selected for this research. It is important to note that regardless of pore water pressure measurement, the variables stress and strain are independent measurements of specimen performance; as such, those two measurements provide reliable information for liquefaction assessment regardless of the frequency of testing.

3.2.10 Post-cyclic reconsolidation

After completion of the cyclic loading stage as per above, specimens were reconsolidated to the initial σ'_{3c} to assess potential post-cyclic volumetric deformations. In this process, at the end of cyclic shearing, specimens were brought back to the initial σ'_1 and σ'_3 values that correspond to the initial applied K_c value and drainage was opened.

3.2.11 Error and uncertainty

The triaxial test is an element test and to be considered an element test, the stresses and strains should be uniformly distributed in the specimen (Saada and Townsend, 1981). This requires designing a triaxial apparatus and test procedure to achieve close to uniform conditions as possible. Deviation from this uniform state can result in errors in the measured properties of the soil specimen.

Any sources of errors should be identified, estimated, and corrected or reduced where possible. On the UBC-CTX, such error can arise from sensors, membrane resistance, pore water drain resistance, piston friction and specimen geometry.

Errors in sensors mainly arise due to non-linearity and hysteresis. These errors were kept to a minimum on the UBC-CTX by calibrating each sensor and against maximum expected loads during triaxial testing and within the linear range of the sensor.

The rubber membrane surrounding the specimen transmits a radial and axial effective stress to the specimen (Germaine and Ladd, 1988). Equations developed by Kuerbis and Vaid, 1990 were used to apply corrections to σ'_1 and σ'_3 based on thin elastic cylindrical shell theory. These corrections involve estimating axial and radial stresses and strains from un-stretched and stretched membrane dimensions, and membrane stiffness.

The efficiency of the pore water drainage system is a major factor contributing to consolidation times and equalization of Δu during undrained shearing. An end drainage system using porous stone discs was selected for the UBC-CTX device due to the complexities associated with incorporating the more effective radial filter drainage in into the design of the silt reconstitution technique. The presence of a porous stone disc increases the friction at the ends of the specimen. This can cause non-uniform stress and strain conditions throughout the specimen during consolidation and shearing, leading to error in reduced parameters (Germaine and Ladd, 1988). It was therefore considered important to keep the size of the porous stone disc to a minimum while still facilitating drainage of pore water in a timely manner. Specimen drainage is a function of hydraulic conductivity (k). It can be observed that k is far greater for silts than clays. On this basis, the size of the porous stone was limited to a diameter of 36 mm, keeping the ratio of porous stone to polished smooth metal to slightly less than 25%. After conducting trial

tests on reconstituted Kamloops silt, the time to reach primary consolidation was estimated to be reached within a reasonable time frame of 60 minutes.

It has been long recognised that rate of loading can influence strength and u response. A detailed discussion on rate of loading can be found in Section 3.2.9.2 and Appendix A.

3.3 Replication

The degree to which the slurry deposition technique is able to replicate specimens at a particular initial effective confining stress level during undrained monotonic shear and undrained cyclic shear is illustrated in Figure 3.13 and Figure 3.14. Excellent repeatability may be noted in these test results.

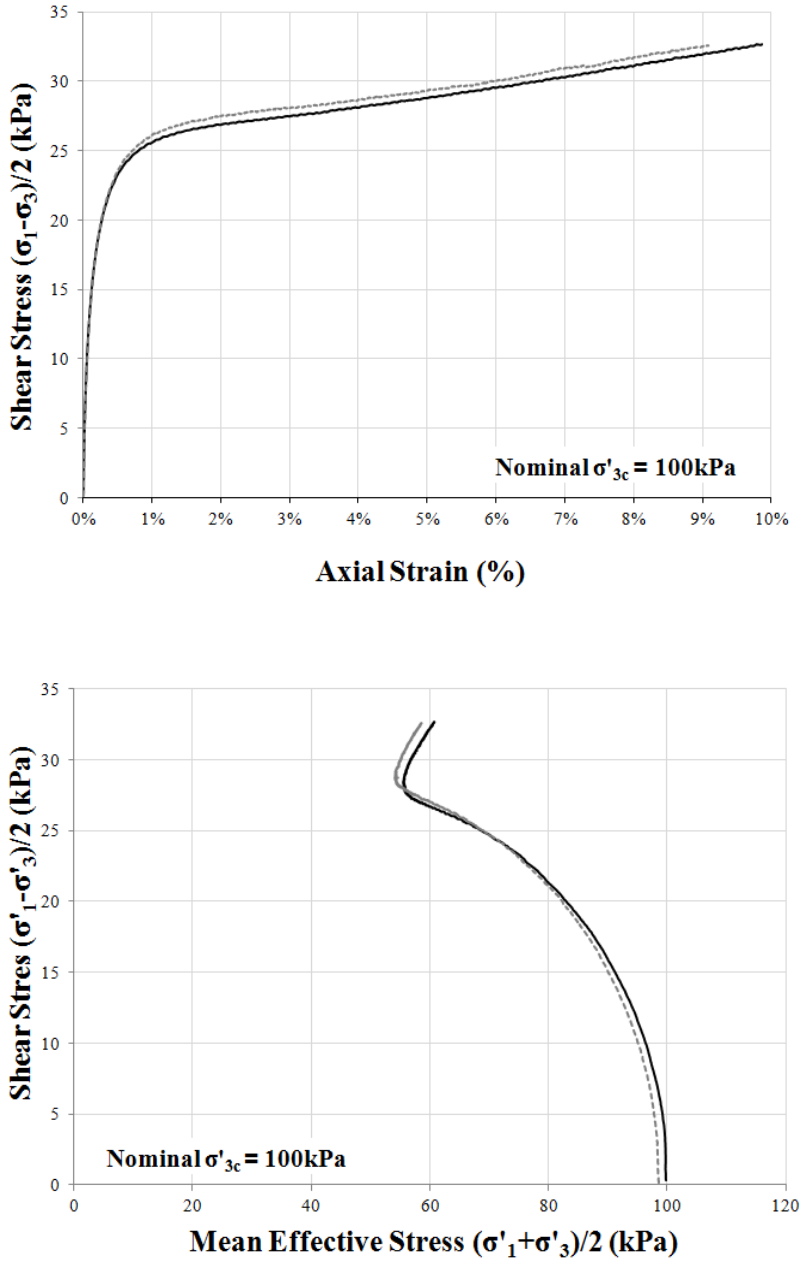

Figure 3.13 Repeatability of the slurry deposited Kamloops silt: Monotonic shear

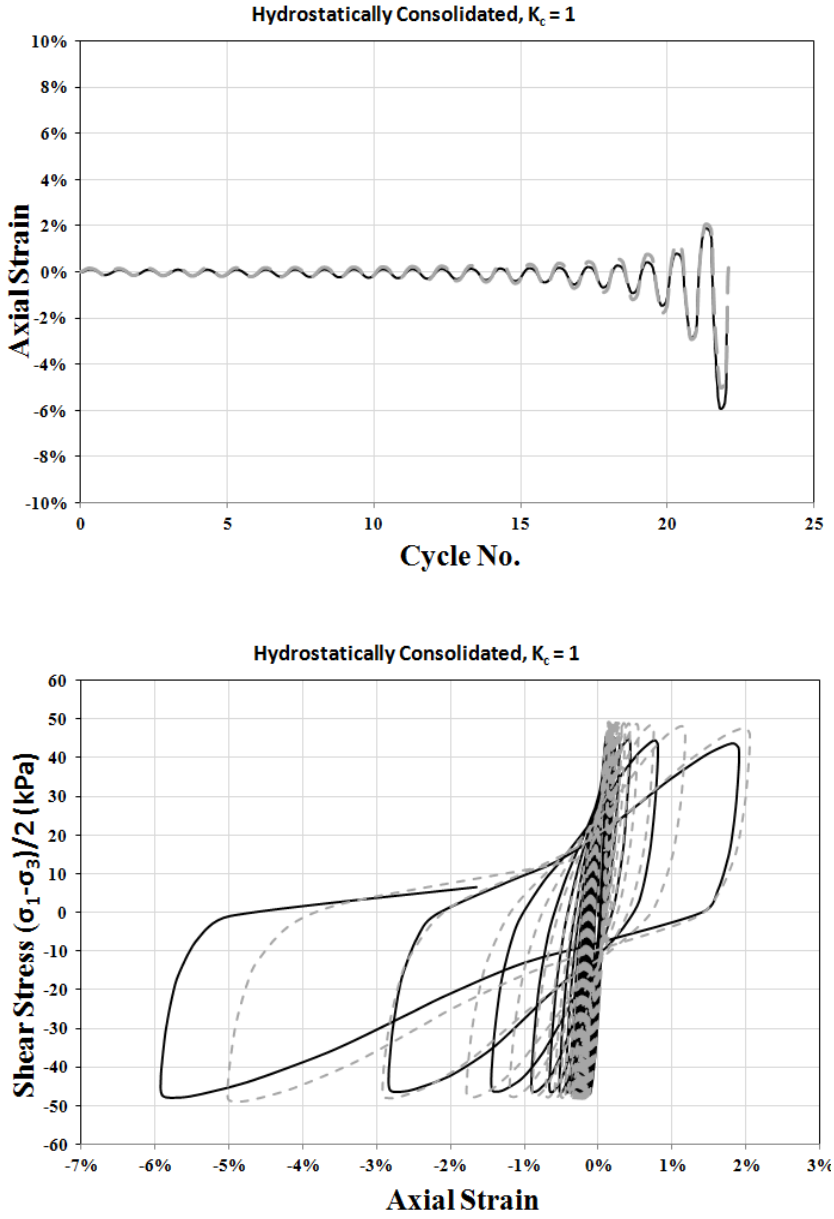

Figure 3.14 Repeatability of the slurry deposited Kamloops silt: Cyclic shear

3.4 Test program

A systematic testing program was undertaken with the main objective of validating the capability of the newly upgraded UBC-CTX device for monotonic and cyclic shear testing. The fundamental mechanical response of Kamloops silt, reconstituted from a slurry state as described in Section 3.2.4, was tested, varying different parameters to investigate the following:

- Undrained monotonic shear response under conventional TC and TE over a range of hydrostatically consolidated σ'_{3c} levels.
- Drained monotonic shear response under conventional TC over a range of hydrostatically consolidated σ'_{3c} levels;
- Undrained cyclic shear loading response over a range of hydrostatically consolidated σ'_{3c} levels;
- Undrained cyclic shear loading response at a single hydrostatic consolidation σ'_{3c} level with application of an initial static shear bias to three target (K_c) levels before cyclic shearing; and
- Post cyclic reconsolidation response over a range of hydrostatically consolidated σ'_{3c} levels, both with and without static shear bias.

Table 3.5 presents a summary of the proposed test program describing each of the test series and parameters investigated.

Table 3.5 Test program

Test Series	Material/Tests	Test ID	Nominal σ'_{3c} (kPa)	CSR = $q_{cyc}/2\sigma'_3$	Static Bias $K_c = \sigma'_1/\sigma'_3$	No. of Tests
I	Kamloops silt: Undrained monotonic shear in conventional triaxial compression and extension, effects of initial hydrostatic effective confining stress	TC100	100	MONOTONIC, $K_c = 1$		6
		TC200	200			
		TC300	300			
		TE100	100			
		TE200	200			
		TE300	300			
II	Kamloops silt: Drained monotonic shear in triaxial compression	DT100	100	MONOTONIC, $K_c = 1$		3
		DT200	200			
		DT300	300			
III	Kamloops silt: Undrained cyclic shear response, effect of initial hydrostatic effective confining stress	IC100-1	100	0.135	$K_c = 1$	12
		IC100-2	100	0.150		
		IC100-3	100	0.180		
		IC100-4	100	0.210		
		IC200-1	200	0.130		
		IC200-2	200	0.170		
		IC200-3	200	0.190		
		IC200-4	200	0.230		
		IC300-1	300	0.120		
		IC300-2	300	0.155		
		IC300-3	300	0.160		
		IC300-4	300	0.185		
IV	Kamloops silt: Undrained cyclic shear response, effect of initial static shear bias, K_c	SC100-1	100	0.155	1.1	9
		SC100-2	100	0.180	1.1	
		SC100-3	100	0.230	1.1	
		SC100-4	100	0.130	1.2	
		SC100-5	100	0.210	1.2	
		SC100-6	100	0.265	1.2	
		SC100-7	100	0.170	1.4	
		SC100-8	100	0.210	1.4	
		SC100-9	100	0.250	1.4	

Total No. Tests: 30

Chapter 4: Experimental Results and Discussion

As mentioned in Section 1.2, the main objective of this study was to upgrade the University of British Columbia (UBC) cyclic triaxial device (CTX) and develop a suitable specimen reconstitution method, enabling triaxial testing of reconstituted low plastic silts at UBC. As part of this development, trial tests were conducted to find a suitable silt specimen preparation procedure (see Section 3.2.4.4). After final refinements were made, reconstituted specimens of Kamloops silt were verified with respect to uniformity and test repeatability (see Section 3.2.4.7 and Section 3.3). Once this initial work was complete, the second objective was to carry out initial key experimental work to investigate the monotonic and cyclic shear response of reconstituted specimens of Kamloops silt. The purpose of doing this initial testing was twofold; 1) To demonstrate the capabilities of the upgraded UBC CTX; and 2) To study the behavioural characteristics of Kamloops silt under monotonic and cyclic shear loading.

The results from the test program performed on specimens of reconstituted Kamloops silt, sourced from the exposed bluffs in Kamloops are presented herein. Details relating to material properties, specimen preparation and test procedures are described in Chapter 3 of this thesis. A summary of the test results, including the range of void ratios obtained from specimens of each test series are presented below in Table 4.1, Table 4.2, Table 4.3 and Table 4.4.

Table 4.1 Test parameters and summary results (Test series I)

Test ID	Skempton's B Value	w_{i-av}	e_i	σ'_{3c} (kPa)	e_c	$K_c=\sigma'_1/\sigma'_3$	$q_{cyc}/2\sigma'_{3c}$	$N_{(\varepsilon_a=2.5\%)}$	ε_{a-max}*	ε_{v-max}	ε_{v-pc}
TC100	1.00	60.1%	1.660	99.6	0.863	1.0	N/A	N/A	9.93%	N/A	N/A
TC200	1.00	60.0%	1.655	203.09	0.801	1.0	N/A	N/A	10.30%	N/A	N/A
TC300	1.00	59.8%	1.651	290.99	0.757	1.0	N/A	N/A	10.50%	N/A	N/A
TE100	1.00	59.9%	1.652	100.21	0.861	1.0	N/A	N/A	-8.71%	N/A	N/A
TE200	1.00	59.9%	1.653	200.49	0.795	1.0	N/A	N/A	-8.32%	N/A	N/A
TE300	0.99	60.0%	1.655	285.02	0.760	1.0	N/A	N/A	-8.34%	N/A	N/A

w_{i-av} = average water content of initial slurry; e_i = void ratio of initial slurry; σ'_{3c} = consolidated hydrostatic effective confining stress; e_c = void ratio of consolidated slurry consolidated ; K_c = effective consolidation stress ratio; q_{cyc} = single amplitude cyclic deviator stress; $N_{(\varepsilon_a=2.5\%)}$ = number of cycles to reach 2.5% axial strain; ε_{a-max} = maximum axial strain; ε_{v-max} = maximum volumetric strain; ε_{v-pc} = maximum post-cyclic volumetric strain.

Table 4.2 Test parameters and summary results (Test series II)

Test ID	Skempton's B Value	w_{i-av}	e_i	σ'_{3c} (kPa)	e_c	$K_c=\sigma'_1/\sigma'_3$	$q_{cyc}/2\sigma'_{3c}$	$N_{(\varepsilon_a=2.5\%)}$	ε_{a-max}*	ε_{v-max}	ε_{v-pc}
DTC100	1.02	60.1%	1.660	100.02	0.981	1.0	N/A	N/A	12.88%	5.05%	N/A
DTC200	1.00	60.1%	1.660	200.19	0.929	1.0	N/A	N/A	12.80%	5.79%	N/A
DTC300	1.00	59.9%	1.654	299.73	0.905	1.0	N/A	N/A	10.70%	5.40%	N/A

Table 4.3 Test parameters and summary results (Test series III)

Test ID	Skempton's B Value	w_{i-av}	e_i	σ'_{3c} (kPa)	e_c	$K_c=\sigma'_1/\sigma'_3$	$q_{cyc}/2\sigma'_{3c}$	$N_{(\varepsilon_a=2.5\%)}$	ε_{a-max}*	ε_{v-max}	ε_{v-pc}
IC100-1	1.00	59.9%	1.654	92.74	0.829	1.0	0.135	98	-8.00%	N/A	4.94%
IC100-2	1.00	60.2%	1.662	92.92	0.903	1.0	0.150	52	-8.41%	N/A	4.62%
IC100-3	1.00	60.1%	1.658	93.22	0.964	1.0	0.180	13	-8.71%	N/A	4.81%
IC100-4	1.00	60.1%	1.659	89.85	0.869	1.0	0.210	4	-8.81%	N/A	3.99%
IC200-1	1.00	59.9%	1.653	185.22	0.827	1.0	0.130	135	-9.05%	N/A	4.74%
IC200-2	1.00	59.9%	1.653	186.77	0.865	1.0	0.170	15	-9.95%	N/A	4.68%
IC200-3	0.98	60.0%	1.656	190.73	0.779	1.0	0.190	6	-9.62%	N/A	4.18%
IC200-4	1.00	59.9%	1.653	186.00	0.818	1.0	0.230	2	-11.17%	N/A	4.70%
IC300-1	0.99	60.3%	1.663	284.12	0.820	1.0	0.120	286	-7.71%	N/A	4.13%
IC300-2	1.00	59.9%	1.654	287.80	0.783	1.0	0.155	22	-9.87%	N/A	4.53%
IC300-3	0.99	60.1%	1.658	283.72	0.872	1.0	0.160	22	-8.05%	N/A	4.26%
IC300-4	0.99	60.0%	1.657	284.31	0.826	1.0	0.185	8	-11.15%	N/A	4.80%

Table 4.4 Test parameters and summary results (Test series IV)

Test ID	Skempton's B Value	w_{i-av}	e_i	σ'_{3c} (kPa)	e_c	$K_c=\sigma'_1/\sigma'_3$	$q_{cyc}/2\sigma'_{3c}$	$N_{(\varepsilon_a=2.5\%)}$	ε_{a-max}*	ε_{v-max}	ε_{v-pc}
SC100-1	0.98	60.3%	1.664	94.50	0.914	1.1	0.155	68	8.49%	N/A	5.03%
SC100-2	1.10	60.0%	1.657	87.07	0.822	1.1	0.180	33	7.33%	N/A	11.24%
SC100-3	0.98	60.0%	1.657	91.83	0.859	1.1	0.230	5	-6.52%	N/A	3.82%
SC100-4	0.99	60.0%	1.657	92.44	0.933	1.2	0.130	267	7.72%	N/A	3.80%
SC100-5	0.98	59.9%	1.653	93.23	0.920	1.2	0.210	10	7.46%	N/A	3.83%
SC100-6	0.99	60.0%	1.657	91.56	0.890	1.2	0.265	3	9.11%	N/A	4.36%
SC100-7	0.98	60.0%	1.656	91.15	0.857	1.4	0.170	25	7.14%	N/A	2.00%
SC100-8	0.98	59.9%	1.653	88.65	0.822	1.4	0.210	12	7.45%	N/A	2.18%
SC100-9	0.98	60.0%	1.655	90.40	0.886	1.4	0.250	3	8.87%	N/A	2.91%

4.1 Monotonic undrained shear loading response

Conventional undrained triaxial shear tests were performed in order to characterize the monotonic stress-strain response of the reconstituted Kamloops silt. The laboratory testing herein focused on testing specimens initially consolidated to different hydrostatic effective confining stress (σ'_{3c}) levels to study the influence of initial effective confining stress; and tests were conducted in triaxial compression (TC) and triaxial extension (TE) shear loading conditions to study the influence of mode of shear.

Specimens were consolidated to initial σ'_{3c} ranging between 100 to 300kPa (Test Series I, Table 3.5). Stress-strain and stress path responses obtained from undrained monotonic shear tests are presented in Figure 4.1 and Figure 4.2 respectively.

In terms of stress-strain characteristics (Figure 4.1), no specimens displayed any notable 'strain softening' type response (except for a very mild strain softening trend that was noted in a TE test conducted with $\sigma'_{3c} \approx$ 100 kPa and 300 kPa. Clearly, the undrained shear strength measured in TE was approximately 20% lower than the shear strength measured in TC. This difference is in accord with the stress-path dependency typically found in gravity deposited sediments, and is considered to be due to the anisotropic soil fabric.

A summary of mobilised undrained shear strength from triaxial tests (s_{u-mob}) at relatively large axial strain (ε_a) are presented below in Table 4.5.

Table 4.5 Mobilised undrained shear strength at relatively large axial strain

Test ID	Nominal σ'_{3c} (kPa)	s_{u-mob}
TC100	100	31
TC200	200	58
TC300	300	94
TE100	100	21
TE200	200	41
TE300	300	62

As may be noted from the stress paths (Figure 4.2), the specimens have deformed initially in a contractive manner and this is followed by a dilative response. This dilative type of behaviour is similar to what has been observed in other reconstituted specimens of low plastic silt prepared using a similar specimen preparation method (Hyde et al. 2006; Sanin. 2010; Wang et al. 2011). The points at which phase transformation (contractive to dilative type behaviour) occur, mobilized angle of friction at maximum obliquity (ϕ'_{MAX}) and mobilised friction angle at phase transformation (ϕ'_{PT}), measured directly from the stress path plot are also identified in Figure 4.2. This plot indicates similar values of ϕ'_{MO} and ϕ'_{PT} in TC and TE modes of shear. In addition, the transformation appears to fall close to the stress ratio at maximum obliquity. Vaid and Chern (1985) suggested

that the ϕ_{PT} is close to the friction angle at steady state ϕ'_{SS} for sands. Due to the dilative tendency of the tested Kamloops silt and physical limitations of the UBC-CTX device, it is difficult to confirm the validity of this for reconstituted Kamloops silt. Additional research work focussing on monotonic testing at larger axial strains could be used to confirm steady state conditions of the Kamloops silt.

Figure 4.3 shows stress paths normalized with respect to initial hydrostatic σ'_{3c}. These normalized stress paths fall within a relatively narrow range. Similar stress path normalizability was also noted by Sanin (2011) for tests conducted on low plastic Fraser River silt using the UBC direct simple shear device. It is also of interest to highlight that this "normalizable" response is similar to that typically observed for normally consolidated clays (Atkinson & Bransby, 1978).

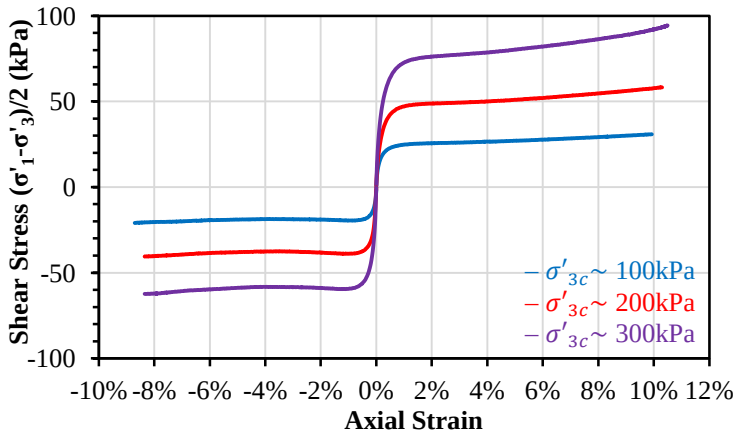

Figure 4.1 Undrained monotonic TC and TE testing on reconstituted specimens of Kamloops silt at varying confining stress levels: Stress-strain curves; σ'_{3c} ~ 100, 200 and 300kPa

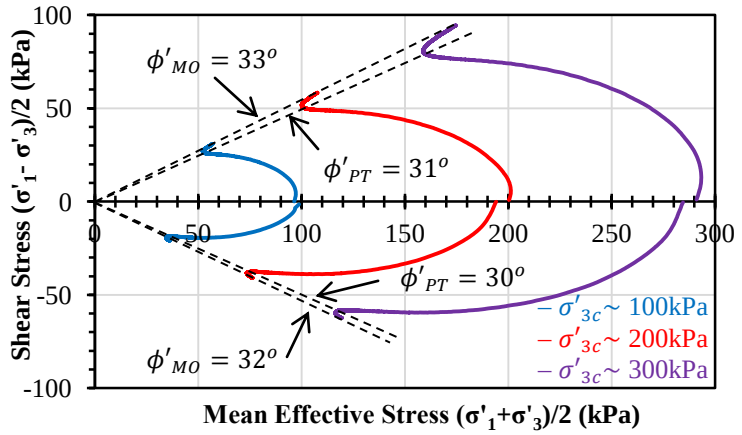

Figure 4.2 Undrained monotonic TC and TE testing on reconstituted specimens of Kamloops silt at varying confining stress levels: Stress path curves; σ'_{3c} ~ 100, 200 and 300kPa

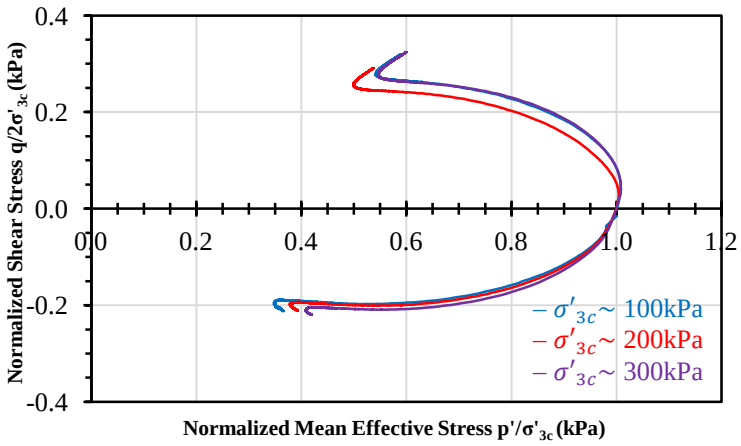

Figure 4.3 Undrained monotonic TC and TE testing on reconstituted specimens of Kamloops silt at varying confining stress levels: Normalized stress path curves; σ'_{3c} ~ 100, 200 and 300kPa

4.2 Monotonic drained shear loading response

CTX tests in Test Series II (see Table 4.2) involved investigating the drained conventional TC shear response of reconstituted Kamloops silt. Specimens were consolidated to the same initial hydrostatic σ'_{3c} levels investigated in test Series I. Stress-strain, volumetric strain, and stress path responses obtained from undrained monotonic triaxial tests are presented in Figure 4.4, Figure 4.5 and Figure 4.6 respectively. In order to facilitate a direct comparison with undrained monotonic shear behaviour, corresponding data derived from undrained monotonic TC shear tests are superimposed onto the stress path plot.

In terms of stress-strain characteristics (Figure 4.4), all the specimens can be considered to have exhibited a strain hardening response. The stress-strain response was normalized with respect to initial hydrostatic σ'_{3c} (Figure 4.7). This plot shows the stress-strain response of the drained shear tests falling within a relatively narrow range. In general, this "normalizable" response is similar to that typically observed for normally consolidated clays (Atkinson & Bransby, 1978).

In terms of volumetric strain characteristics (Figure 4.5), all specimens experienced a contractive type response with the specimen volume reducing at all strain levels. It is also noted that a similar volumetric strain response was observed at all initial hydrostatic σ'_{3c} levels. This similarity in volumetric strain has also been observed in normally consolidated clays (Atkinson & Bransby,

1978). It is likely that the test conducted at initial hydrostatic $\sigma'_{3c}\sim$ 100kPa, has almost reached a point of maximum contractive behaviour. However, this could not be confirmed due axial strain limitations of the UBC-CTX device.

As may be noted from the stress path response (Figure 4.6), at all initial hydrostatic σ'_{3c} levels, the stress path follows a straight line response at a slope of 1.0. This is in agreement with the total stress path response that is usually observed truly drained conventional TC shear tests. As noted above, the test conducted at initial hydrostatic $\sigma'_{3c}\sim$ 100kPa has likely reached a point of maximum contractive behaviour. The mobilised friction angle at maximum contraction ϕ'_{MC} measured from this point was observed to be similar to the ϕ'_{PT} measured from undrained TC shear tests. Wijewickreme (1986) suggests that for sands, the correspondence between ϕ_{MC} and ϕ_{PT} should only be made for soils that exhibit an initially contractive response. The results of this testing suggest that this qualification may perhaps also extended to normally consolidated reconstituted low plastic silt. It should be noted that the drained TC shear test conducted at initial $\sigma'_{3c}\sim$ 300kPa had to be terminated early due to the limiting capacity of the load cell.

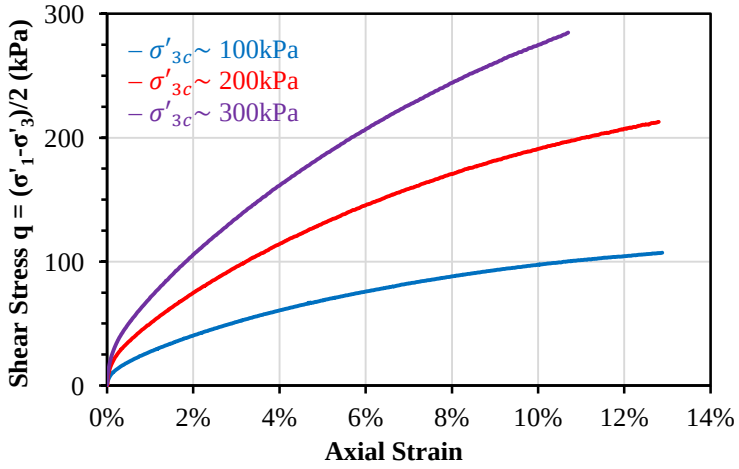

Figure 4.4 Drained monotonic TC testing on reconstituted specimens of Kamloops silt at varying confining stress levels: Stress-strain curves; σ'_{3c} ~ 100, 200 and 300kPa

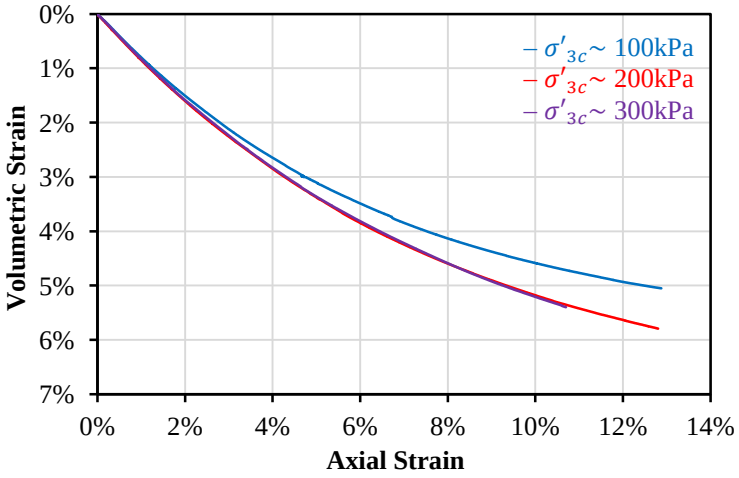

Figure 4.5 Drained monotonic TC testing on reconstituted specimens of Kamloops silt at varying confining stress levels: Volumetric strain curves; σ'_{3c} ~ 100, 200 and 300kPa

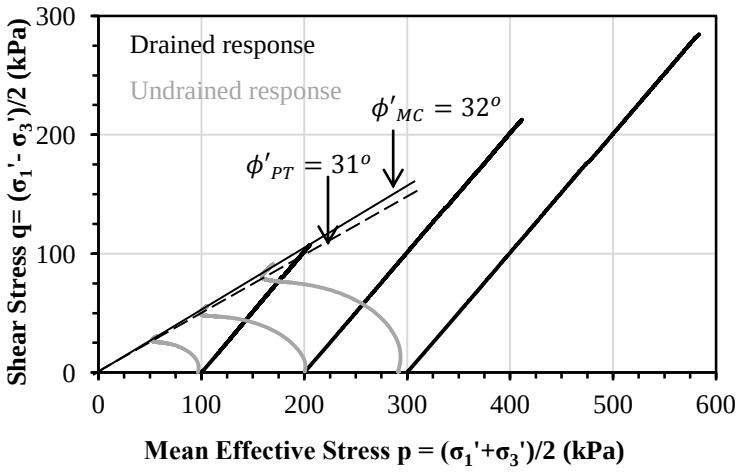

Figure 4.6 Drained monotonic TC testing on reconstituted specimens of Kamloops silt at varying confining stress levels: Stress path curves; σ'_{3c} ~ 100, 200 and 300kPa. (Undrained response superimposed)

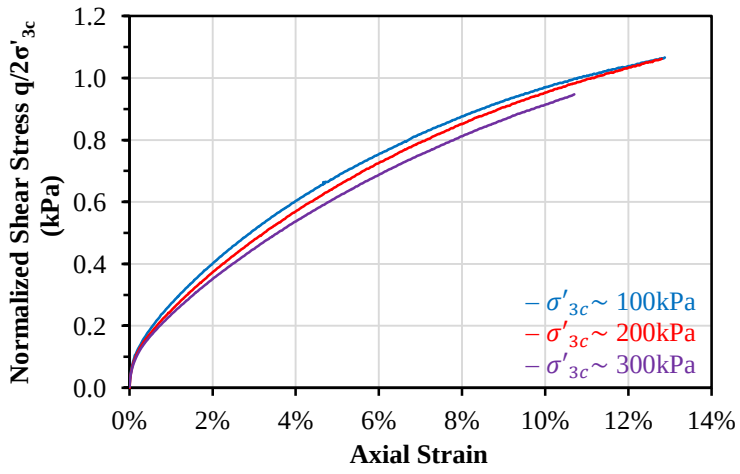

Figure 4.7 Drained monotonic TC testing on reconstituted specimens of Kamloops silt at varying confining stress levels: Normalized stress path curves; σ'_{3c} ~ 100, 200 and 300kPa

4.3 Cyclic shear loading response

The following sections present the results of key laboratory tests assessing the cyclic shear response of reconstituted Kamloops silt. The effects of the following parameters on the cyclic shear response of the material are investigated: (i) effect of initial confining stress – from tests conducted on specimens consolidated to different initial hydrostatic σ'_{3c} with no static shear bias (Test Series III, see Table 4.3); (ii) the effect of the initial static shear bias – studied using tests conducted on specimens consolidated under different initial static shear stress conditions (Test Series IV, see Table 4.4).

4.3.1 Effect of initial effective confining stress

4.3.1.1 General stress-strain and pore water pressure response

Test Series III investigated the effects of the initial effective confining stress on the cyclic loading response of Kamloops silt. As indicated in Table 3.5, the effect of initial effective confining stress was investigated at three different hydrostatic σ'_{3c} levels: 100, 200 and 300 kPa. The intent here is to present typical test results and then examine and highlight some of the key observations and findings emerging from these results.

The applied single amplitude cyclic deviator stress (q_{cyc}) corresponding to tests conducted at three different cyclic stress ratio (CSR) levels with an initial hydrostatic $\sigma'_{3c}\sim$ 100kPa are presented in Figure 4.8. For clarity purposes, this plot is shown to a maximum of 10 loading cycles. The observed axial strain (ε_a) and excess pore water pressure (Δu) development with number of loading cycles as a result of these applied q_{cyc} values are presented in Figure 4.9 and Figure 4.10 respectively. In the pore water pressure response, the excess pore water pressure ratio is normalized with respect to initial hydrostatic effective confining stress r_u [$\Delta u/\sigma'_{3c}$]. The corresponding stress strain and stress path responses at different CSR values and initial $\sigma'_{3c}\sim$ 100kPa are presented in Figure 4.11, Figure 4.12 and Figure 4.13. Following a similar format, the results of tests with an initial hydrostatic $\sigma'_{3c}\sim$ 200 kPa and 300 kPa are presented in Figures C.1 to C.12 of Appendix C.

In response to cyclic loading, all specimens exhibit gradual increase of ε_a and r_u with increasing number of loading cycles. As expected, the rate of r_u generation increases with increasing applied CSR. For example, at $\sigma'_{3c}\sim$ 100kPa, and a CSR value of 0.170, r_u approached unity within 15 cycles compared to a test a CSR value of 0.230 where r_u approached unity within 2 cycles. It is also important to note that for all tests, r_u eventually reached unity at relatively low axial strains (2-4%). For example, with a CSR value of 0.150 and $\sigma'_{3c}\sim$ 100kPa, r_u approached

unity within 50 cycles when axial strain reached 2%. It is also of interest to note that significant accumulation of shear strain occurred even at moderate levels of loading. For example at initial hydrostatic σ'_{3c}~ 100kPa - a test with a CSR value of 0.190 reached axial strains in the order of 10% within 5 cycles compared to at test with a CSR value of 0.130 where there was almost no axial strain was observed after 100 cycles of loading.

With respect to stress-strain response, at all initial hydrostatic σ'_{3c} levels, specimens can be considered to have exhibited a cumulative development of axial strain and gradual reduction in shear stiffness, accompanied by gradual reduction in effective confining stress. With respect to stress path, it is reasonable to state that all specimens are showing an initially cumulatively contractive response. This cyclic mobility type response is similar in form to the undrained (constant-volume) cyclic shear responses from cyclic shear tests on natural silts, fine grained mine tailings, and clays (Zergoun and Vaid, 1994; Wijewickreme et al., 2005; Sanin, 2010; Seidalinova, 2014; Soysa, 2015) and dense reconstituted sand (Sriskandadakumar 2004). It is of importance to note, that this cyclic mobility type response was observed irrespective of the initial hydrostatic consolidation stress level (σ'_{3c}).

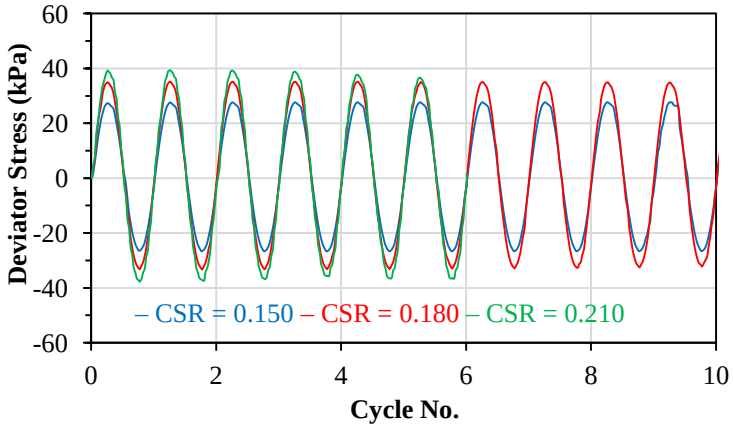

Figure 4.8 Undrained triaxial cyclic shear test on reconstituted specimen of Kamloops silt: Applied single amplitude deviator stress (q_{cyc}) vs. number of loading cycles for different CSR values; σ'_{3c} ~ 100; K_c=1.0

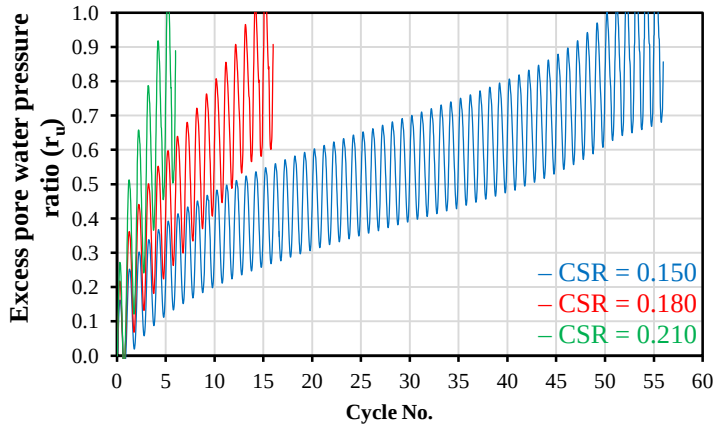

Figure 4.9 Undrained triaxial cyclic shear test on reconstituted specimen of Kamloops silt: Excess pore water pressure ratio (r_u) vs. number of loading cycles for different CSR values; σ'_{3c} ~ 100; K_c=1.0

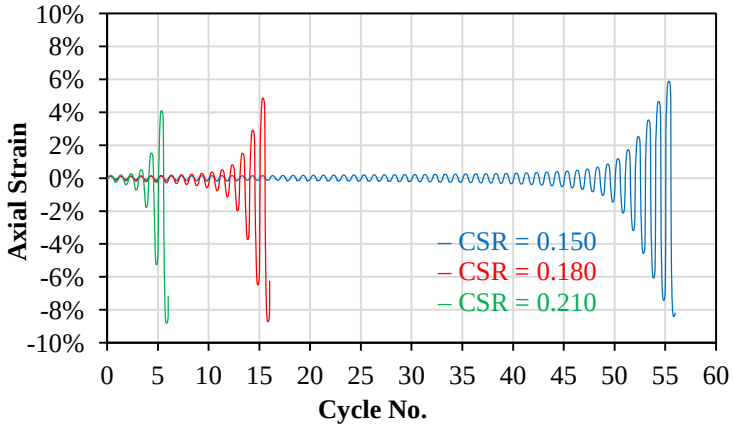

Figure 4.10 Undrained triaxial cyclic shear test on reconstituted specimen of Kamloops silt: Axial strain (ε_a) vs. number of loading cycles for different CSR values; σ'_{3c} ~ 100; K_c=1.0

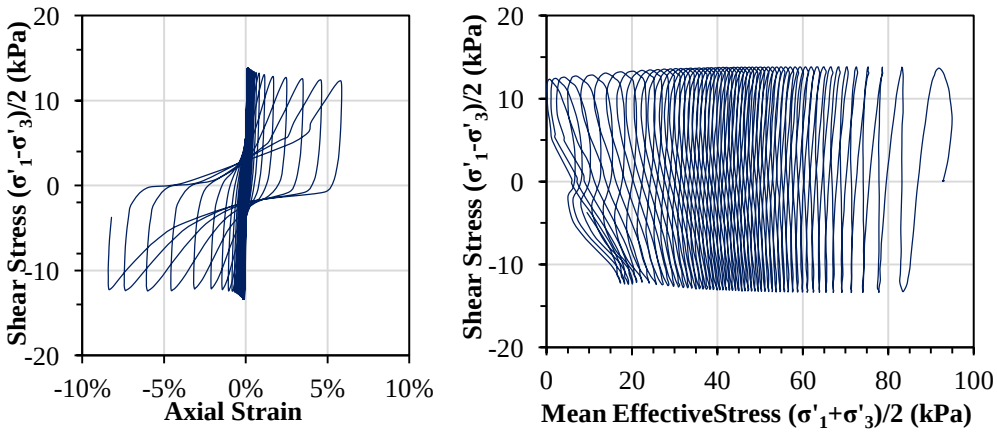

Figure 4.11 Undrained triaxial cyclic shear test on reconstituted specimen of Kamloops silt: Stress-strain and stress path curves; σ'_{3c} ~ 100kPa; CSR = 0.150; K_c=1.0.

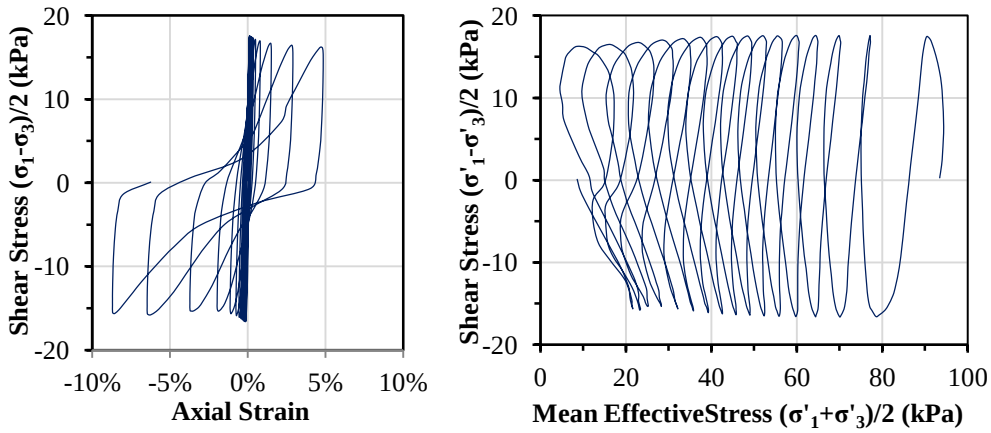

Figure 4.12 Undrained triaxial cyclic shear test on reconstituted specimen of Kamloops silt: Stress-strain and stress path curves; σ'_{3c} ~ 100kPa; CSR = 0.180; K_c=1.0

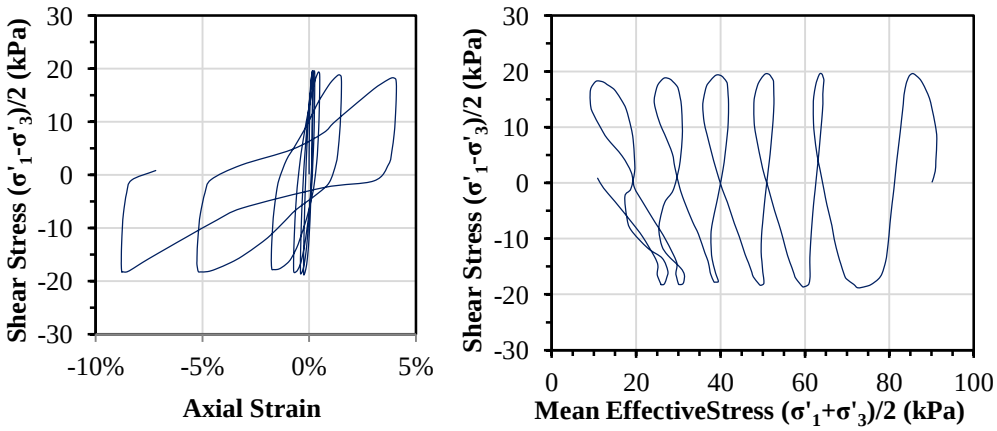

Figure 4.13 Undrained triaxial cyclic shear test on reconstituted specimen of Kamloops silt: Stress-strain and stress path curves; σ'_{3c} ~ 100kPa; CSR = 0.210; K_c=1.0

4.3.1.2 Cyclic shear resistance

It is also of interest to examine the cyclic shear resistance ratio (CRR) of reconstituted Kamloops silt by comparing the response observed from triaxial

testing under different applied cyclic loadings and effective confining stress levels. In order to facilitate this comparison, the number of load cycles required to reach a single-amplitude axial strain ε_a= 2.5%, in a given applied CSR, was defined as $N_{\varepsilon_a=2.5\%}$. This 2.5% single-amplitude axial strain in a triaxial soil specimen is essentially equivalent to reaching 3.75% single-amplitude axial strain in constant volume cyclic direct simple shear (CDSS). An identical definition has been previously used to assess the cyclic shear resistance of sands by the U.S. National Research Council (NRC 1985), and has been adopted in many previous liquefaction studies at UBC.

The applied cyclic stress ratio [CSR = $(q_{cyc}/2\sigma'_{3c})$] is plotted against number of cycles to reach single-amplitude ε_a= 2.5% at initial hydrostatic $\sigma'_{3c}\sim$ 100kPa, 200kPa and 300kPa is presented in Figure 4.14. The data points seem to fall on a single trend-line suggesting that cyclic resistance is relatively insensitive to confining pressure and that the response is influenced only by the mobilised CSR. It is important to note that this 'normalizable' type behaviour is also in accord with the coincidence of normalized stress paths found from monotonic shear tests of the same soil, as described in Section 4.1. Similar behaviour has been observed for normally consolidated low plastic Fraser River silt under constant volume CDSS (Sanin & Wijewickreme, 2005; Sanin, 2010; and Soysa, 2005) and for normally consolidated Cloverdale clay in cyclic triaxial tests (Zergoun and Vaid,

1994). These results are in harmony with the typical behavioural frameworks noted for normally consolidated clay (e.g. Atkinson, 1993).

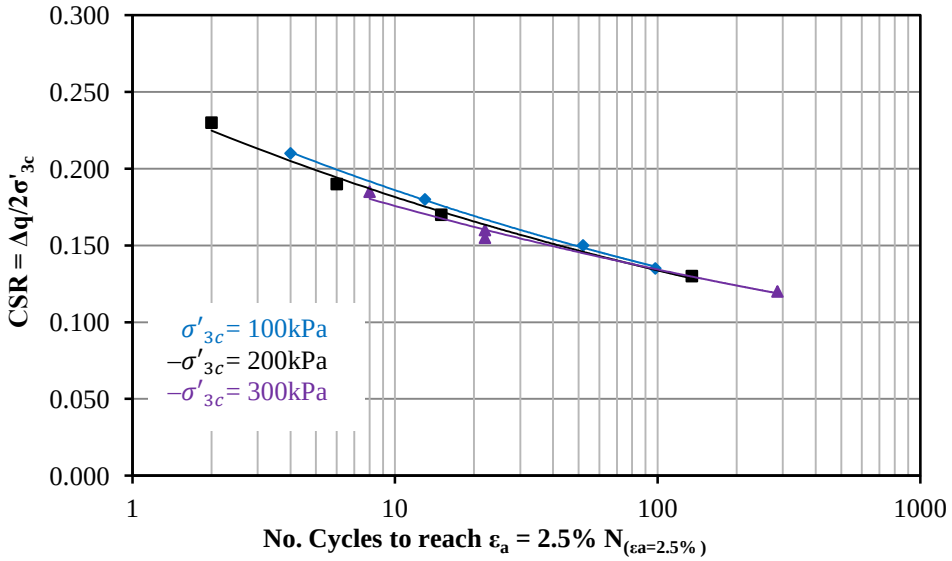

Figure 4.14 Cyclic resistance ratio from undrained cyclic triaxial tests on reconstituted specimens of Kamloops silt at varying initial effective confining stress levels; K_c = 1.0

The results of the undrained cyclic triaxial tests performed at initial hydrostatic $\sigma'_{3c}\sim$ 100kPa, 200kPa and 300kPa can also be plotted in the form of cyclic strength ratio defined as the ratio of the applied single amplitude cyclic deviator stress, q_{cyc}, to the undrained shear strength (s_{u-mob}) obtained from the undrained monotonic triaxial compression shear tests (see Table 4.5) and is shown in Figure 4.15. This approach has been previously been used to interpret the results of cyclic testing for clays (e.g. Zergoun & Vaid 1994; Andersen 2009; Idriss and Boulanger 2008). The data points seem to fall on a single trend-line also

suggesting that the cyclic resistance of reconstituted Kamloops silt is not sensitive to initial effective confining stress levels up to 300kPa. The observations are also in accord with the normalized behaviour observed from undrained monotonic triaxial loading. Additional testing would need to be carried out to confirm if this 'normalizable' type behaviour can be extended effective confining stress levels higher than 300kPa.

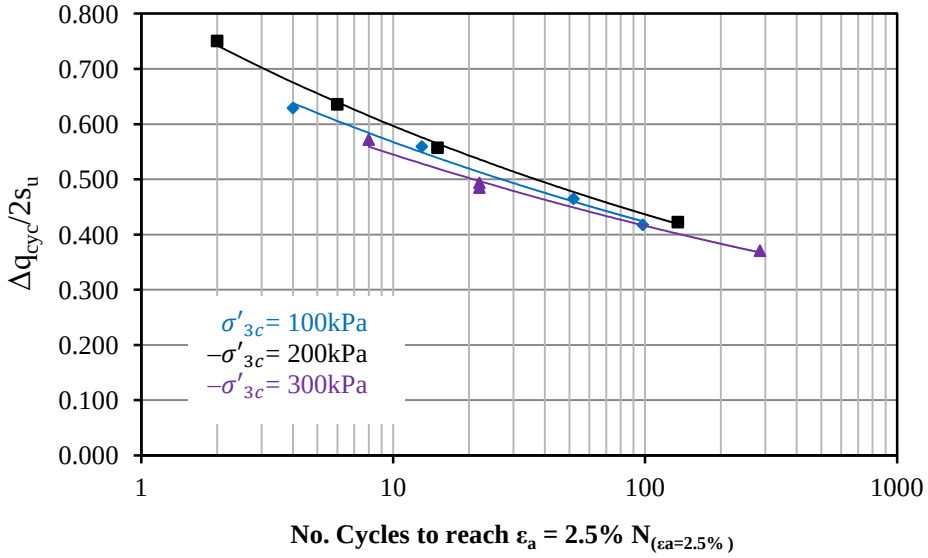

Figure 4.15 Cyclic strength ratio (q_{cyc}/s_u) from undrained cyclic triaxial tests on reconstituted specimens of Kamloops silt at varying initial confining stress levels

It is also of interest to review the above observations with respect to the generally accepted response of relatively clean sands. In sands, the cyclic resistance generally increases with increasing density; for a given relative density, the cyclic resistance in sands has been noted to decrease with increasing confining stress

(Seed & Harder, 1990). In addition to the effects of density and confining pressure, the difference in particle fabric alone could lead to significant differences in cyclic resistance ratios (Kuerbis, 1989; Khalili & Wijewickreme, 2008). The observations presented herein suggest that, the dilative tendency arising due to stress densification seems to have been overcome by the possible contractive tendency due to the increase in confining stress.

4.3.2 Effect of initial static shear bias

4.3.2.1 General stress-strain and pore-water pressure response

As indicated in Table 3.5, the effects of static shear bias were investigated for three different values of $K_c = (\sigma'_1/\sigma'_3)$: 1.1, 1.2 and 1.4 (Test Series IV). The typical applied q_{cyc}; development of excess pore water pressure ratios r_u [$\Delta u/\sigma'_{3c}$]; and development of axial strain (ε_a) cyclic loading for one selected CSR value of 0.21 and comparing different values of K_c are presented in Figure 4.16, Figure 4.17, and Figure 4.18 respectively. The corresponding cyclic loading, stress-strain and stress path responses are presented in Figure 4.19, Figure 4.20, and Figure 4.21.

As may be noted, cyclic mobility type strain development was observed in all of the tests throughout the cyclic loading process. Again, liquefaction in the form of strain softening, accompanied by loss of shear strength did not manifest itself

regardless of the K_c value and applied CSR level. However, the buildup of excess pore ware pressure with the increase in number of cycles could result in significant cyclic shear strains even at moderate levels of cyclic loading. A comparison of tests conducted at CSR value of 0.21 indicates that there is a marked increase of the rate of development of excess pore water pressure (with respect to number of applied CSR cycles) with increase in K_c level.

It is noted that at some of the CSR stress levels a softening effect can be seen, especially long duration tests at large number loading cycles, as can be seen in Figure 4.21. It is believed this is due to a problem related to the pneumatic stress controlled loading system.

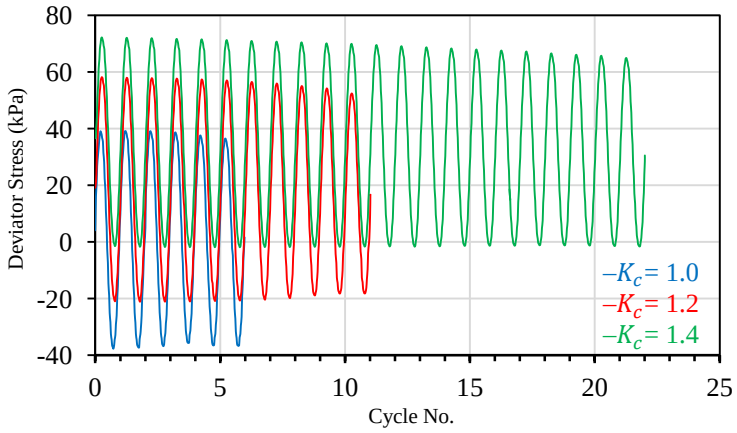

Figure 4.16 Undrained triaxial cyclic shear test on reconstituted specimen of Kamloops silt: Applied single amplitude deviator stress (q_{cyc}) vs. number of loading cycles for different K_c values; σ'_{3c} ~ 100; CSR = 0.21

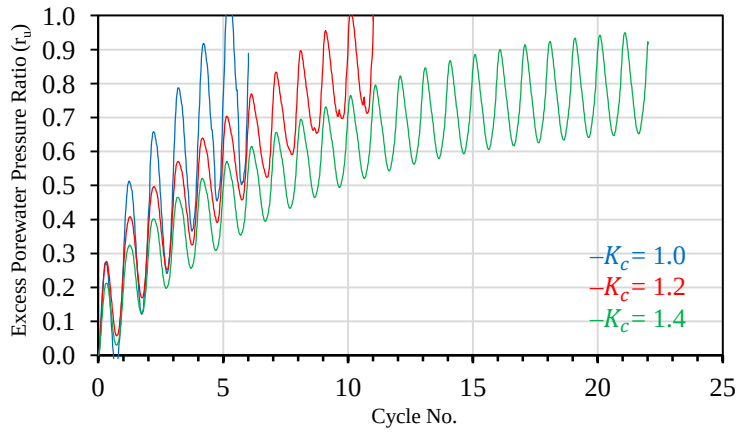

Figure 4.17 Undrained triaxial cyclic shear test on reconstituted specimen of Kamloops silt: Excess pore water pressure ratio (r_u) vs. number of loading cycles for different K_c values; σ'_{3c} ~ 100; CSR = 0.21

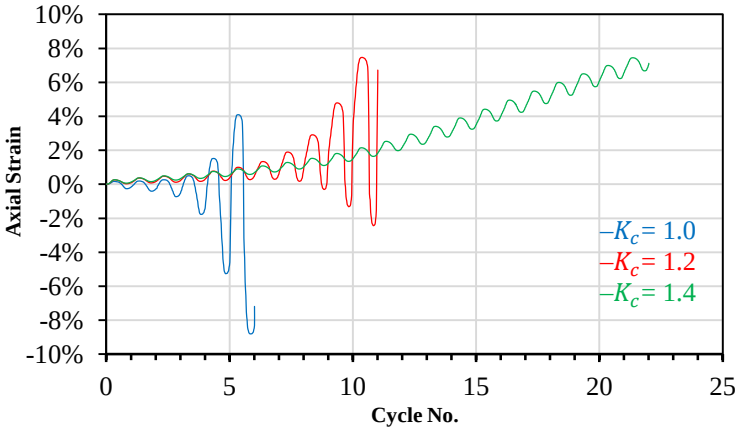

Figure 4.18 Undrained triaxial cyclic shear test on reconstituted specimen of Kamloops silt: Axial strain (ε_a) vs. number of loading cycles for different K_c values; σ'_{3c} ~ 100; CSR = 0.21

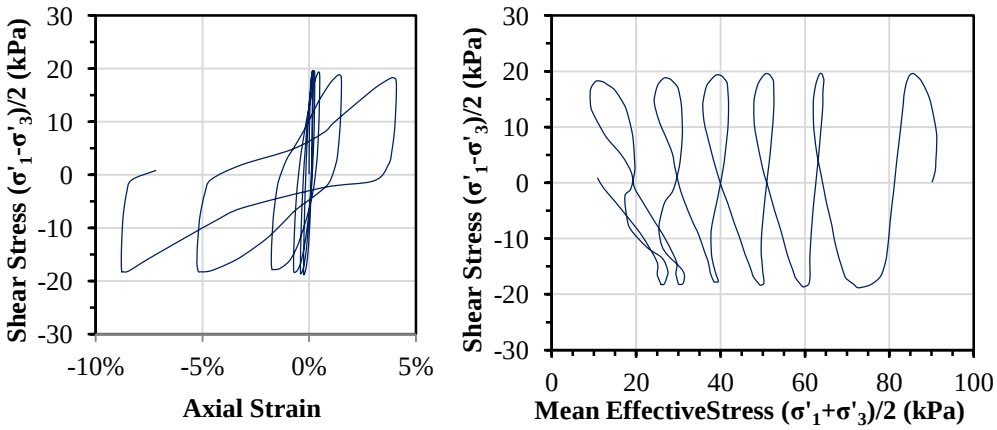

Figure 4.19 Undrained triaxial cyclic shear test on reconstituted specimen of Kamloops silt: Stress-strain and stress path curves; σ'_{3c} ~ 100kPa; CSR = 0.210; K_c=1.0

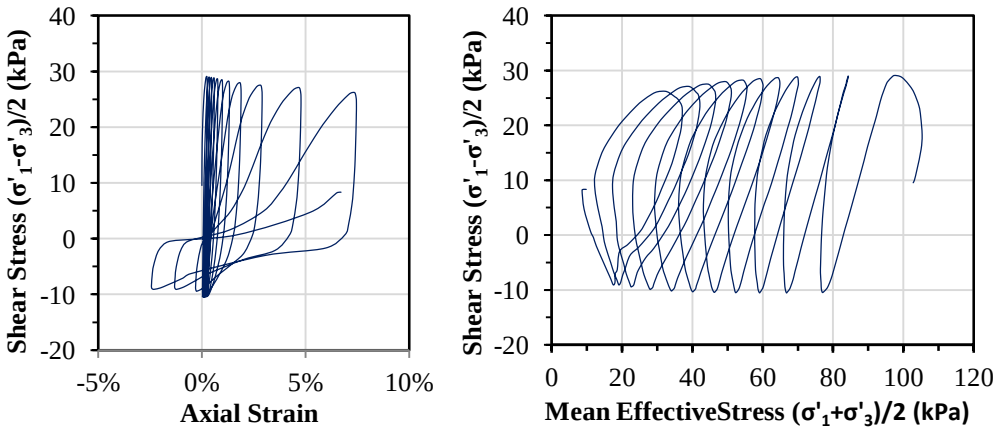

Figure 4.20 Undrained triaxial cyclic shear test on reconstituted specimen of Kamloops silt: Stress-strain and stress path curves; σ'_{3c} ~ 100kPa; CSR = 0.210; K_c=1.2

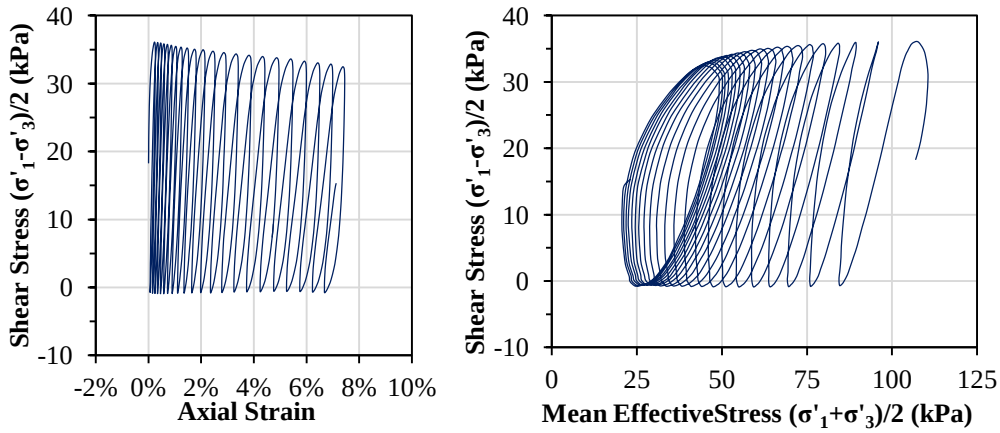

Figure 4.21 Undrained triaxial cyclic shear test on reconstituted specimen of Kamloops silt: Stress-strain and stress path curves; σ'_{3c} ~ 100kPa; CSR = 0.210; K_c=1.4

4.3.2.2 Cyclic shear resistance

The number of load cycles ($N_{\varepsilon_a=2.5\%}$) required to reach a single-amplitude axial strain ε_a = 2.5% under a given applied CSR was plotted in Figure 4.22 to examine the effect of K_c on cyclic shear resistance. The relationship for each value of K_c can be represented by trend-lines. Comparison of these trend-lines reveals that the CRR of the tested material is relatively insensitive to the applied static shear bias. A slight increase in CRR is observed from $K_c = 1$ to $K_c = 1.1$, and no distinct change in CRR was observed between $K_c = 1.1$, 1.2 and 1.4. A similar trend is has been seen in cyclic triaxial testing of dense Fraser River sands where an increase in CRR has been observed with increase in static shear bias level (Sivathayalan & Ha, 2011).

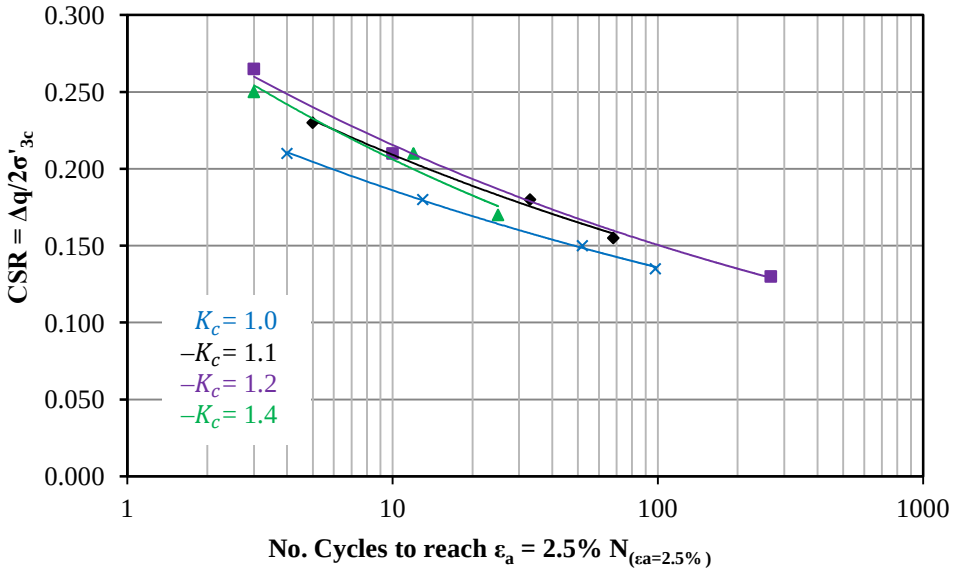

Figure 4.22 Cyclic resistance ratio from constant volume cyclic DSS tests on reconstituted specimens of Kamloops silt at varying initial static shear bias (K_c) levels; $\sigma'_{3c} \sim 100$

4.3.3 Comparison with typical cyclic response of sands

It is useful to make a comparison between the stress-strain and excess pore water pressure response observed for reconstituted Kamloops silt (tests both with and without initial static shear bias) and those observed from tests on sands. Previous observations by Vaid and Chern (1985) on the triaxial shear response of Ottawa sand are used to make this comparison. This work has shown that relatively loose Ottawa sand ($D_{ri} \sim$ 30%, e_i = 0.725) developed a strain softening limited liquefaction response (as described in Section 2.2) under triaxial cyclic shear loading regardless of the consolidation stress. This abrupt loss of shear stiffness is clearly in accord with the idea of liquefaction "triggering" as noted previously

during other research on sands (Castro 1969; Ishihara et al. 1975). On the other hand, when the same Ottawa sand was tested under at a slightly denser sate (D_{ri} ~ 45%, e_i = 0.700), it has been observed that the material would exhibit a dilative cyclic mobility type response (as described in Section 2.2). The observations from tests conducted in this study suggest that the shear behaviour of reconstituted Kamloops silt, which exhibited gradual excess pore water pressure development with progressive degradation of shear stiffness in undrained cyclic shear loading regardless of initial σ'_{3c}, K_c or CSR level, is more similar to dense sand in the behavioural pattern than to relatively loose sand.

4.3.4 Post-cyclic reconsolidation

Typical post-cyclic reconsolidation volumetric strain (ε_{v-pc}) versus time responses of reconstituted Kamloops without initial static shear bias (Test Series III - Table 3.5) are presented in Figure 4.23. For all tests in this series, similar ε_{v-pc} levels were observed regardless of the applied CSR and initial effective confining stress levels.

Sanin (2010) indicated from constant volume direct simple shear testing on Fraser River silt that cyclic excess pore water pressure is a key factor that control post cyclic volumetric strain. A comparison of ε_{v-pc} obtained from cyclic triaxial testing of reconstituted Kamloops silt (Test Series III - Table 3.5) with the results

of Sanin (2010) are presented in Figure 4.24. The results indicate the measured ε_{v-pc} from Test Series III are in close agreement with the results obtained by Sanin (2010).

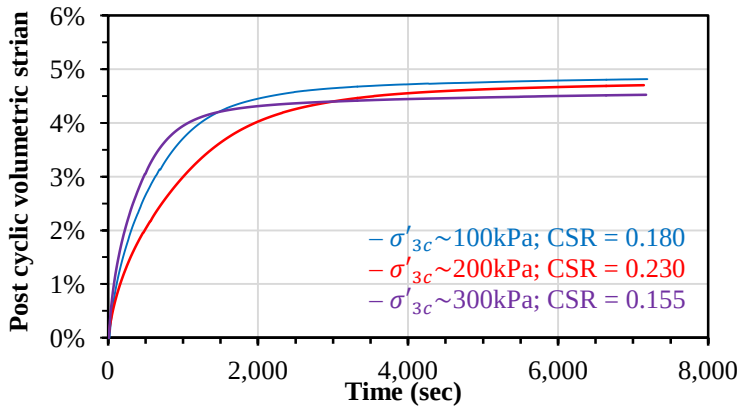

Figure 4.23 Typical post cyclic volumetric strain (ε_{v-pc}) versus time characteristics of reconstituted Kamloops silt during post cyclic consolidation (Test series III)

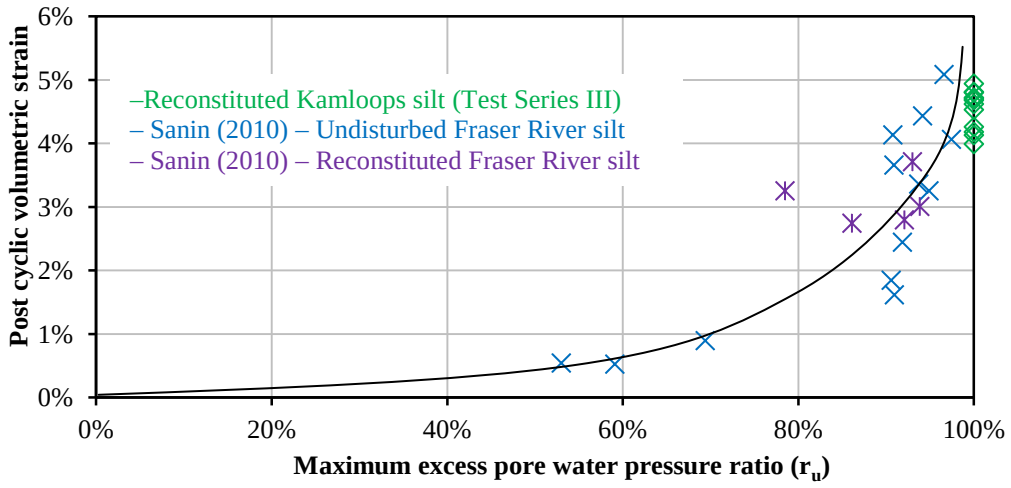

Figure 4.24 Post cyclic volumetric strain (ε_{v-pc}) versus excess pore water pressure ratio (r_u) of reconstituted Kamloops (Test series III) and normally consolidated Fraser River Silt (Sanin, 2010).

4.3.5 Error in pore water pressure measurement

It is noted that in all cyclic shear tests, effective stress paths reached impossibly high effective stress ratios toward the end of tests. The effective stress paths are dependent on the measured total stress and pore water pressure. The total stress is directly measured and should have good accuracy; on the other hand, the pore water pressure is measured at the end of the specimen and may be subject to pore water pressure inequalisation effects. As such, the likely cause is strain-rate related non-uniform pore water pressure distribution within the specimen and a delay in pore water pressure response at the base of the specimen. Due to the time constraints and the requirement to conduct a meaningful number of tests in this

study a sinusoidal frequency of 0.1 Hz was adopted for this research. In any case, the stress and strain measurements are independent of the pore water pressure measurements and as such, stress strain plots can be considered in isolation for liquefaction triggering assessment. Furthermore, if any such error exists with the pore water pressure measurements these errors are likely systematic and the pore water pressure measurements could be used for comparative purposes and identifying general trends.

Chapter 5: Summary and Conclusions

The UBC triaxial apparatus was upgraded and a specimen preparation technique was developed to allow conventional monotonic and cyclic shear tests to be carried out at UBC. Once verified in terms of specimen uniformity and test repeatability, this specimen preparation technique was then used to examine the undrained shear response of low-plastic, fine grained reconstituted natural silt (Kamloops silt) using data from conventional monotonic and cyclic triaxial tests. This research focussed on: (i) Technological advancement in preparing uniform specimens of reconstituted silt for triaxial testing that yield repeatable test results; and (ii) Understanding the effects of the following factors on the monotonic and cyclic loading response of low plastic silt (Kamloops silt): initial effective confining stress and initial static shear bias. This chapter summarizes the key contributions, and presents conclusions and recommendations originating from the research.

For the purpose of clarity, this information is presented as separate sections for each of the following areas of work (i) Upgrade of the UBC triaxial device; (ii) Development of a suitable reconstitution technique for silts; (iii) Monotonic shear response of reconstituted low plastic Kamloops silt; (iv); Cyclic shear response and post-cyclic reconsolidation response of reconstituted low plastic Kamloops silt; and (v) Recommendations for future research.

5.1 Upgrade of the UBC triaxial device

In order to conduct conventional triaxial monotonic shear and cyclic triaxial shear testing, upgrades to the UBC triaxial device were required. Such modifications included: (i) a new cell design to accommodate silt specimens with specimen dimensions of approximately 73mm and 150mm high and; (ii) upgrade of the data acquisition system to provide the necessary function generators (FG) for cell pressure and deviator stress control and full time monitoring of sensor variables during all stages of the triaxial test. The dimensions of the specimens were selected to be similar to undisturbed specimens that have been extruded previously from modified Shelby tubes at UBC (Sanin, 2010; Seidalinova, 2014; Soysa, 2015).

5.2 Development of specimen preparation methods

In order to investigate the fundamental characteristic response of low plastic silts, a specimen reconstitution technique suitable for element testing of silts was developed. In element testing, homogenous (uniform) reconstituted specimens, yielding repeatable results are required. The research undertaken in this thesis involved developing a slurry consolidation method to reconstitute silt specimens for conventional triaxial monotonic and cyclic shear testing. It was demonstrated that this method would lead to relatively uniform specimens in terms of density (void ratio), particle size distribution. This preparation method resulted in high

levels of saturation with measured Skempton's B values in excess of 0.98 and very good repeatability of test results. It is understood that the specimen reconstitution method can have a profound influence on the soil particle fabric. Although particle fabric was not directly investigated, the slurry consolidation method was considered to be the most appropriate method for simulating the deposition of natural silts, when compared to the only other viable method for fine grained soils which is moist tamping.

5.3 Undrained monotonic response of reconstituted Kamloops silt

Normally consolidated specimens tested in triaxial compression (TC) and triaxial extension (TE) at various initially consolidated isotropic consolidation stress up to a maximum value of 300kPa showed that the reconstituted Kamloops silt initially behave in a contractive manner followed by a dilative response. In addition, the stress paths were found to be "normalizable" with respect to initial hydrostatic effective confining stress. Additional testing would be required to validate this "normalizable" behaviour at higher effective confining stresses. In terms of stress-strain response, all specimens showed a slight strain hardening type behaviour that is typical of material undergoing a shear-induced dilative response. At all tested initial effective confining stress levels, the undrained shear strength measured in TC was found to be 20% larger than the undrained shear strength measured in TE. This difference is in accord with the stress-path dependency

typically found in gravity deposited sediments, and is considered to be due to the anisotropic soil fabric.

5.4 Drained monotonic response of reconstituted Kamloops silt

Under conventional drained TC loading, normally consolidated specimens of reconstituted Kamloops silt displayed a reduction in volume (contractive behaviour) up to a maximum tested axial strain level of about 13 %. Volumetric strains were found to be independent of initial consolidated hydrostatic confining stress up to a maximum value of 300kPa. In terms of stress-strain response, specimens exhibited a strain hardening type response which was "normalizable' with respect to initial hydrostatic effective confining stresses up to a maximum value of 300kPa. Additional testing would be required to validate this "normalizable" behaviour at higher effective confining stresses.

5.5 Cyclic shear response of reconstituted Kamloops silt

Liquefaction in the form of strain softening, accompanied by loss of shear strength, was not observed regardless of the applied cyclic stress ratio (CSR). Under triaxial undrained cyclic loading, reconstituted Kamloops silt exhibited a cumulative increase in axial strain with increasing number of load cycles (i.e. cyclic-mobility-type strain development mechanism), similar to the observed behaviour of dense sands and natural Fraser River silt.

This type of behaviour was observed regardless of the initial confining stress, initial static shear bias, identified as effective consolidation stress ratio (K_c) in triaxial testing, or applied CSR level. No strain softening/and or loss of shear strength was observed in any of the tests that were conducted under different values of the above variables. The cyclic resistance ratio (CRR) of normally consolidated reconstituted Kamloops silt was not sensitive to the initial consolidated hydrostatic effective confining stress (σ'_{3c}) for the tested stress range of 100kPa < σ'_{3c} < 300kPa. The tests results also indicated that the CRR is relatively insensitive to the effective consolidation stress ratio (K_c) with a slight increase in CRR observed from K_c = 1 to K_c = 1.1 and no notable change between from K_c = 1.1 and K_c = 1.2.

5.6 Limitations and recommendations for future research

In addition to the research findings presented above, the investigation has also led to the identification of a number of limitations and suggestions for future research as given below:

- It is anticipated that the specimen preparation method causes some initial stress non-uniformities. These stress non uniformities are expected to have an insignificant effect on tests conducted at effective confining stress levels greater than 100kPa. However, the effect of these initial induced

shear stresses should be further investigated if tests using this reconstitution method are conducted at effective hydrostatic consolidation stresses of less than 100kPa.

- In all undrained cyclic triaxial tests, effective stress paths exhibited impossibly high stress ratios toward the end of cyclic shear testing. This is believed to be due to a strain rate effect causing pore water pressure non equalisation within the specimen during shear. Liquefaction assessment, in terms of degradation in shear stiffness and accumulation of strain can still be considered accurate in isolation to the pore water pressure response. Howevever, future laboratory testing, using the UBC-CTX apparatus and UBC-TSC device, should investigate effect of strain rate on the pore water pressure response. Numerical simulations involving finite element or finite difference solutions could also be carried out in an attempt to quantify the delay in pore water pressure at the base of the specimen and come up with an estimate the actual pore water pressure response at the centre of the specimen, where most of the shear induced pore water pressures are expected to occur.
- The current study investigated the effect of effective confining stresses stress levels up to 300kPa. There is a need to extend the study to include higher effective confining stress levels, particularly if studying deeper marine soil deposits typically found in lower mainland BC.

- Due to physical limitations of the UBC-CTX device, drained and undrained monotonic shear tests were carried out to maximum axial strains in the order of 10%. It is recommended that modifications be made to the cell design to allow additional research to be conducted at larger axial strains.
- Additional research should be undertaken with the objective of comparing laboratory element behaviour with data obtained from constant volume direct simple shear testing and hollow cylinder testing to further investigate the influence of mode of shear on the monotonic and cyclic shear response of natural and reconstituted silts.
- During cyclic shear testing, a softening effect of the applied cyclic shear stress was observed and is believed to be a problem related to the pneumatic system. It is suggested that the stress controlled cyclic loading be futher improved with feedback in the data aquisition and control system to esnure that the applied shear stress level is uniform and corrected as the loading reduces.

References

Andersen, K.H. (2009). Bearing capacity under cyclic loading - offshore, along the coast and on land. The 21st Bjerrum Lecture presented in Oslo, 23 Nov. 2007. *Canadian Geotechnical Journal,* 46(5), p. 513-535.

Atkinson, J.H., Bransby, P.L. (1978). The mechanics of Solids, An Introduction to Critical State Soil Mechanics, McGraw Hill Book Company (UK) Ltd.

Atkinson, J. (1993). An introduction to the mechanics of soils and foundations. McGraw Hill, US.

Bishop, A.W., Henkel, D.J. (1957). The measurement of soil properties in the triaxial test, London, William Clowes and Sons, Limited, London and Beccles, p. 1-180.

Boulanger, R.W., Seed, R.B. (1995). Liquefaction of sand under bidirectional monotonic and cyclic loading. *Journal of Geotechnical Engineering,* 121(12), p. 870-878.

Boulanger, R.W., Meyers, M.W., Mejia, L.H., Idriss, I.M. (1998). Behavior of a fine-grained soil during the Loma Prieta earthquake. *Canadian Geotechnical Journal*, 35(1), p. 146-158.

Bradshaw, A.S., Baxter, C.D.P. (2007). Sample preparation of silts for liquefaction testing. *Geotechnical Testing Journal.* 30(4), Paper ID GTJ100206, 9 pages.

Bray, J.D., Sancio, R.B. (2006). Assessment of the Liquefaction Susceptibility of Fine-Grained Soils. *Journal of Geotechnical and Geoenvironmental Engineering,* 132(9), p. 1165-1177.

Carraro, J.A.H., Prezzi, M. (2007). A New Slurry-Based Method of Preparation of Specimens of Sand Containing Fines. *Geotechnical Testing Journal.* 31(1). Paper ID GTJ100207, 11 pages.

Castro, G. (1969). Liquefaction of sands. PhD. Thesis, Harvard University, Cambridge, Mass.

Donahue, J.L., Bray, J.D., riemer, M.F. (2007). The liquefaction susceptibility, resistance, and response of silty and clayey soils.

El Hosri, M.S., Biarez, H., Hicher, P.Y. (1984). Liquefaction characteristics of silty clay. Proceedings of the 8th World Conference on Earthquake Engineering. Prentice-Hall, Englewood Cliffs. N.J. 3. p. 277-284.

Finn, W.D.L., Bransby, P.L., Pickering, D.J. (1970). Effect of Strain History on Liquefaction of Sand. *Journal of the Soil Mechanics and Foundations Division,* ASCE, 96(SM6), p. 1917-1934.

Fulton, R.J. (1965). Silt Deposition in Late-Glacial Lakes of Southern British Columbia. *American Journal of Science,* vol. 263, 553-570.

Geremew, A.M., Yanful, E.K. (2011). Laboratory Investigation of the Resistance of Tailings and Natural Sediments to Cyclic Loading. *Geotechnical and Geological Engineering,* 30(2), p. 431-447.

Germaine, J.T., Ladd, C.C. (1988). Triaxial Testing of Saturated Cohesive Soils, Advanced Triaxial Testing of Soil and Rock, ASTM STP 977, Robert T. Donaghe, Ronald C. Chaney, and Marshall L. Silver, Eds., American Society of Testing and Materials, Philadelphia, 1988, pp. 421-459.

Guo, T., Prakash, S. (1999). Liquefaction of Silts and Silty-Clay Mixtures. *Journal of Geotechnical and Geoenvironmental Engineering,* 5(8), p.706-710.

Guo, Y., Wang, Y. (2009). Experimental Study about the Influence of Initial Water Content in Wet tamping Method on Static Triaxial Test Results of Silt. *Engineering Journal of Geotechnical Engineering*, 13 pages.

Høeg, K., Dyvik, R., Sandbaekken, G. (2000). Strength of undisturbed versus reconstituted silt and silty sand specimens. *Journal of Geotechnical and Geoenvironmental Engineering*, 126(7), p. 606-617.

Hyde, A.F.L., Higuchi, T., Yasuhara, K. (2006). Liquefaction, Cyclic Mobility, and Failure of Silt. *Journal of Geotechnical and Geoenvironmental Engineering,* 132(6) p. 716-735.

Idriss, I.M., Boulanger, R. (2008). Soil liquefaction during earthquakes. Earthquake Research Institute. Pub No. MNO-12, p. 237.

Ishihara, K., Tatsuoka, F., Yasuda, S. (1975). Undrained deformation and liquefaction under cyclic stresses. *Soils and Foundations*, 15(1), p. 29-44.

Ishihara, K., Yamazaki, F. (1980). Cyclic simple shear tests on saturated sand in multi-directional loading. *Soils and Foundations,* Japanese Society of Soil Mechanics and Foundation Engineering, 20(1), p. 45-59.

Ishihara, K. (1993). Liquefaction and flow failure during earthquakes. *Geotechnique,* 43(3), p. 351-415.

Kuerbis, R.H. (1989). The Effect of Gradation and Fines Content on the Undrained Loading Response of Sand. M.A.Sc. Thesis, The University of British Columbia. Retrieved from cirble.ubc.ca.

Khalili, A., Wijewickreme, D. (2008). New Slurry Displacement Method for Reconstitution of Highly Gap-Graded Specimens for Laboratory Element Testing. *Geotechnical Testing Journal.* 31(5). Paper ID GTJ101373, 9 pages.

Kim, H., Daliri, F., Simms, P., Sivathayalan, S. (2011). The influence of desiccation and overconsolidation on monotonic and cyclic shear response of thickened gold tailings. In 2011 Pan-Am CGS Geotechnical Conference. Toronto.

Kuerbis, R.H., Vaid, Y.P. (1990). Corrections for Membrane Strength in the Triaxial Test. Technical Note. American Society for Testing and Materials. p. 361-369.

Ladd, C.C. (1964). Stress-strain behavior of saturated clay and basic strength principles: Research in Earth Physics - Research Report R64-17, Massachusetts Institute of Technology.

Ladd, R.S. (1974) Specimen Preparation and Liquefaction of Sands. *Journal of the Geotechnical Engineering Division,* ASCE, 100(GT10), Proc. Paper 10857, p. 1180-1184.

Lambe, T.W. (1951). Soil Testing for Engineers, John Wiley & Sons, Inc. N.Y.

Lee, K.L., Seed, H.B. (1967). Dynamic strength of anisotropically consolidated sand. Proceedings of the American Society of Civil Engineers, 93(SM5), p. 169-190.

Lefebvre, G., Pfendler, P. (1996). Strain rate and pre-shear effects in cyclic resistance of soft clay. *Journal of Geotechnical Engineering*, 122(1), p. 21-26.

Mathews, P.P. (1971). Glacial lakes and Ice Retreat of South-Central B.C. Transactions of the Royal Society of Canada. 3(38), sec 4, p. 39-57.

Miura, S., Toki, S. (1982). A sample preparation method and its effect on static and cyclic deformation-strength properties of sand. *Soils and Foundations.* 22(1), p. 61-77.

Miura, S., Toki, S., Tanizawa, F. (1984). Cone penetration characteristics and its correlation to static and cyclic deformation-strength behaviors of anisotropic sand. *Soils and Foundations.* 24(2). p. 58-74.

Mulilis, J.P., Seed, H.B., Chan,C.K., Mitchell, J.K., Arulanandan, K. (1977). Effects of sample preparation on sand liquefaction. *Journal of the Geotechnical Engineering Division*, ASCE. 103(GT2), p. 91-108.

Negussey, D., Wijewickreme, D, Vaid, Y.P., (1988). Constant Volume Friction Angle of Granular Materials. *Canadian Geotechnical Journal*, 25(1), p. 50-55.

Oda, M., Koishikawa, I., Highuchi, T. (1978). Experimental study of anisotropic shear strength of sand by plane strain test. *Soils and Foundations*, 18(1), p. 25-38.

Prakash, S., Sandoval, J.A. (1992). Liquefaction of low plasticity silts. *Soil Dynamics and Earthquake Engineering.* p. 373-379.

Puri, V.K. (1990). Liquefaction aspects of loessial soils". Proc. 4th U.S. National Conference on Earthquake Engineering. Earthquake Engineering Research Institute., El Cerito, California (3), p. 755-762.

Quigley, R.M. (1976). Mineralogy, Chemistry and Structure of the Penticton & South Thomson Silt Deposits. Research Report to B.C. Department of Highways, Faculty of Engineering Science, University of Western Ontario, London, Ontario.

Saada, A., Townsend, F. (1981). State of the art: laboratory strength testing of soils. Laboratory shear strength of soil, ASTM STP, 740:7-77.

Sanin, M.V., Wijewickreme, D. (2006). Cyclic shear response of channel-fill Fraser River Delta silt. *Soil Dynamics and Earthquake Engineering.* vol. 26. p. 854-869.

Sanin, M.V. (2010). Cyclic Shear Loading Response of Fraser River Delta Silt. PhD. Thesis, The University of British Columbia.

Schofield, A., Wroth, P. (1968). Critical state soil mechanics. McGraw-Hill Inc., US.

Seed, H.B., Lee, K.L. (1967). Cyclic Stress Conditions Causing Liquefaction of Sand. *Journal of the Soil Mechanics and Foundations Division*, ASCE, 93(SM1), p. 47-70.

Seed, H.B., Duncan, J.M., Idriss, I.M. (1975). Criteria and methods for static and dynamic analysis of earth dams: Criteria and assumptions for numerical analysis of dams. Swansea, Univ. Wales, Swansea, United Kingdom (GBR).

Seed, H.B., Harder, L.F. (1990). SPT-based analysis of cyclic pore pressure generation and undrained residual strength. Proceedings of the H. Bolton Seed Memorial Symposium, 351-376.

Seidalinova, A. (2014). Monotonic and cyclic shear loading response of fine-grained gold tailings. MASc. Thesis, The University of British Columbia.

Sivathayalan, S., Ha, D. (2004). Effect of initial stress state on the cyclic simple shear behaviour of sands. Cyclic Behaviour of Soils and Liquefaction

Phenomena, Triantafyllidis (ed). Taylor & Francis Group, London, p. 207-214.

Sivathayalan, S., Ha, D. (2011). Effect of static shear stress on the cyclic resistance of sands in simple shear loading. *Canadian Geotechnical Journal*, 48, p. 1471-1484.

Soysa, A.N. (2015). Monotonic and Cyclic Shear Loading Response of Natural Silts. MASc. Thesis, The University of British Columbia.

Sriskandakumar, S. (2004).Cyclic loading response of Fraser River sand for validation of numerical models simulating centrifuge tests. PhD thesis, Department of Civil Engineering, The University of British Columbia, Vancouver, BC.

Troncoso, J.H. (1986). Critical state of tailing silty sands for earthquake loadings. *Soil Dynamics and Earthquake Engineering*, 5(3), p. 248-252.

Vaid, Y.P., Finn, W.D.L. (1979). Static shear and liquefaction potential. *Journal of the Geotechnical Engineering Division*, ASCE, 105(GT10), p. 1233-1246.

Vaid, Y.P., Negussey, D. (1988). Preparation of Reconstituted Sand Specimens. Advanced Triaxial Testing of Soil and Rock. R.T. Donaghe, R.C. Chaney, M.L. Silver Eds., ASTM International, West Conshohocken, PA, p. 405-417.

Vaid, Y.P., Chern, J.C. (1985). Cyclic and monotonic undrained response of sands. In V. Khosla (Ed), Advances in the Art of Testing Soils Under Cyclic Conditions, Sponsored by the Geotechnical Engineering Division New York in conjunction with the ASCE Convention, p. 120-147. Detroit, Michigan.

Vaid, Y.P., and Thomas, J. (1995). Liquefaction and postliquefaction behavior of sand. *Journal of Geotechnical Engineering,* ASCE, 121(2), p. 163-173.

Vaid, Y.P., Sivathayalan, S., and Stedman, D. (1999). Influence of Specimen-Reconstituting Method on the Undrained Response of Sand. *Geotechnical Testing Journal.* Vol. 22. p. 187-195.

Vaid, J.P., Stedman, J.D., Sivathayalan, S. (2001). Confining stress and static shear effects in cyclic liquefaction. *Canadian Geotechnical Journal,* 38(3), p. 580-591.

Wang, S., Luna, R., Stephenson, R.W. (2011). A Slurry Consolidation Approach to Reconstitute Low-Plasticity Silt Specimens for Laboratory Triaxial Testing. *Geotechnical Testing Journal.* 34(4). p. 1-9.

Wijewickreme, D. (1986). Constant Volume Friction Angle of Granular Materials MASc. Thesis, The University of British Columbia.

Wijewickreme, D., Sanin, M.V., Greenaway, G.R. (2005). Cyclic shear response of fine-grained mine tailings. *Canadian Geotechnical Journal.* vol. 42. p. 1408-1421.

Yamamuro, J.A., Lade, P.V. (1997). Static liquefaction of very loose sands. *Canadian Geotechnical Journal,* 34(6), p. 905-917.

Zergoun, M., Vaid, Y.P. (1994). Effective stress response of clay to undrained cyclic loading. *Canadian Geotechnical Journal.* vol. 31. p. 714-727.

Appendices

Appendix A Rate of loading

A.1 Drained shear tests

During drained shear, the rate of axial shear must be sufficiently slow for pore water movement throughout the specimen so that pore water pressure everywhere equals back pressure. Experimental evidence shows that 95% dissipation of pore pressure is sufficient to yield accurate drained results (Germaine and Ladd, 1988) The choice of suitable deformation rate for the drained shear tests conducted in this study has been selected based on a method suggested by Bishop and Henkel (1957) and later by Germaine and Ladd (1988), and is based on consolidation theory.

Firstly, the coefficient of consolidation (c_v) is calculated from the consolidation phase of the triaxial test. Bishop and Henkel (1957) suggest using the initial slope of the consolidation versus square root of time curve to estimate t_{100}. A typical consolidation curve was used to estimate t_{100} and is shown below in Figure A.1.

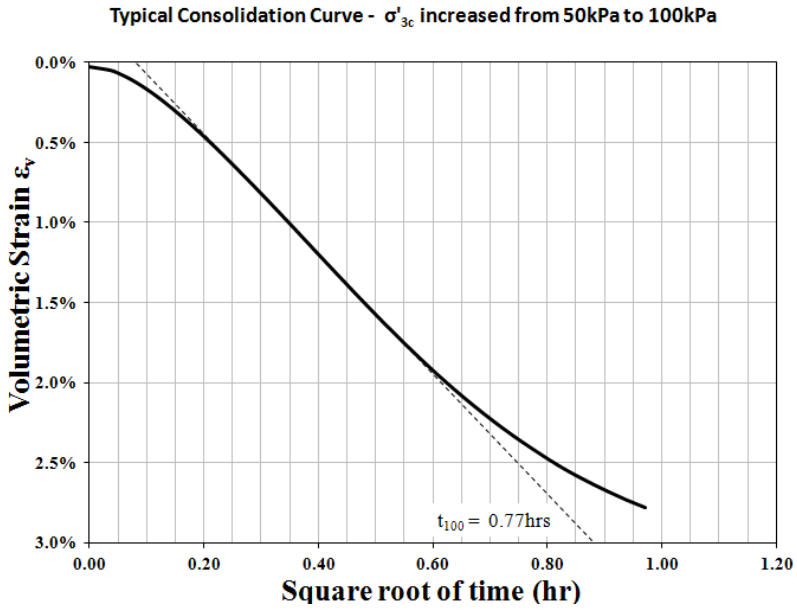

Figure A.1 Estimation of time for 100% consolidation (t_{100}) from typical consolidation curve

From Figure A.1 t_{100} is estimated at 0.77 hours (46 minutes). For specimens with one-way drainage, the following relation can be used to estimate calculate the coefficient of consolidation (c_v):

$$c_v = \frac{\pi h^2}{t_{100}} = \frac{\pi \left(\frac{145mm}{2}\right)^2}{46min} = 359 \ \frac{mm^2}{min} \qquad (1)$$

where *h* is equal to half of the height of the drainage path.

Knowing c_v, the time to failure for a specimen with one-way drainage can then be estimated using the following relation:

$$t_f = \frac{26.7h^2}{c_v} = \frac{26.7\left(\frac{145}{2}\right)^2}{359} = 391 \text{ min} = 6.51\ hrs \quad (2)$$

An appropriate rate of strain for drained shear, a strain rate at failure needs to be determined. Based on the monotonic drained shear tests, the specimen tested with an initial effective confining stress, (σ'_{3c}) was seen to approach the critical state line at an axial strain of 13% and, as such, this strain level will be taken as the axial strain to failure for drained tests (ε_{afd}).

Knowing an estimate of ε_{afd} axial strain at failure and t_f, a strain rate of 2%/hr has been calculated for drained triaxial tests. This rate of axial strain was adopted for all drained shear tests.

A.2 Undrained triaxial tests

During undrained shear testing, the rate of axial shear must be sufficiently slow to ensure equalization of excess pore water pressure across specimen, allowing for reliable pore water pressure. The choice of suitable deformation rate for the drained shear tests conducted in this study has been selected based on a method suggested by Germaine and Ladd (1988).

The time to the first significant measurement can be estimated using the following expression

$$t_s = 2t_{100} \quad (3)$$

Where $t_{100}$is the time for 100% consolidation, estimated in Section A.1. Using this expression, the time to the first significant measurement was estimated to be 92 minutes.

Similarly to drained shear tests, an appropriate rate of strain at failure needs to be determined. Based on the monotonic undrained shear test results, effective stress paths were seen to approach the critical state line at an axial strain of 10% and, as such, this strain level will be taken as the axial strain to failure for undrained tests (ε_{afu}).

Knowing an estimate of ε_{afu} axial strain at failure and t_s, a strain rate of 10%/hr has been calculated for drained triaxial tests. To ensure full equilibrium of internal specimen drainage, undreamed triaxial shear tests were conducted at a much slower rate of axial strain of 6% per hour.

Appendix B Additional cyclic shear test results

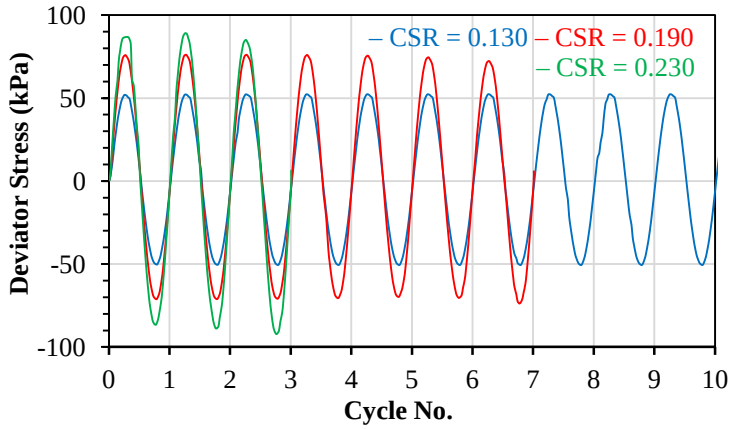

Figure B.1 Undrained triaxial cyclic shear test on reconstituted specimen of Kamloops silt: Applied single amplitude deviator stress (q_{cyc}) vs. number of loading cycles for different CSR values; σ'_{3c} ~ 200; K_c=1.0.

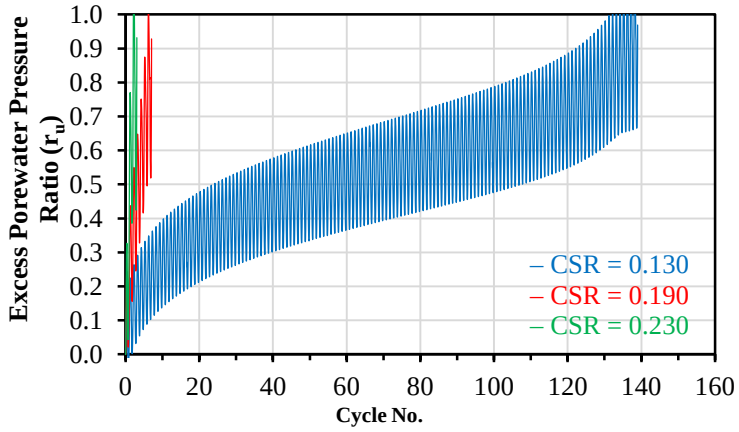

Figure B.2 Undrained triaxial cyclic shear test on reconstituted specimen of Kamloops silt: Excess pore water pressure ratio (r_u) vs. number of loading cycles for different CSR values; σ'_{3c} ~ 200; K_c=1.0.

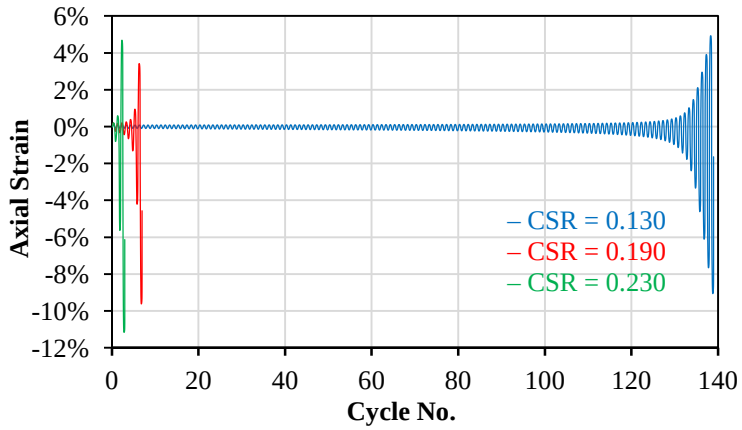

Figure B.3 Undrained triaxial cyclic shear test on reconstituted specimen of Kamloops silt: Axial strain (ε_a) vs. number of loading cycles for different CSR values; σ'_{3c} ~ 200; K_c=1.0.

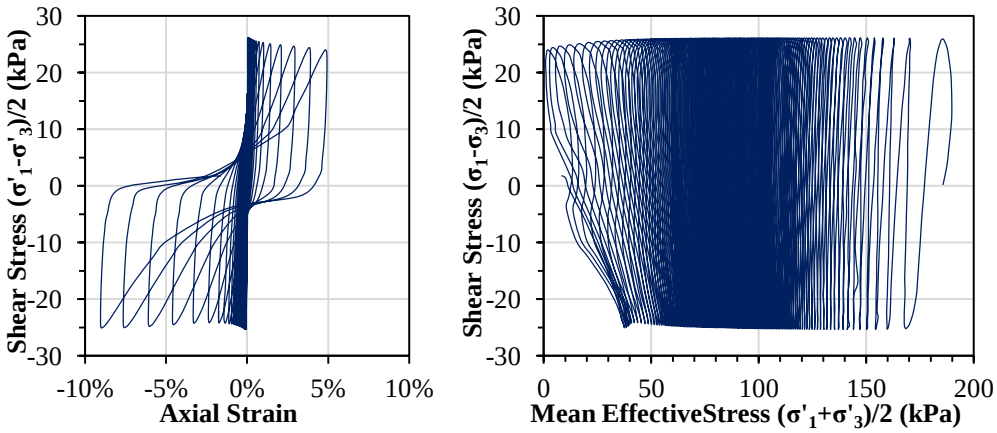

Figure B.4 Undrained triaxial cyclic shear test on reconstituted specimen of Kamloops silt: Stress-strain and stress path curves; σ'_{3c} ~ 200kPa; CSR = 0.130; K_c=1.0.

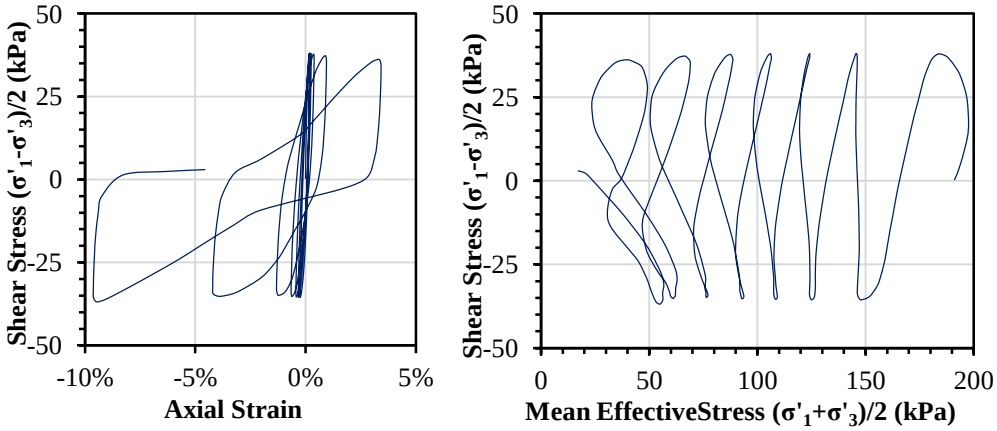

Figure B.5 Undrained triaxial cyclic shear test on reconstituted specimen of Kamloops silt: Stress-strain and stress path curves; σ'_{3c} ~ 200kPa; CSR = 0.190; K_c=1.0.

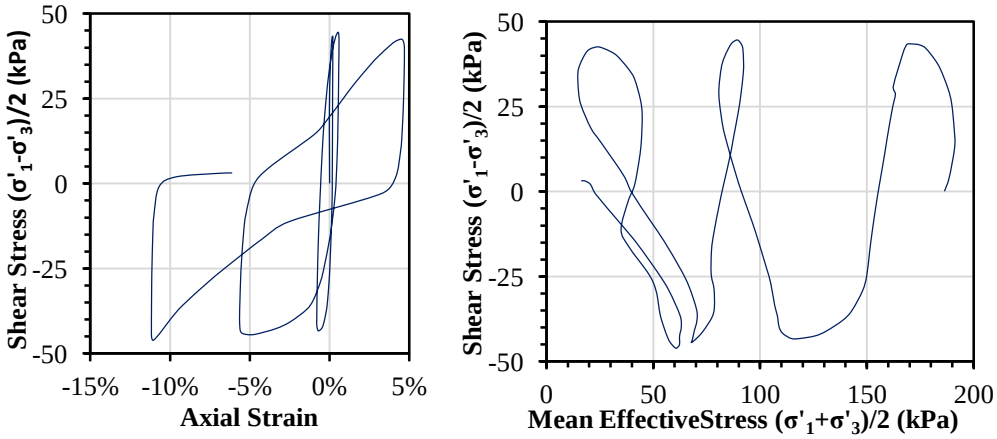

Figure B.6 Undrained triaxial cyclic shear test on reconstituted specimen of Kamloops silt: Stress-strain and stress path curves; σ'_{3c} ~ 200kPa; CSR = 0.230; K_c=1.0.

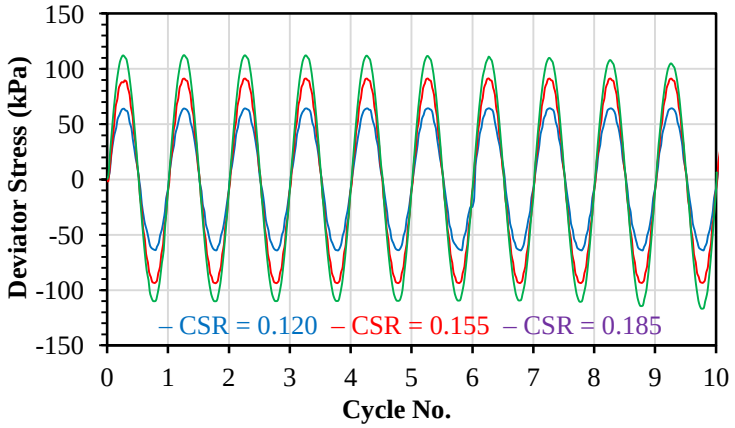

Figure B.7 Undrained triaxial cyclic shear test on reconstituted specimen of Kamloops silt: Applied single amplitude deviator stress (q_{cyc}) vs. number of loading cycles for different CSR values; σ'_{3c} ~ 300; K_c=1.0.

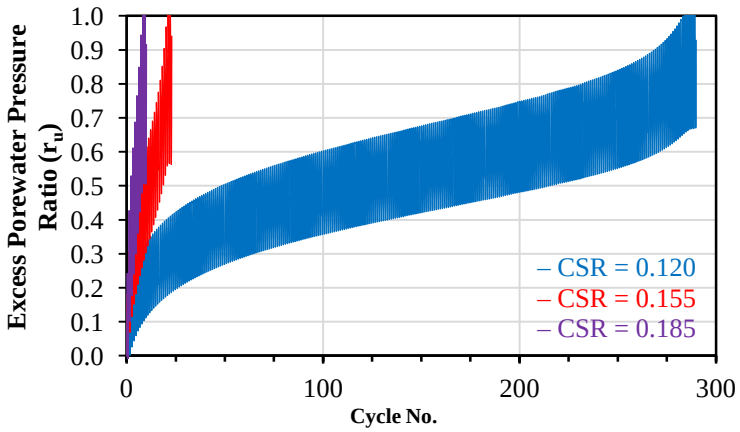

Figure B.8 Undrained triaxial cyclic shear test on reconstituted specimen of Kamloops silt: Excess pore water pressure ratio (r_u) vs. number of loading cycles for different CSR values; σ'_{3c} ~ 300; K_c=1.0.

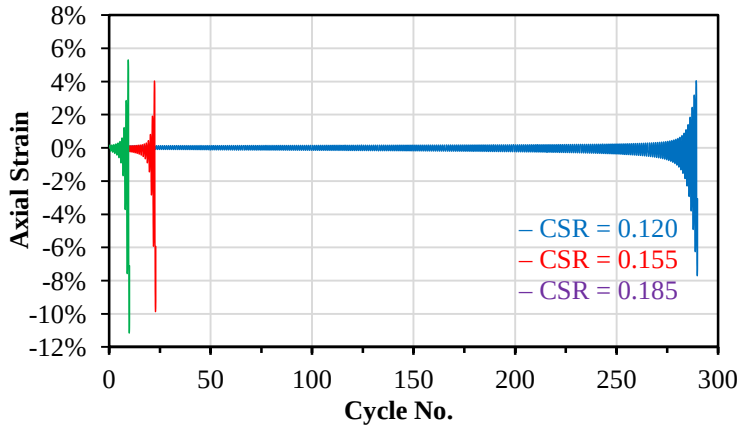

Figure B.9 Undrained triaxial cyclic shear test on reconstituted specimen of Kamloops silt: Axial strain (ε_a) vs. number of loading cycles for different CSR values; σ'_{3c} ~ 300; K_c=1.0.

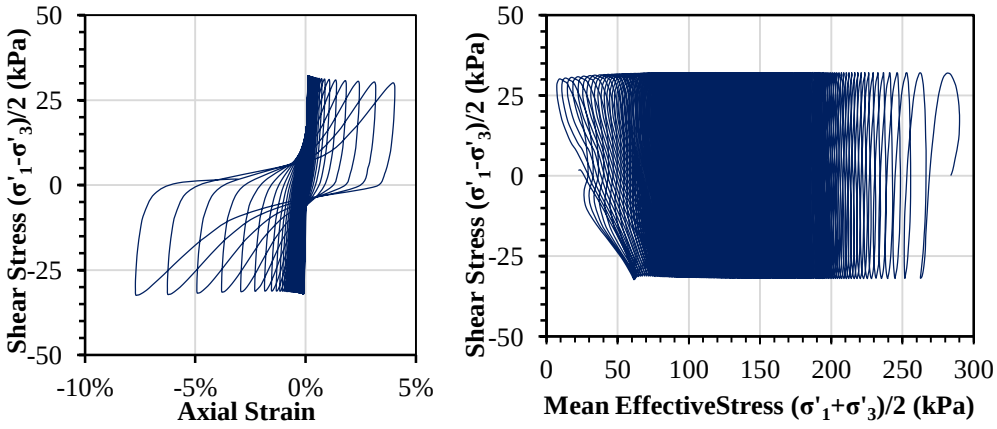

Figure B.10 Undrained triaxial cyclic shear test on reconstituted specimen of Kamloops silt: Stress-strain and stress path curves; σ'_{3c} ~ 300kPa; CSR = 0.120; K_c=1.0.

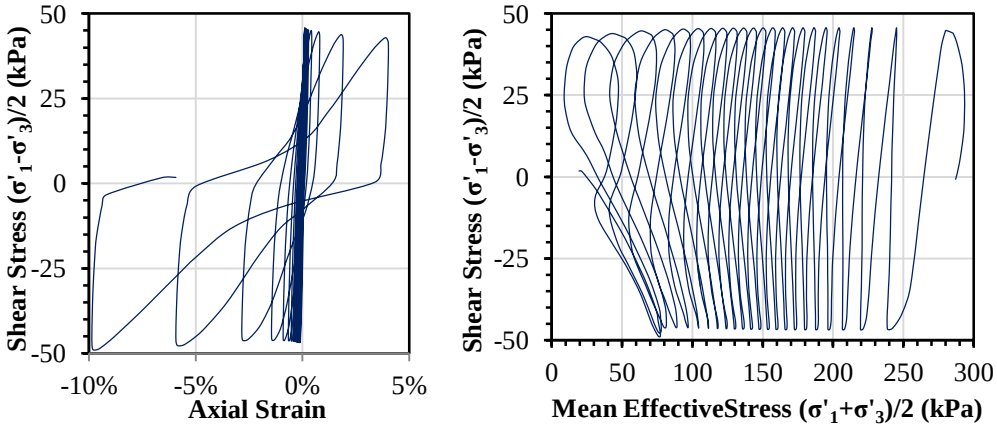

Figure B.11 Undrained triaxial cyclic shear test on reconstituted specimen of Kamloops silt: Stress-strain and stress path curves; σ'_{3c} ~ 300kPa; CSR = 0.155; K_c=1.0.

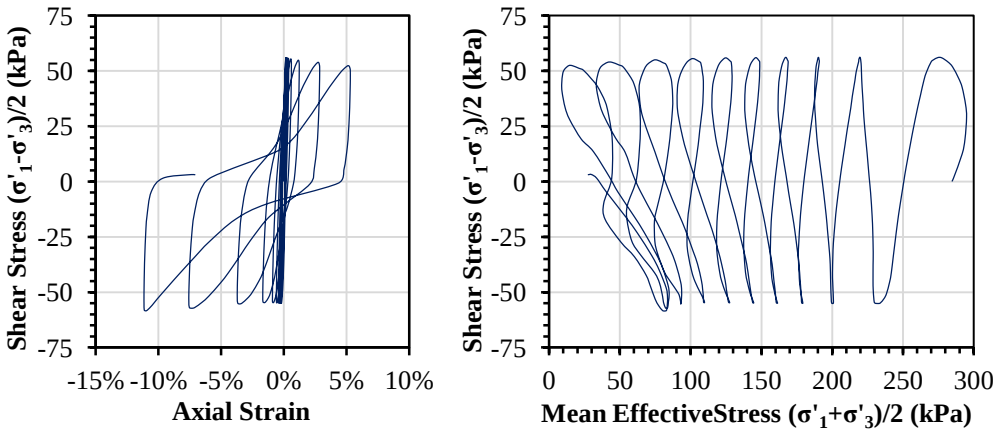

Figure B.12 Undrained triaxial cyclic shear test on reconstituted specimen of Kamloops silt: Stress-strain and stress path curves; σ'_{3c} ~ 300kPa; CSR = 0.185; K_c=1.0.